# *IN VIVO* MEASUREMENTS OF HUMAN TONGUE ELASTICITY USING A VOLUME-BASED ASPIRATION METHOD

**Towards a personalized biomechanical tongue model**

S.Boonstra
*Technical Medicine – Master Thesis*
University of Twente
09-01-2019

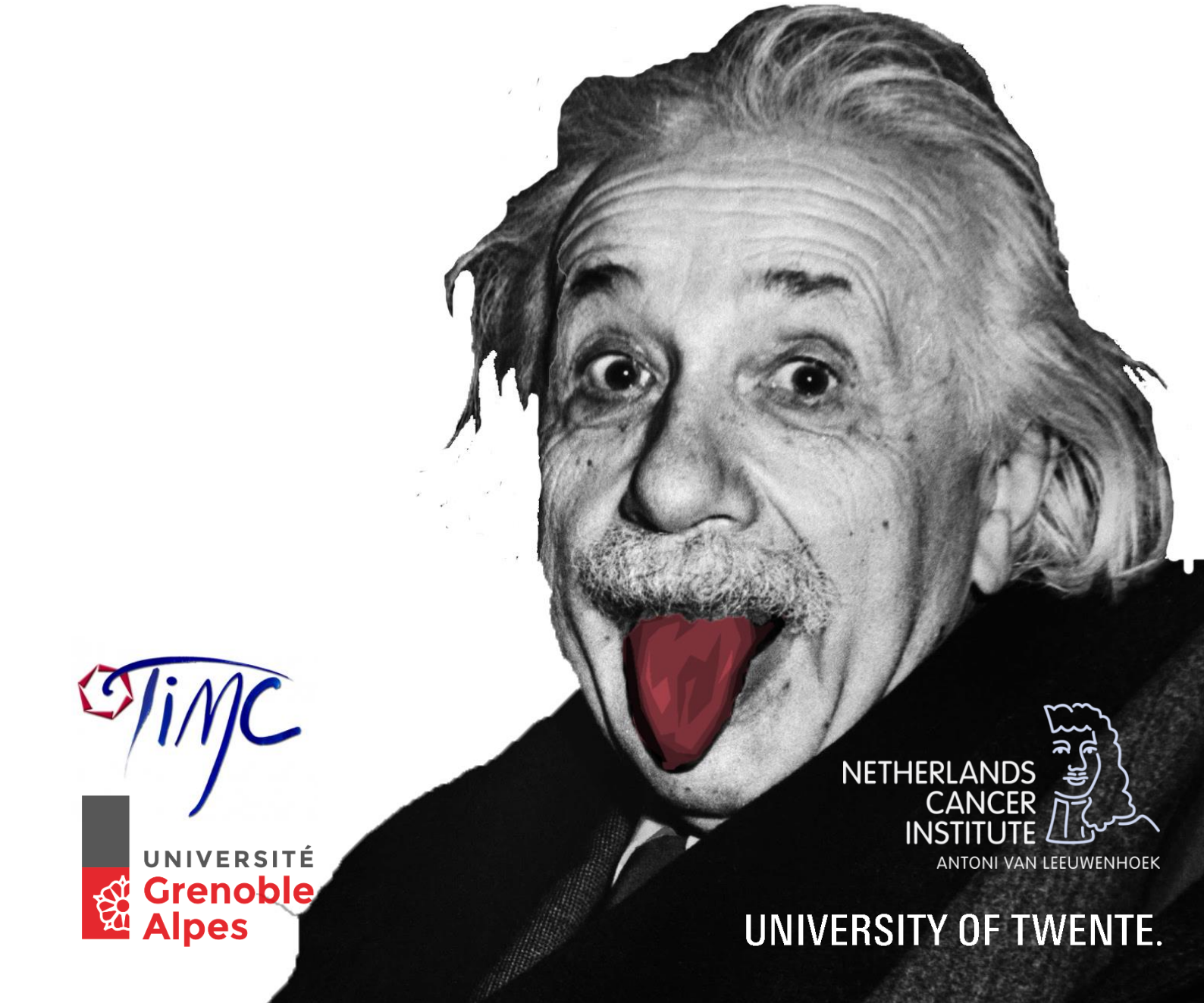

# *IN VIVO* MEASUREMENTS OF HUMAN TONGUE ELASTICITY USING A VOLUME-BASED ASPIRATION METHOD

## TOWARDS A PERSONALIZED BIOMECHANICAL TONGUE MODEL

Sander Boonstra

Technical Medicine – Medical Imaging and Intervention

January 2018 – January 2019

**Masters Graduation Committee**

| | |
|---|---|
| Chairman and technical supervisor | Dr.ir. F. van der Heijden,<br>MIRA institute for Biomechanical Engineering and Technical Medicine<br>University of Twente, Enschede, The Netherlands |
| Clinical supervisor | Prof.dr. L.E. Smeele,<br>Department of Head and Neck Oncology and Surgery<br>Netherlands Cancer Institute, Amsterdam, The Netherlands |
| Technical Supervisor NKI | K.D.R. Kappert, MSc<br>Department of Head and Neck Oncology and Surgery<br>Netherlands Cancer Institute, Amsterdam, The Netherlands |
| Mentor | Dr. M. Groenier<br>Technical Medicine<br>University of Twente, Enschede, The Netherlands |
| Additional member | M.E. Kamphuis, MSc<br>Researcher/teacher<br>University of Twente, Enschede, The Netherlands |

# Preface

About sixteen months ago I started one of the biggest adventures of my life so for: exploring the beautiful South America for three months. But before I left, I wanted to be sure to have a position to graduate. In the year before I did a 10 weeks internship in the Netherlands Cancer Institute and had a really good time. So, before I left I contacted the members of the Virtual Therapy project with the question if there was a graduation assignment. Luckily, there was. Based on my previous internships I wanted to have a more practical assignment with a lot of experiments and measurements on subjects. There was one project that could offer this: measurements of the human tongue elasticity. All of the aforementioned was realized, but in the end it was not a typical Technical Medicine internship since a large part can be seen as 'biomedical engineering'. I remember being in Cusco (Peru) and calling with Kilian on how we could shape my project to a more concrete assignment. Crucial for this thesis became my visit to the laboratory of Techniques for biomedical engineering and complexity management and Informatics, Mathematics and Applications (TIMC-IMAG) in Grenoble (France). Here I was assisted by Yohan Payan, Nathanael Connessn and Seyed-Ali Elahi. I couldn't have done this thesis without their help, so I am very grateful for all the hours of help they gave me (and still give, via email and skype). I really enjoyed working with them as they were always open for discussion and provided constructive feedback. I learned a lot from them in a really short period of time. I want to thank the members of the Virtual Therapy project for giving me the opportunity and motivation to spend three weeks in Grenoble for my research. Also, for thrusting me and giving me the responsibility to strengthen the collaboration with the research group in Grenoble. I want to thank Maarten van Alpen for always taking the time to look at my results and provide feedback. Also great thanks to Freeke Porte, Bence Halpern, and all the M2 students for making my stay at the NKI a pleasant time. A special thanks to Kilian Kappert for not only being my daily supervisor but also becoming a friend. The last year we worked extensively together on several projects and always tried to enjoy it as much as possible. Last, I want to thank my parents, brother, girlfriend, and friends. Without them I would have never been the person I am today. When in doubt, having lack of motivation or in times of adversity they always had, and will always have, my back.

# Summary

**Introduction:** Treatment of locally advanced head and neck cancer has a high risk of loss of functionality. Speech, mastication and swallowing are complex functions that are easily affected. The term "functional inoperability" is used by physicians when unacceptable function loss after surgery is to be expected. It is hard to reach a consensus for the majority of surgical interventions regarding functional inoperability, making effective patient counselling on the expected outcome an arduous task. To make a better prediction of the functional loss after treatment the Virtual Therapy project was launched. One of the aims of the Virtual Therapy project is to develop a biomechanical tongue model to simulate different treatment options and predict the functional outcome on founded expectation. To make this tongue model patient-specific, it is important to have knowledge of the elastic properties of tongue tissue. Since the elastic properties of the tongue are practically unknown, we should first investigate the elastic properties of healthy tongue tissue. It is of importance to be able to measure the elastic properties *in vivo* for applications such as a biomechanical tongue model. In this study a cohort with 16 healthy volunteers was studied to estimate the elastic properties of the human tongue using an *in vivo* measurement technique, as a first step towards extending the biomechanical tongue model of the Virtual Therapy project with the elastic properties of the human tongue. Also, the feasibility of the used measurement technique was assessed.

**Method:** A volume-based aspiration method for *in-vivo* mechanical characterization of soft tissue, called LASTIC, was used to estimate the elastic properties of tongue tissue. An inverse Finite Element Analysis of the aspiration experiment using the Gent hyperelastic material model provided the Young's modulus of 16 healthy subjects. The Gent model contains two parameters, the Young's modulus and a strain limiting factor $Jm$ .

**Results:** An overall mean Young's modulus of 4.83 kPa with a standard deviation of 1.73 kPa was found. For the dimensionless parameter $Jm$ we found an average value of 0.32±0.11. The volume-based measurement technique showed a good reproducibility within each subject with an Intra Class Correlation of 0.78.

**Conclusion:** The results presented in this report gave a good estimation of the elastic behavior of tongue tissue. Although the Gent model does not include viscoelastic behavior, it provided great insight in what the elastic response might be. Also, we obtained a lot of data which can be evaluated using different material models in the future as well. The design of LASTIC and its ability to provide contrast between the mechanical local behavior of different materials, makes it a very promising and feasible technique to measure the elastic properties of the human tongue. A first step towards extending the biomechanical tongue model of the Virtual Therapy project with the elastic properties of the human tongue was made.

***Index Terms*— Aspiration, Elasticity, In vivo, Virtual Therapy, Volume-based, Finite Element Analysis, Functional inoperability**

# Table of contents

# 1. INTRODUCTION

According to the Dutch Cancer Registry, almost 3100 people have been newly diagnosed with head and neck cancer (HNC) in 2017 in the Netherlands, taking up to almost 3% of all newly diagnosed cancers. The total number for oral cavity and tongue cancer is 930 and 395, respectively. On average 1/3 of the tumors in the oral cavity is located in the tongue[1]. Dutch figures for cancer in the oral cavity and oropharynx show a five-year survival rate of 62% and 48% respectively over the period 2011 to 2015[2]. Oral cancers are believed to be a multifactorial disease and tobacco and alcohol are considered the major risk factors. They appear to have a synergistic effect[3–5]. Other risk factors are dietary habits, occupational activities, socioeconomic status, exposure to external agents and genetic susceptibility[6].

For advanced oral and oropharyngeal cancer, stage III and IV according to the TNM classification, two main curative treatment modalities are currently available: surgery (with or without adjuvant radiotherapy) and chemoradiotherapy. For oral cancer surgery is preferred, followed by adjuvant radiotherapy in case of non-radical resection or the histological presence of bad prognostic indicators[7]. Next to traditional surgery, radiation and chemotherapy other treatment modalities like $CO_2$ laser surgery, transoral robotic surgery and photodynamic therapy can be used. Important tumor characteristics for the choice of treatment are its size, location, extension, histology, and stage. Also the patient's age, condition, compliance and own choice are taken into consideration for the choice of treatment[6].

The best treatment should maximize the patient's survival and minimize the effect on the quality of life (QOL). Post-operative QOL depends largely on the patient's functional outcome of the treatment. Resection of tumors and critical structures in the oral cavity or oropharynx can lead to loss or impairment of essential functions like speech, mastication, and swallowing. Such function loss may lead to other problems like depression and deficient intake[8,9]. Therefore, treatment of oral cavity and oropharyngeal cancer can lead to a serious decrease in the QOL[10,11]. Although the aforementioned functions seem straightforward, complexly coordinated contractions of multiple muscles are required for the associated motions. Proper timing, muscle strength, coordination, and sensibility are of vital importance to perform the right motions. Function loss will be induced when one of these factors is compromised[7]. Surgical reconstruction can preserve functionality, but some degree of impairment may remain[12]. Where surgical removal has a more direct influence on the functional outcome, radiation and chemoradiation often show a delayed effect. Nevertheless, the functional sequelae can be substantial. Xerostomia and fibrosis are common side effects of (chemo)radiation. In Appendix A an overview of the anatomy of the tongue is given, showing the complexity of all muscle structures in the tongue.

Traditionally, tumors were considered inoperable if vital structures were invaded. This is called anatomically inoperable[12]. Nowadays, the surgical focus is shifted to the preservation of function, introducing a new term: functional inoperability. Functional inoperability refers to tumors that can only be radically resected with the unacceptable postoperative functional loss. Functional inoperability is a hard threshold in the middle of a grey area. This area is grey because the agreement between physicians on whether surgery is functional inoperable is low[13]. Also, there are no objective tools yet to predict the functional outcome in full detail.

In the Netherlands, A.M. Kreeft performed a study about the way Dutch physicians agree on functional inoperability for HNC patients. She concluded that assessment of functional inoperability is highly dependent on personal experience and preferences of the physician, i.e. no absolute consensus was found[12,13]. Due to the lack of clear guidelines and many patient-specific factors, it is very difficult to preoperatively predict the resulting loss of function after surgery[7]. This makes it arduous to reach an objective consensus in the multidisciplinary meetings and to counsel the patient properly on the expected outcome. Although severely needed, no standardized evaluation tool exists to help predict a personalized functional outcome of oral cancer therapies. In order to improve this situation, the *Virtual Therapy* project was established. This project was launched to develop a more objective evidence-based approach to predict patient-specific oral function post-treatment[7]. It aims to guide the decision-making process by incorporating a biomechanical model which can simulate post-treatment functionality.

Physically based models are widely used in the field of biomedical engineering to represents human organs geometrical, and mechanical behavior[14]. Unfortunately, virtual simulators are mostly limited to a single preset model. The rise of Computer Assisted Planning and Computer Aided Surgery sparks the need for patient-specific models[14]. The Virtual Therapy project focuses on

the oral cavity and the oropharynx, and therefore the model should be able to predict movements and load-bearing tasks of the tongue, lips and other structures in these areas in order to present the individual treatment effects on mastication, swallowing, and speech. The present study will focus on the tongue. Currently, the biomechanical model of the tongue is created in ArtiSynth. ArtiSynth is developed at the University of British Columbia to create and simulate solid and deformable structures in mainly the upper airway. It is a toolkit in JAVA[15].

In order to create a personalized model, a conforming mesh of the patient's tongue geometry needs to be generated. Within the Virtual Therapy project, an atlas of the human tongue using manually labeled magnetic resonance (MR) images is in development. The aim is to implement an atlas-based segmentation method. Using image registration techniques the atlas image can be aligned with a new, unseen, image to segment the tongue geometries of a patient and extrapolate the generic tongue model to a personalized model. Although, this shows promising results the largest challenge is still ahead. Namely, the extension of the model with proper and patient-specific biomechanical properties using an appropriate material model. Currently, the elastic properties of the biomechanical tongue model are based on assumptions and probabilities while the movement and deformation of the model are highly dependent on these properties. Also, after treatment, the elastic properties of the tongue are strongly influenced by fibrotic changes. Therefore, fibrosis and other effects on tissue elasticity should be studied closely. However, the elastic properties of just the healthy tongue tissue are still not clear, let alone the properties of fibrotic tissue. Therefore, this report will focus on measuring the elastic properties of healthy human tongue tissue *in vivo,* as a first step towards the extension of the biomechanical tongue model.

## 2. THEORY: TECHNICAL BACKGROUND

To understand the goals of this study and the method section, it is essential to know the terminology and techniques that were used. In this chapter, some background will be provided about elasticity and the biomechanical modeling. If these terms are familiar, one can continue in section 2.2, where some background on different measurement techniques is given. In section 2.3 and 2.4, the introduced measurement technique in this study is explained.

### *2.1. Elasticity and biomechanical modeling with FEM*

The elasticity of a material, known as the Young's modulus ( $E$ ), is a measure of the stiffness of a material. It describes the tendency of the material to return to its original size and shape after experiencing uniaxial stress and is defined as the ratio between stress (the force per unit area) and strain (proportional deformation) according to Hooke's law[16]:

$$E = \frac{F/A}{\Delta L / L_0} = \frac{\sigma}{\varepsilon} \tag{1}$$

Where $\sigma$ represents stress as a function of the force $F$ per unit area $A$. The strain is represented by $\varepsilon$ with $L_0$ as the original length of the object and $\Delta L$ the elongation or compression of the object. In Figure 1 a schematic representation of uniaxial stress on an object and the resulting strain is shown.

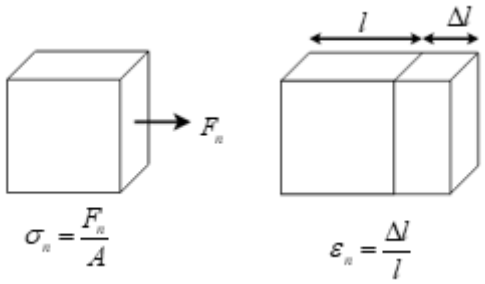


Figure 1: Schematic representation of stress (left) and strain (right).

Usually, a biomechanical model is created using the Finite Element Method (FEM). FEM is used in engineering to divide structures into smaller parts wherein physical properties, like stress and strain, can be calculated and subsequently be used for calculation of certain property changes of the complete structure using a numerical method. FEM is often referred to as the numerical technique used to perform the calculations in order to solve the problem or to perform a simulation of an experiment that describes the relationship between two physical properties. Analyzing a phenomenon with FEM is often referred to as Finite Element Analysis (FEA).

In an FEA a 2D or 3D object is divided into multiple smaller parts, which are called elements. This is called the Finite Element (FE) model. The FE model is partly responsible for the biomechanical simulation. In this report, we will first focus on a 2D FE model since 2D models require significantly less computational power compared to 3D models when performing an FEA[17]. An example is shown in Figure 2.

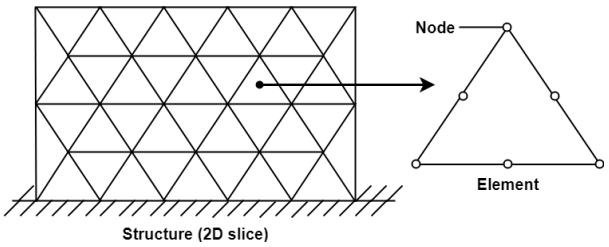


Figure 2: Example of a 2D Finite Element structure.

In a 2D FE model, an element is an area defined by nodes as seen in Figure 2. In a visual representation of an element, these nodes function as vertices, but during an FEA they are more than that. The nodes contain information about the material properties. At each time step, a new state for each node is calculated. This can be a state of position, speed or other physical quantities, such as stress and strain. The latter two is what we are interested in. Using interpolation the new state of each node can be calculated for each position within the element after each time step.

Once the FE model is created that represents or approximates the desired geometry of the structure to simulate, one needs a mathematical model that describes the state of the nodes at each time step. In physics and engineering the relationship between two physical quantities, like stress and strain, are described by a constitutive law that is specific for a material or substance. Equation 1 is the constitutive law for the Young's modulus, it describes the linear relationship between uniaxial stress and the resulting strain for materials that exhibit linear elastic behavior. However, the complex muscular and connective tissue of the human tongue can exhibit nonlinear, time-dependent, inhomogeneous and anisotropic behavior[18]. Therefore, Hooke's Law will not be suitable to describe the stress and strain relationship inside the tongue tissue. Several constitutive laws exist using complex polynomial function. For example, the multiparametric Yeoh or Mooney Rivlin strain energy functions. In this report, the constitutive law of the Gent model will be used. The robust Gent model is praised by its simplicity, yet its effectiveness in describing the behavior of many elastomeric and biological materials[19,20]. The strain energy function $W_G$, for incompressible, isotropic, hyperelastic materials according to the Gent model is as follows:

$$W_G = -\frac{EJ_m}{6}\ln\left(1-\frac{I_1-3}{J_m}\right) \qquad (2)$$

In this basic Gent model $I_1$ represents the first invariant of the left Cauchy-Green strain tensor. $W_G$ only depends on the first invariant and therefore the Gent model belongs to the generalized neo-Hookean material models such that $W = W(I_1)$[19]. The dimensionless parameter $J_m$ defines the maximum value of elongation $(I_1 - 3)$ that can be undergone by the material. It introduces strain limitation. One recovers the parent neo-Hookean if $J_m \to \infty$. The parameter $E$ represents the Young's modulus of the material and is expressed in kilopascals (kPa). Based on this relationship we can use the Young's modulus as an elastic parameter in an FEA.

The strain tensor is the tensor that describes the deformation of the material, i.e. the elements in the FE model. To get a better understanding of this term and about invariants, an introduction to continuum mechanics is given in Appendix B. Without prior knowledge about continuum mechanics, it is recommended to read Appendix B first before continuing to the next sections.

### *2.2. In vivo measurement techniques*

In the past, several constitutive laws are proposed in literature, but only a few propose a constitutive law based on real data. This is because of the complexity of measuring the mechanical response of tongue tissue under physiological loading conditions[18]. To our knowledge, only three papers have used experimental data to address this issue and performed *ex vivo*[21] and *in vivo* experiments [22,23]. All of them assumed a hyperelastic material model using a strain energy approach like we will in this report. The mechanical behavior of living tissues varies between *in vivo* and *ex vivo* conditions[24], it is thus of importance to be able to measure the elastic properties *in vivo* for applications such as the biomechanical tongue of the Virtual Therapy project.

One commonly known technique to measure the elastic properties of human tissue *in vivo* is elastography. Nowadays this technique is implemented commonly in ultrasound (US) and magnetic resonance (MR) systems to noninvasively assess the elastic properties of tissue. Elastographic images are mainly performed using a dynamic source to create shear waves. When shear waves, or transverse waves, are generated inside the tissue the elasticity can be measured.

One of the main dynamic methods is Magnetic Resonance Elastography (MRE). In MRE external mechanically induced shear waves are used to determine the viscoelastic properties of tissue. One study performed by Cheng et al. 2011 determined the

viscoelastic properties of the tongue in patients with obstructive sleep apnea (OPA)[23]. The results looked very promising, but we aim to perform intra-operative measurements on the tissue in the future (See Chapter 3), which is not possible with MRE.

A more practical way to measure elasticity is shear wave imaging (SWI) in ultrasound. The tongue can be measured by simply placing the ultrasound probe on the submental space of the subject. SWI in ultrasound can be divided into three main techniques. 1) A dynamic stress can be applied to the tissue using an external mechanical vibration device in 1D transient imaging (1D-TE) or 2) focusing acoustic radiation force impulses (ARFI) in point shear wave elastography (pSWE) and 3) 2D shear wave elastography (2D-SWE)[25]. When using an acoustic radiation force the shear waves are measured perpendicular to the push pulse propagation. The speed of shear waves $v_s$ and the density of the material $\rho$ have a direct relationship with the material Young's modulus according to:

$$E = 3\rho v_s^2 \tag{3}$$

ARFI technique would be the most practical method since it is used with direct grayscale guidance, showing the exact anatomical location of the tissue and the location where the measurement is obtained. However, earlier studies by our research group showed that SWE is not a reliable technique to determine the Young's modulus for anisotropic tissue like the tongue. In Appendix J some background information about acoustic waves and elastography is given. In addition, a brief overview of our SWE results is presented.

Based on the aforementioned constraints and limitations of both MRE and SWE and the desire to perform intra-operative measurements on humans, researchers tried to design new devices. For intra-operative measurements, the procedure should be non-traumatic and performed under sterile conditions. Also, the measurement procedure should meet the space and time limitation in the operating room (OR).

To comply with these requirements, several devices of small sizes and low weights are proposed in literature using different measurement methods[26–32]. Of all these methods, the aspiration technique is the most widely used technique due to its simplicity and robustness[33]. Even some commercial aspiration devices are designed for the dermatology market (e.g. Cutometer from Courage and Khazaka, Germany)[34]. The aspiration method especially provides a good method to control the applied experimental boundary conditions[35] and limits the relative displacement of the tissues compared with the device.

The aspiration device works in the following way: a chamber with an aperture is placed on the tissue and the pressure is lowered inside the chamber. Consequently, the tissue is aspirated inside the chamber through the aperture while the aspiration pressure is measured during the experiment. In order to measure the deformation of the tissue, most authors propose to measure the aspirated height of the tissue. Several methods are proposed such as ultrasound[35,36], mechanical stops[37] or optical methods using a camera measuring the height directly or with mirrors or prisms. Since ultrasound requires the use of a large machine and mechanical stops only provide one value, the optical method seems preferable to provide pressure versus apex height characteristic curves over time.

The in-house built Light Aspiration device for *in vivo* Soft TIssue Characterization (LASTIC), developed by Schiavone et al. 2018, provides such curves. It uses aspiration to deform soft tissue within a small suction cup with a circular aperture [22]. Several models of LASTIC using an optical method have been developed in the past years and were used to *in vivo* measure the elastic properties of the human brain, tongue, and skin[14,21,22,38]. However, like all other optical aspiration methods, these techniques underline some major limitations regarding sterilization and handling. First, the electronic parts cannot withstand severe sterilization processes. Meaning, these complex designs are not suitable for intra-operative measurements. Schiavone et al. 2009[38] tried using an external camera so the aspiration chamber was able to meet the required severe sterilization, but due to misalignment of the external camera measurement errors were induced. This underlines the second limitation: the use of cameras and mirrors require accurate positioning with respect to each other in order to measure the correct tissue apex height. Overcoming this problem leads to rigid and large devices[14]. Since the aspiration method requires direct placement of the aspiration chamber on the tissue, these devices are not suitable for intra-oral measurements. To overcome these limitations a new and disposable version of LASTIC has been developed. The design of the aspiration experiment has shifted from measuring tissue deformation by the apex height in millimeters to a rate-based volume measurement[33]. Hereby, all electronic

parts are eliminated and only a small and light aspiration chamber is needed to perform the measurements.

This new measurement technique provides a quantitative elasticity measurement, which could be included directly into the biomechanical ArtiSynth model and, therefore, it is a promising added value for the Virtual Therapy project. It is introduced in the next section.

### 2.3. *Rate-Based volume measurement*

During the *in vivo* and *in situ* test, the measurement technique is simply composed of a syringe pump, a manometer and an aspiration chamber with a circular aperture with a certain aperture diameter (AD). On Figure 3, a schematic overview of the setup is shown.

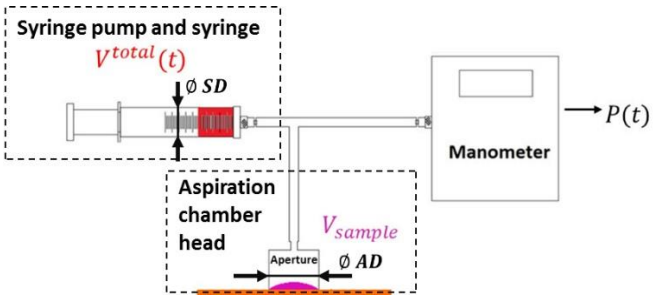


Figure 3: Measurement principle of rate-based volume measurement. *Image retrieved from Elahi et al. 2018*[33].

When performing a measurement on a sample, i.e. tissue, the total volume removed by the syringe pump $V^{total}$ and the associated pressure $P$ is measured during the test over time. However, the volume removed by the syringe pump $V^{total}$ is obviously different from the tissue volume $V_{sample}$. This difference is mainly due to volume changes in the system because of the applied pressure, and the system volume $V_{system}$ is compressible due to air expansion and elasticity of the components (connections, tubes, syringe, etc.). The total removed volume $V^{total}$ can, therefore, be seen as the sum of the aspirated tissue volume $V^{RB}_{sample}$ and the volume changes due to system compressibility $V_{system}$ :

$$V^{total}(P) = V^{RB}_{sample}(P) + V_{system}(P) \quad (4)$$

The system volume function $V_{system}$ is experimentally obtained during the first step by testing an undeformable material, referred to as the rigid test. In this experimental setting, the aspirated tissue volume $V^{RB}_{sample}$ sample remains zero and the system volume compressibility $V_{system}$ can be directly measured using:

$$V_{system}(P) = V^{total}_{rigid}(P) \quad (5)$$

Combining the system volume $V_{system}$ (equation 4 and equation 5), the aspirated tissue volume $V^{RB}_{sample}$ can naturally be estimated by:

$$V^{RB}_{sample}(P) = V^{total}(P) - V_{system}(P) \quad (6)$$

In Figure 4 a schematic representation of the experimental acquired curves according to equation 4 and 5 are shown in blue and red, respectively. In green, the calculated tissue volume versus pressure curve according to equation 6 is shown. In Appendix C a more in-depth explanation of the volume based measurement can be found.

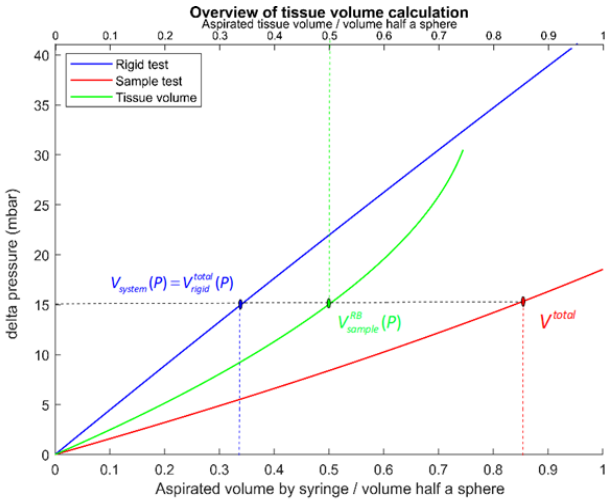


Figure 4: Schematic representation of the experimental acquired curve. In blue, the curve of the rigid test is depicted. In red the total volume curve of the sample test is shown. The calculated tissue volume versus pressure curve is shown in green.

Before a measurement is started an airtight connection between the tissue and aperture is obtained by creating an initial depression $P_0$ within the aspiration chamber. Consequently, some initial and unknown tissue volume $V_{0,sample}$ is aspirated through the aperture. This is shown in Figure 5.

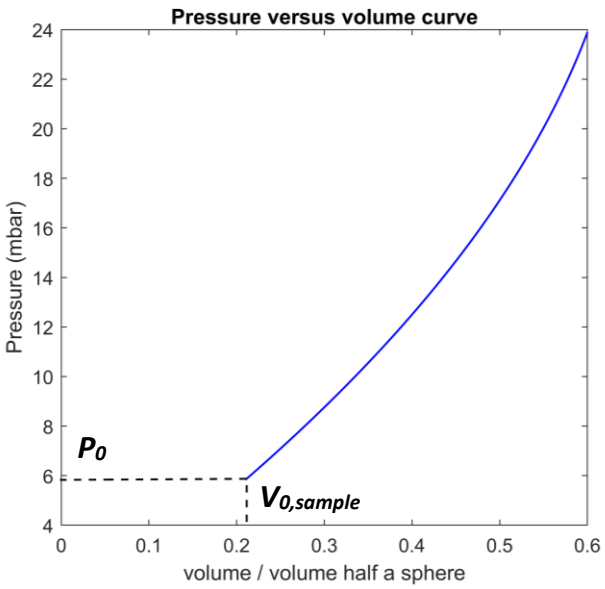


Figure 5: Representation of the tissue volume versus pressure curve of the tissue sample acquired by the experiment. The initial tissue volume $V_{0,sample}$ and corresponding pressure points until $P_0$ are unknown.

For real-time measurements, a software tool was developed that automatically estimates the initial tissue volume $V_{0,sample}$ using a linear estimation based on the slope of the first ten measurement points. Therefore, we could monitor the aspirated tissue volume during the aspiration experiment. This was tested on silicon phantoms as well and showed good results. However, the phantoms showed a linear elastic response while tissue is known to show a nonlinear response. Therefore the estimation of $V_{0,sample}$ was reevaluated. See Appendix E. Based on the reevaluation the raw measurement data was used to estimate the initial aspirated volume $V_{0,sample}$ by extrapolating all the measurement points using a second-degree polynomial fit.

The rate-based method has been extensively tested and validated. The signal-to-noise ratio of the optical and rate-based volume measurement was assessed by comparing all results with a reference obtained in identical conditions. The complete performance test can be found in Elahi et al. 2018[33]. It showed that the rate-based volume method proves to have a similar or lower measurement error than the optical method mentioned before with a measurement error close to zero for different aperture diameters. It is essential that the syringe diameter used in the syringe pump is properly chosen, the smaller the diameter the smaller the measurement error. But the volume of the syringe should be sufficient to aspirate the desired tissue volume as well. Also, no leakage should occur during the tests.

### *2.4. Estimation of the constitutive law with inverse FEA*

The aspiration experiment itself does not provide the constitutive law of the tissue, i.e. the Young's modulus. The measurements only give the relation between the local depression applied to the external surface of the tissue and the resulting aspirated tissue volume. The result is a tissue volume versus pressure curve as described in equation 6 and shown in Figure 4 in green. To derive the constitutive law from the experiment, i.e. the assumed relationship between stress and strain inside the tissue, a four-step optimization scheme can be used:

1. Assume a given constitutive law with a given set of parameters. In our case, the Gent model is assumed.
2. Build and simulate a Finite Element Analysis (FEA) of the aspiration experiment
3. Compare the results, i.e. volume versus pressure curve, of the FEA with the aspiration experiment.
4. Deduce better values of the constitutive law parameters from this comparison in order to improve the fit of FEA simulation with the measurement.

Step 3 and 4 are repeated until the comparison in step 3 gives satisfactory results.

So, the elastic parameters of the soft tissue are estimated by inverting an FEA of the aspiration experiment. Using an optimization scheme the best fit between the experimental results and the FEA is computed. The FEA used in this study will be explained in section 4.3.

## 3. RESEARCH GOALS

During this project, the main goal was to set up a new research project within the research line of the Virtual Therapy project. We want to take a first step towards improving the biomechanical tongue model with human-specific elastic properties of healthy tongue tissue.

To understand the goal of the new research line it is important to know that we divide the elastic properties of the human tongue into two features, namely the active and passive elasticity. The elastic properties of the human tongue are expected to be influenced by muscle activation of the tongue muscles, even at rest muscle tonus is present. Therefore, we consider the elastic

properties of the tongue, even at rest, as the active. The real tissue stiffness can only be measured when there is no muscle tone at all. This is defined as passive elasticity. We believe the latter can only be measured when a subject is under general anesthesia since this is the only reasonable way to get almost complete relaxation of the tongue muscle *in vivo*.

The ultimate goal is to estimate passive and active tongue muscle elasticity *in vivo*. A study cohort of patients, with no pathology or impaired functionality in the oral cavity and oropharynx, measured before (active elasticity) and during general anesthesia (passive elasticity) are expected to show a difference between the active and passive elastic properties of the tongue, respectively. But, the proposed measurement technique has never been used for our desired purposes and should, therefore, be evaluated before we subject a patient cohort to our measurements. A study cohort of healthy volunteers should be studied first to estimate a realistic range and variation for the elastic properties of the human tongue and to evaluate the proposed measurement technique. Therefore, a clinical study was designed to perform these measurements on the aforementioned cohorts. The research protocol was approved by the local Ethics Committee (METC AVL – code 031) and can be found in Appendix L.

In the present feasibility study, only the cohort with healthy volunteers was studied to estimate the elastic properties of the human tongue using an *in vivo* measurement technique. The latest version of the LASTIC device[33] was used to perform these measurements as described in section 2.3.

This is the first time *in vivo* data of the human tongue is acquired on this scale. Therefore the main research question is: Can LASTIC be used to measure the elastic properties of the human tongue *in vivo*?

While conducting our measurements a couple of questions have to be taken into consideration:

1. Is LASTIC a feasible technique to estimate differences in (tongue tissue) elasticity?
2. What are the constraints we will be facing during our measurements and how can we solve these?
3. What constitutive law is appropriate to get a good estimation of the elastic behavior of tongue tissue?
4. What is a simple and effective way to simulate the tongue in an FE model for Finite Element Analysis, without running computationally expensive simulations?

As this is a first step towards estimating the elastic properties of tongue tissue *in vivo* we do not expect to provide a universal constitutive law of human tongue tissue elasticity. This report will, therefore, primarily focus on showing the results of the rather difficult experiments on *in vivo* human tongue elasticity. The goal is to provide an initial estimation of a range for the elastic values of human tongue tissue. In this report, only the results of the measurements on the healthy cohort are provided.

In addition, an evaluation of the proposed measurement tool for estimating the elastic properties of human tongue tissue is included. It should be suitable to deliver an input for the biomechanical tongue model to improve it with human-specific elastic properties of healthy tongue tissue, and fibrotic tissue in the future as well.

## 4. METHODS AND MATERIALS

### *4.1. The aspiration chamber*

A major constraint we faced was the limited space of the oral cavity. The aspiration chamber should thus be light and small in order to access the tongue properly. In all previous aspiration chambers, the depression was applied directly above the tissue. However, this requires wider mouth opening due to the tubes that need to access the aspiration chamber. Also, the subject is more likely to put external pressure on the chamber with the mouth itself as it is very hard to keep the mouth wide open for a long period of time. To overcome this constraint a lateral suction cup was developed and tested so the tubes can access to chamber from the side. The tubes of the system can be directly attached to this chamber. In Figure 6 the design is shown.

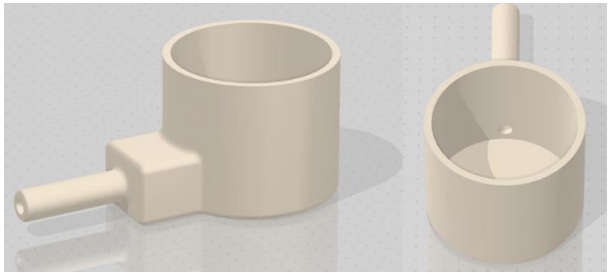

Figure 6: Design of the new aspiration chamber. The inner aperture diameter (AD) was set to 10 mm, the outer diameter to 11 mm. The wall thickness is 0.5 mm

The aspiration chamber was designed in Solidworks (SolidWorks Corp., Waltham, Massachusetts, USA) and fabricated using 3D printing technology. The Formslabs Form 2 printer (Formlabs, Somerville, Massachusetts, USA) with Dental SG Resin was used. The resin is biocompatible and autoclave proof and, therefore, suitable for our purposes. The aspiration chamber was tested on silicon phantoms and showed similar results as the previous designs. The 3D printed aspiration chamber is completely airtight and no leakage due to torque was observed.

### *4.2. Risk analysis*

In order to start our measurements, we had to be sure the procedure was non-traumatic for the tongue tissue. We designed a program to perform real-time measurements in order to observe the amount of aspirated tissue volume during a test. To reduce the risk of possible tissue damage due to the mechanical stress applied on the tongue, we created a safeguard. Several articles describe that human cells and tissue will be damaged after applying 50% or more strain to the tissue for 5-10 minutes[39,40]. Therefore, we had to perform measurements without reaching this limit.

The formula for uniaxial strain is $\varepsilon = \frac{\Delta L}{L_o}$ where $L_o$ represents the original length of the material and $\Delta L$ the elongation or compression of the material. An example of a square of 1 by 1 ($dx = 1, dy = 1$) imposed by stress is shown in Figure 7.

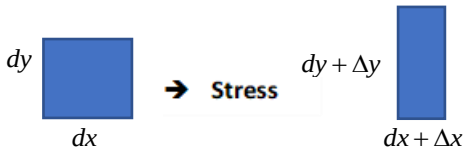


Figure 7: Schematic example of strain due to stress on a square

After applying stress on the square its shape changes and the new dimension becomes $dx + \Delta dx$ and $dy + \Delta dy$. According to the previously mentioned equation, we can define strain in the x-direction and the y-direction according to: $\varepsilon_x = \frac{\Delta dx}{dx}$ and $\varepsilon_y = \frac{\Delta dy}{dy}$, respectively. To calculate the total strain on the material we use $\varepsilon_{tot} = \sqrt{\varepsilon_x^2 + \varepsilon_y^2}$. If $\varepsilon_{tot}$ equals 0.5 it means that the total strain applied to the material is 50%.

In LASTIC we had several parameters to work with. First of all, we have the radius of the aperture. Based on finite element simulations with ANSYS software (Ansys, Canonsburg, PA, USA) we observed that aspirating a volume of 50% of a half sphere will lead to a total maximum strain of around 50%. So the volume of the tissue deformation should not be more than 50% of a half sphere. Based on phantom experiments and FEA we also saw that the volume of 50% of half a sphere was sufficient to calculate the Young's modulus of the material. Knowing the radius of the aperture the volume of 50% of a half sphere can be calculated according to:

$$V = \frac{1}{4} \cdot \frac{4}{3} \pi r^3 = \frac{1}{3} \pi r^3 \qquad (7)$$

Where $r$ is the radius. With real-time processing, the aspirated volume during each measurement could be monitored. If the aspirated volume reached the volume of 50% of a half sphere the measurement was stopped, this was the limit. If the limit was reached the system gave a warning to the user, who had to turn off the aspiration pump. One could also set the target volume of the aspiration pump to a certain limit but then the measurement would have stopped immediately. To be sure we reached the right volume the system had to continue to measure for several seconds (e.g. 3 seconds). In this way, possible volume alterations caused by the system itself were eliminated. Figure 8 shows a schematic representation of half a sphere volume.

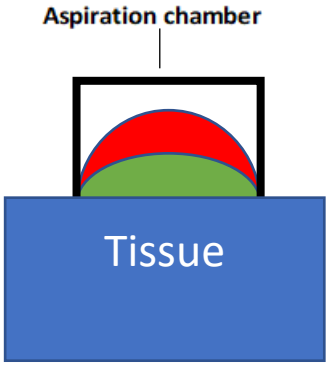


Figure 8: Schematic representation of aspiration limit. Red shows half sphere volume. Green is 50% of a half sphere and our limit

So, by setting the maximum aspirated volume to 50% of half sphere we indirectly set the maximum strain limit around 50%. By only applying it for a few seconds we assured no damage to the tissue was done. If the volunteer experienced pain and wanted to terminate the measurement all pressure could be released with the turn of one valve so direct and safe removal of the aspiration chamber was assured

In Appendix D an overview (in Dutch) is given of possible risks and adverse events regarding the measurements and how to prevent them. This was part of the application for the ethics committee.

### 4.3. *Inverse analysis*

The elastic parameters of the soft tissue were identified by inverting an FEA of the aspiration experiment as described in section 2.4. Ansys mechanical APDL software (Ansys Student 19.1, Ansys, Canonsburg, PA, USA) was used to build and simulate the FEA. All other operations and calculations were done using Matlab R2018a (The Mathworks Inc., Natick, MA, USA).

The optimization of the FEA fit was done automatically. The unconstrained multivariable optimization function (fminsearch) of the Matlab Optimization Toolbox was used to minimize our cost function using a derivative-free method. With a simple cost function, the goodness of fit was evaluated. Our cost function calculated the residual sum of squares ( $RSS$ ) according to:

$$RSS = \sum_{i=1}^{n} (P_i^{\exp} - P_i^{sim}(x_i))^2 \qquad (8)$$

Where $P_i^{\exp}$ is the $i^{th}$ value of pressure of the experiment, $x_i$ the $i^{th}$ value of the explanatory variable, i.e. volume, and $P_i^{sim}(x_i)$ is the predicted value of $P_i^{\exp}$ .

In Figure 9 the used FE model to represent the tongue with its boundary conditions is shown. The tests were modeled in 2D with axis symmetry for computational purposes, i.e. only half of the sample is simulated during the FEA. Since only a small volume was aspirated the deformation of the tissue is small and was considered superficial. Therefore, the bottom layer of the nodes was assumed not the be affected by the applied load and was fixed for horizontal and vertical displacements. The outer side of the tissue was allowed to move freely. The sample was meshed with 2543 quadratic triangular 6-node (T6) elements. The aspiration chamber elements were only fixed for horizontal displacements to simulate a load-free chamber. The load, i.e. pressure on the tissue surface inside the aspiration chamber, is also applied on the aperture in the opposite direction. This is depicted by the red lines. Because of cylinder stresses inside the thin aspiration chamber, the pressure on the chamber is compensated by a surfratio.

The friction coefficient $\mu$ to model the experimental contact properties between the aperture and the sample is unknown. On a scale from 0 (frictionless contact) to 1 (maximum friction), the coefficient was assumed to be 0.2, because of the moist surface of the tongue. The displacement of the tissue surface inside the aperture was used to compute the aspirated volume at each pressure step. Each test was performed using 12 pressure steps. The appropriate pressure step was calculated by dividing the pressure needed in the experiment to reach 0.50 of the shape ratio by 12.

The apex of the tongue was simulated with a radius of 25 mm and a thickness of 15 mm. The radius of the aperture was 5 mm and the aperture wall thickness was 0.5 mm. Since soft tissue is assumed to be nearly incompressible a Poisson's ratio $v$ of 0.49 was chosen to model the compressibility of tongue tissue.

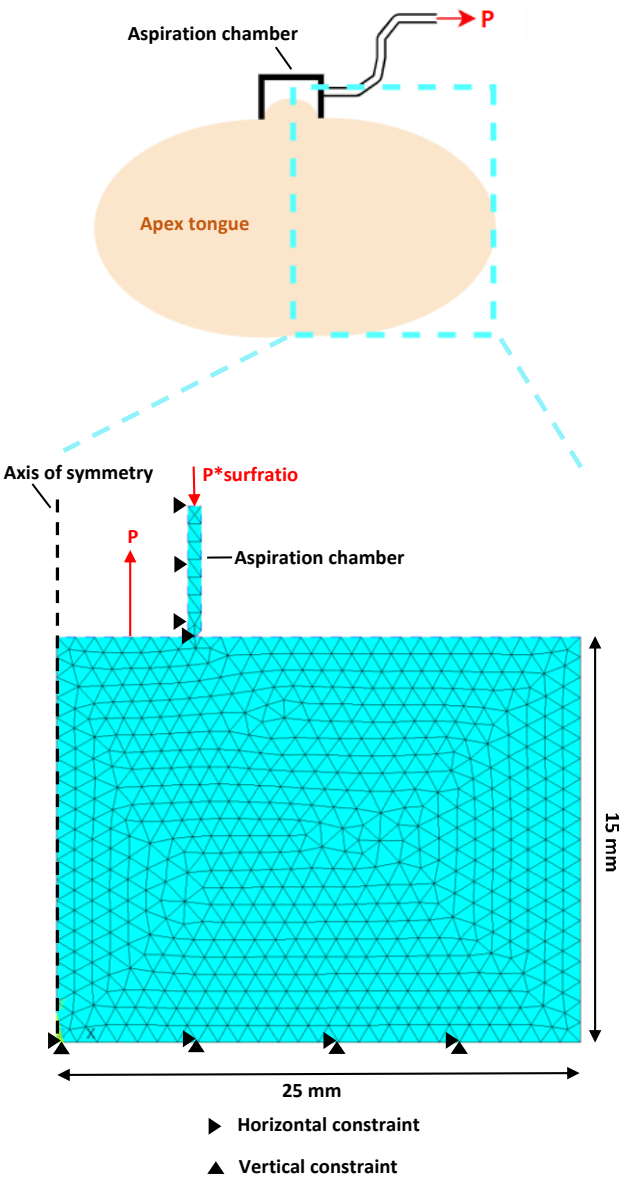


Figure 9: **Top:** Due to axisymmetric conditions only half of the sample needs to be simulated in the FEA. **Bottom:** Schematic of the FE model and boundary conditions of the aspiration experiment at the start of the measurement. The bottom is constrained for horizontal and vertical displacement. The aspiration chamber only for horizontal displacement. The outer side of the tissue was allowed to move freely.

In Figure 10 the result of the FEA is shown. The colors correspond to the amount of displacement of the elements in the y-direction in meters according to the color bar below. Based on the displacement of the nodes of the tissue surface inside the aspiration chamber the volume of the aspirated tissue in the FEA was calculated.

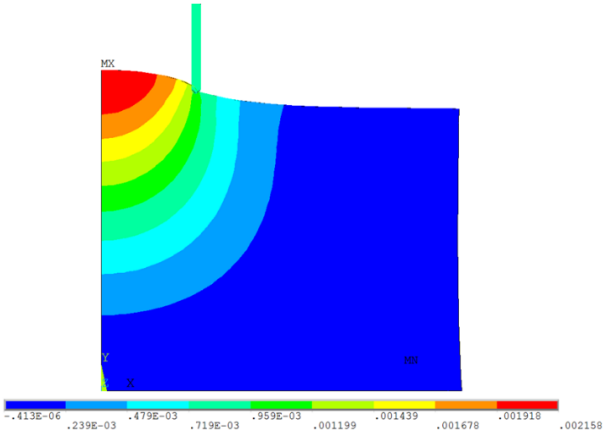


Figure 10: Result of the FEA. The colors correspond to the amount of displacement of the elements in the y-direction in meters.

### *4.4. Preliminary tests*

As mentioned in section 2.1, the human tongue can exhibit nonlinear, time-dependent, inhomogeneous and anisotropic behavior. It is therefore considered to be a viscoelastic material showing time-dependent strain. In other words, the rate at which the strain is applied affects the elastic response of the tissue. In order to investigate the effect of the aspiration rate (AR) on the volume versus pressure curve and to distinguish possible differences in the (visco)elastic response of the tissue, preliminary tests were done on three volunteers. Each subject was measured at an AR of 0.2, 0.4, 0.8 and 1.2 ml/min. For each AR the measurement was repeated three times and the average curve was calculated. The results of these preliminary test are shown in Appendix F. In conclusion, it seemed that the AR does not have a substantial effect on the tongue muscle elastic response while the subject is awake. Therefore, one fixed AR was chosen for the remainder of this study. For practical reasons, the AR was set at 0.6 ml/min. Although the wide spread observed in the pressure versus volume curves did not lead to a high variation in the Young's modulus, each subject will be measured ten times in order to calculate an accurate average curve for the FEA.

### *4.5. Measurements of healthy subjects*

During all measurements, the fully conscious was asked to position the tongue in a relaxed position at the floor of the mouth. Figure 11 shows how a measurement was performed. The aspiration chamber was first connected to a flexible tube followed by a rigid tube, which was fixed by a rigid holder close to the subject's mouth. The rigid tube reduces the systems compressibility, making it more robust. The rigid holder ensured no movement by external influences of the aspiration chamber once it was placed on the tongue. The flexible tube avoided the application of an external load to the aspiration chamber. This was to maintain an airtight connection with the tissue and to minimize the pressure on the tissue by the aspiration chamber itself.

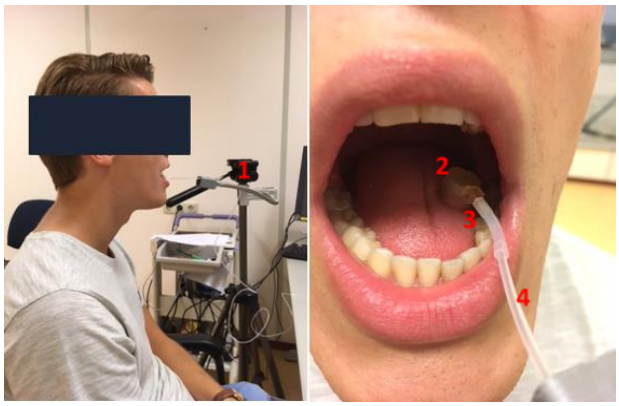


Figure 11: On the left, the position of the subject during a measurement is shown with a rigid holder close to the mouth (1). On the right, the positioning of the aspiration chamber (2) is shown, with the flexible tube (3) and rigid tube (4).

For each subject, a new rigid test was performed. The sample tests were performed immediately after the rigid test. Based on the results of the preliminary test each subject was measured ten times at an AR of 0.6 ml/min. The average curve of all ten measurements was used for the FEA. The aspiration experiment was performed on the apex of the tongue. The aspiration chamber was positioned left or right from the midline of the tongue. Left and right were considered equal, but the aspiration chamber was kept on the same spot for all measurements. The mouth could be partially closed as long as the tube and aperture were not touched or pressed on the tissue by the mouth itself. Intervals of around 30 seconds between each measurement were maintained to avoid possible stress softening or residual strain. Stress softening is observed when a soft sample is loaded, unloaded, and then reloaded in cycles and the required stress to get the same strain level decreases. Because of cyclic loading positive strain can be observed in an unloaded sample. This is known as residual strain.

### 4.6. Subject data

For this feasibility study, we included 16 healthy volunteers with an average age of 28.4±8 years. Subjects gave their informed consent to the experimental procedure as required by the Helsinki declaration (1964) and the local Ethics Committee (METC AVL – code 031). The subject characteristics can be found in Table 1. All volunteers can be divided by gender into two comparable groups. In total, we included 9 men and 7 women with an average age of 30±10 and 26±2.4 years, respectively.

Table 1: subject characteristics

| Subject | Age | Gender |
|---|---|---|
| H01 | 27 | M |
| H02 | 24 | M |
| H03 | 26 | M |
| H04 | 27 | M |
| H05 | 30 | M |
| H06 | 30 | F |
| H07 | 24 | F |
| H08 | 58 | M |
| H09 | 24 | M |
| H10 | 25 | F |
| H11 | 24 | M |
| H12 | 24 | F |
| H13 | 24 | F |
| H14 | 28 | F |
| H15 | 29 | F |
| H16 | 30 | M |

### 4.7. Data evaluation and statistics

In order to assess the repeatability of the procedure the intra rater repeatability was calculated using the intraclass correlation coefficient (ICC) with a mixed model. This way the reproducibility within each subject is assessed with one single observer. To evaluate possible differences between men or women, an unpaired t-test was performed. An F-test was performed to test if the variance of both distributions was equal. For the statistical tests, IBM SPSS Statistics 22 (IBM, Armonk, New York, USA) software was used.

## 5. RESULTS

For the remainder of this report, the aspirated tissue volume is depicted as a ratio of half a sphere volume.

### 5.1. Healthy volunteers

In Appendix H the results of the FEA on the mean curve of each subject is shown in Table 4. Including the Young's modulus $E$, the parameter $Jm$, the initial unknown tissue volume $V_{0,sample}$, and the $RSS$ of the fitting process. In Appendix G the same results of each individual measurement of each subject is shown. All subjects were measured ten times. However, in five of the volunteers, some measurements were excluded. When retrospectively inspecting the acquired curves, noise due to unwilling movement of the tongue was observed. For subject H03, H11, and H16 we obtained 9 measurements. Only 7 and 8 measurements were included for H08 and H12, respectively.

In Figure 12 the results of the fitting process of the FEA is shown for subject H01, H02, H04, and H05. The average tissue volume versus pressure curve of all 16 healthy volunteers can be seen in Figure 13. Most of the subject reached a tissue volume ratio of 0.5 at an average pressure between 12 and 20 millibars. In order to visualize the variation between the subjects a histogram was created, which can be seen in Figure 14.

An overall mean Young's modulus of 4.83 kPa with a standard deviation of 1.73 kPa was found. For the dimensionless parameter $Jm$ we found an average value of 0.32±0.11. Two subjects, H06 and H08, showed a remarkable higher pressure for aspirating the same tissue volume, i.e. showed stiffer behavior, which might indicate them as outliers.

When sorting the found Young's modulus $E$ from low to high, as seen in Figure 15, we observed that the parameter $Jm$ is decreasing. Also, the initial unknown tissue volume $V_{0,sample}$ becomes smaller. Note that the values for $Jm$ and $V_{0,sample}$ are depicted on the right y-axis.

Figure 16 shows all ten measurements including the average curve of subject H04 and H05. The curves of subject H04 are shown on the left. Among all subjects, subject H04 showed the smallest spread observed between all curves. On the right to the curves of subject H05 are shown, showing one of the widest spread that was observed in all subjects. In Figure 17 the corresponding histograms are shown. When looking at the curves in Figure 16 and the histograms in Figure 17, a higher variation in Young's modulus is seen for subject H05 with the widest spread and a much lower variation for subject H04 with the smallest spread. For subject H05 the curves reach the 0.5 volume ratio between 15 and 25 millibars. This seems to be a really wide spread and it could be expected to give very different Young's modulus

for each curve, but it is noteworthy that the standard deviation for the Young's moduli is only 0.69 kPa.

In order to check whether there is a difference in the calculated Young's modulus when taking the average of all measurements or by only taking the average curve and then performing the FEA, simulations were performed for all measurements of each subject. Comparing the mean Young's modulus of all measurements showed similar results as taking the average curve and then performing the FEA. In all subjects, performing an FEA on only the mean curve results in a slightly lower mean Young's modulus. The mean difference was 0.15±0.19 kPa.

### *5.2. Statistical analysis*

The ICC was 0.78 at a 5% significance level, which represents good agreement within each subject. For the unpaired t-test, a p-value was found of 0.64. at a 5% significance level, stating there is no significant difference between males and females in our cohort. The F-test gave a p-value of 0.85, i.e. no significant difference in variance was found between men or women.

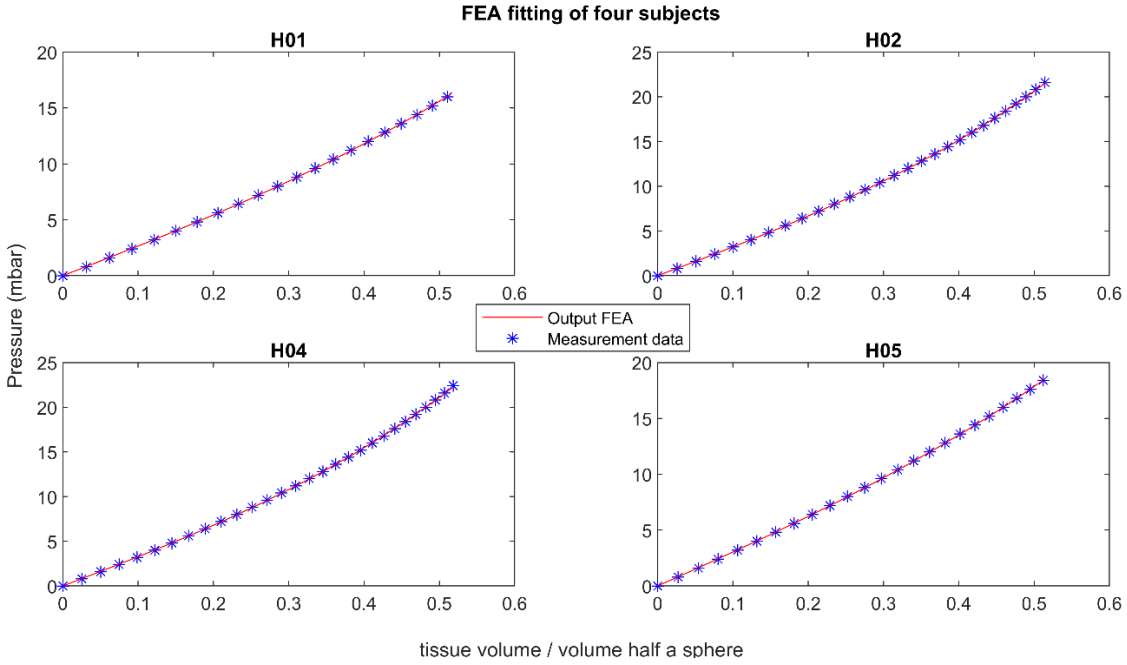


Figure 12: Result of the FEA fitting for four subjects.

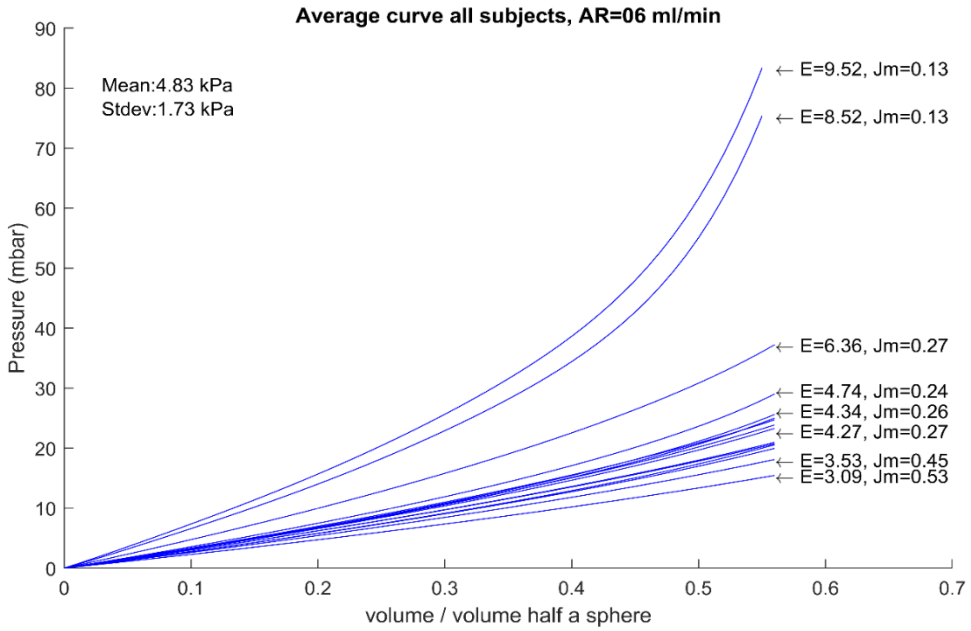


Figure 13: The mean tissue volume versus pressure curve of each subject.

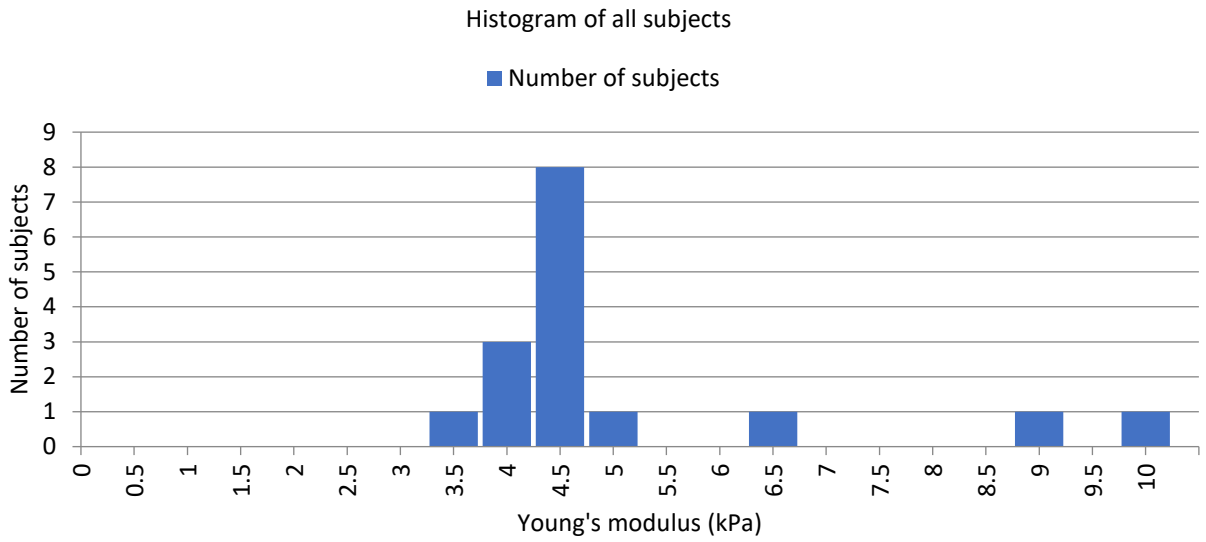


Figure 14: Histogram of estimated Young's modulus of all subjects.

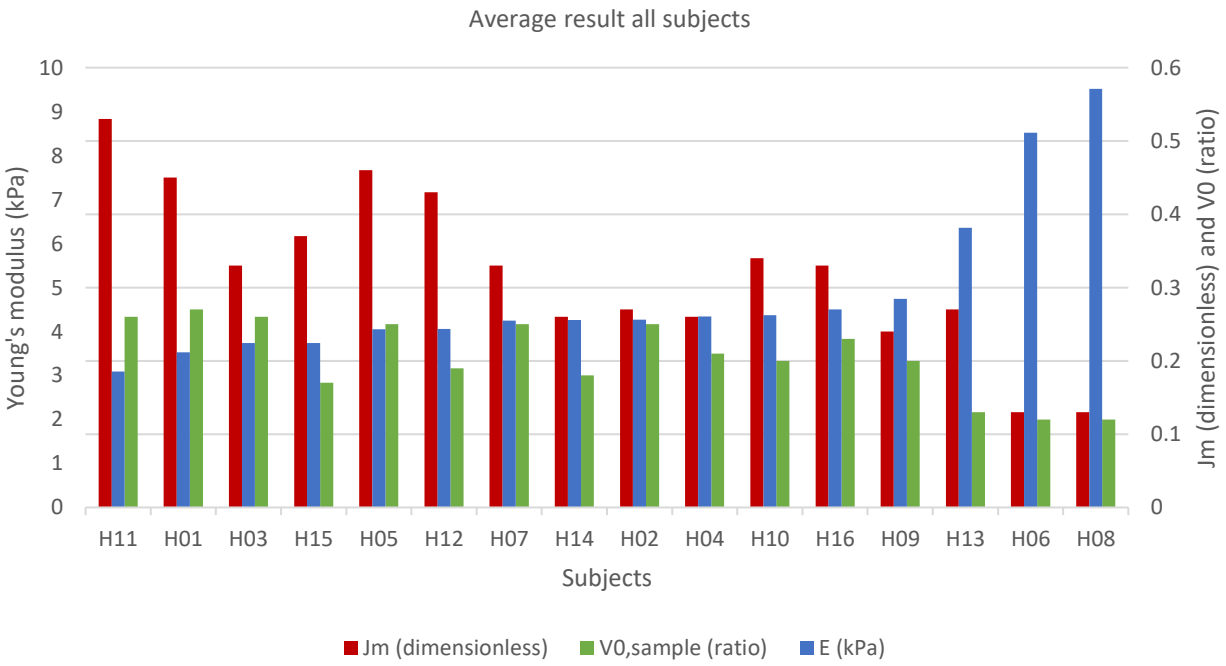


Figure 15: The Young's modulus of each subject blue from high to low is shown in blue and found on the left y-axis. The corresponding value of $Jm$, and $V_{0,sample}$ are shown in red and green, respectively, and are depicted on the right y-axis

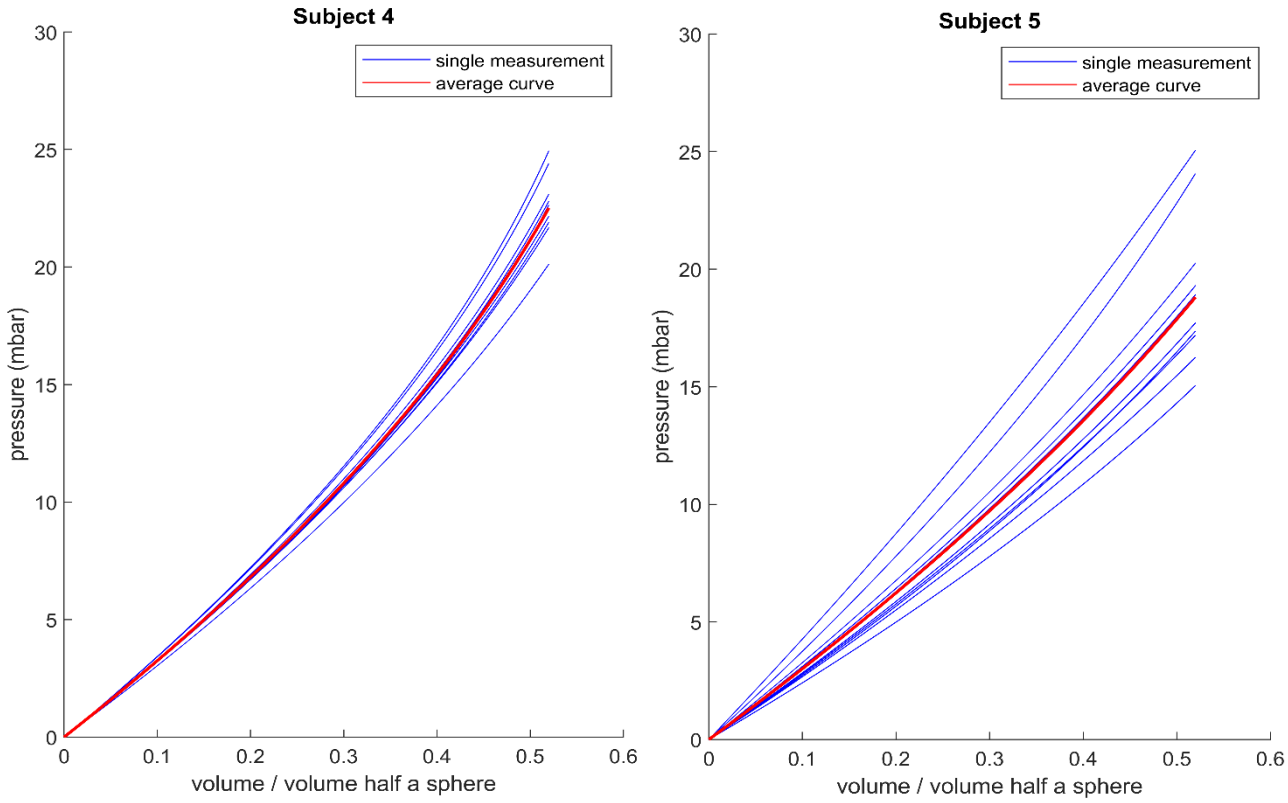


Figure 16: The tissue volume versus pressure curve of all measurements (blue) and the mean curve (red) for subject H04 on the left and H05 on the right.

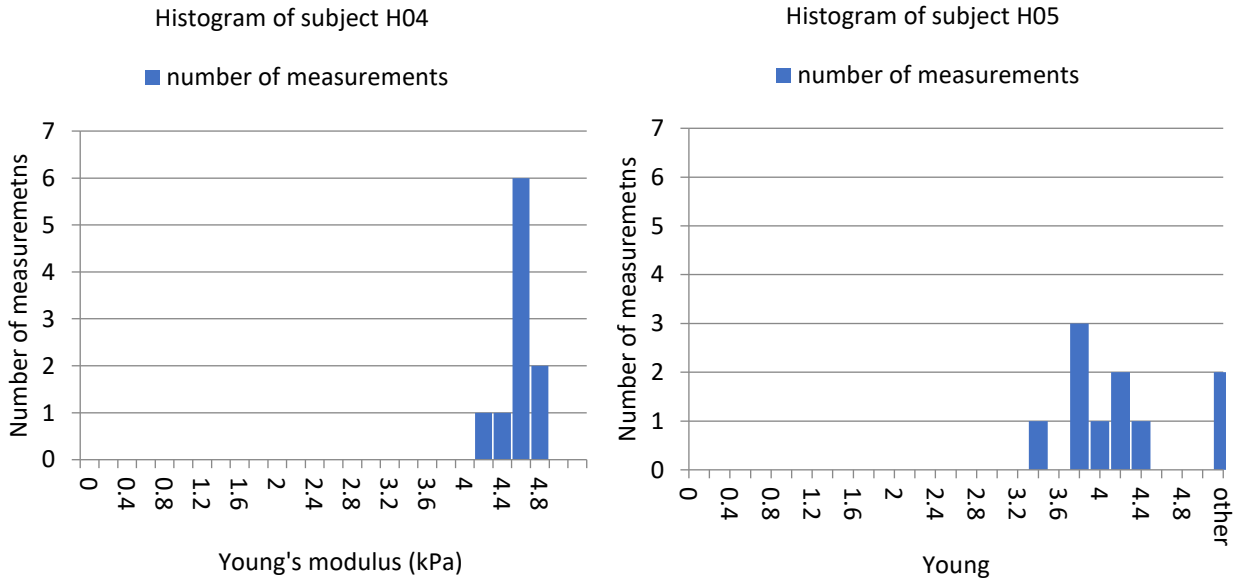


Figure 17: Histogram of estimated Young's modulus of all measurement for subject H04 (left) and H05 (right).

## 6. DISCUSSION

In this feasibility study, we showed the results of experiments on *in vivo* human tongue elasticity. The elastic properties of human tongue tissue of 16 healthy volunteers were estimated using a volume-based aspiration method. Coupled with an inverse FEA the Young's modulus of each measurement was provided. The results provided an estimation of the elastic behavior the tongue tissue. Based on our data we gained a lot of new insights regarding the measurement procedure as well as the FEA, which will be discussed in the following sections.

### *6.1. The Results*

The curves in Figure 16 and the results in the histograms in Figure 17, showed a higher variation for $E$ for subject H05 who showed the widest spread between the curves. A much lower variation for subject H04, who showed the smallest spread between the acquired curves, was seen. For subject H05 the curves reached the 0.5 volume ratio between 15 and 25 millibars. This seems to be a really wide spread and it could be expected to give very different Young's modulus for each curve, but the standard deviation for the Young's modulus is still relatively small at only 0.69 kPa. There are two possible explanations for having a wide spread but low standard deviations. First, there might be something wrong with the measurement protocol. All measurements were done within a short interval (30 seconds). Meaning there could be a buildup of tension within the tissue and attraction of fluid and therefore influencing the outcome of the consecutive measurement. The tissue should be completely recovered before the next measurement is started. However, the variation between the curves is completely random in all subjects. In Appendix G the results of all measurements of each subject is shown in chronological order. The response of the tissue is not becoming more elastic or stiff after consecutive measurements. We do not observe stress softening of residual strain effects. Also by visual inspection, the healthy *in vivo* tissue seemed to recover very quickly and no marks of the aperture were seen after a couple of seconds. So we believe our measurement protocol was not wrong. The second reason could be unwanted muscle contraction or movement of the tongue during the experiment. Subject H04 was able to keep the tongue real steady during all measurements and showed a small spread with only a standard deviation of 0.13 kPa. This strengthens the hypothesis that the variation in the acquired curves is caused more by unwilling tongue movement rather than the reproducibility of the experiment within short intervals. This assumption could be validated in our future study when a patient awake shows large differences between measurements and none when under general anesthesia.

Another explanation for a wide spread between the curves but a low standard deviation for the Young's modulus is the factor $Jm$. Since both parameters are used for the fitting process. One could argue that the factor $Jm$ should be the same in each subject, which would automatically lead to larger differences in the estimated Young's modulus. Since both parameters are unknown for tongue tissue both were used as input parameters for the FEA.

By taking the mean Young's modulus of all measurements we obtain similar results as by taking the average curve and then performing the FEA. In all subjects, performing an FEA on only the mean curve resulted in a slightly lower mean Young's modulus. However, the mean difference is only 0.15±0.19 kPa in comparison to taking the mean of al separate measurements. This is an acceptable difference in our opinion, since running an FEA on only the average curve will reduce the computational time tremendously.

Two of the measured subjects might be indicated as outliers. However, looking at the data there is no direct explanation for this behavior. No error was found in the rigid test. Although, a new rigid test was performed for each subject, each rigid test can be expected to give a nearly similar output for each subject. This was indeed the case. The next possibility could be an error in the sample test. The most likely error is that the initial volume inside the system was not equal between the rigid and sample test. In general when the aspiration experiment is started an immediate drop in pressure is observed and the measurement is started right after. Only when the measurement is started the aspirated volume over time is obtained. Sometimes it took some time before a drop in pressure was seen, probably because of leakage. In this case, the measurement should be restarted. Waiting for a drop in pressure and starting the measurement with a delay leads to an underestimation of the volume inside the system since the aspiration was already started. Eventually, this leads to a higher pressure at equal volumes compared to a correct measurement. It is unlikely this mistake was made ten times for these two subjects. Another explanation of why the two subjects showed a stiffer behavior is that a different part of the tongue was

measured. In Appendix I some additional test are included. One subject was measured on the body of the tongue as well. A similar steep curve for the body of the tongue, measured with an AD of 10 mm, was observed for the two possible outliers. Since the measurements were done while the mouth was partially closed, the two subjects could have systematically placed the aperture more to the body of the tongue instead of the apex, without the observer noticing. Therefore, the conclusion should either be that their measured tongue tissue is indeed stiffer or that the aspiration chamber was placed on the wrong part of the tongue. Unfortunately, the latter cannot be checked retrospectively

When sorting the found Young's modulus $E$ from low to high, as seen in Figure 15, we observed that in general the parameter $Jm$ is decreasing. Also, the initial unknown tissue volume $V_{0,sample}$ becomes smaller in general. Looking at the constitutive law of the Gent model this is what could be expected. For stiffer behavior, which is represented by a steeper and more progressive curve, the $Jm$ is lowered to simulate strain stiffening. Also, less tissue volume is aspirated for the same initial negative pressure when the tissue is stiffer.

The ICC showed satisfying results. The ICC showed good agreement between the measurements, stating that the reproducibility of the measurements within each subject is good. However, some caution is advised when interpreting the ICC because in our study only one observer performed the measurements. To perform the volume-based measurements efficiently with LASTIC some prior experience is required.

### *6.2. Comparison with literature*

For the first time, human tongue *in vivo* data was acquired on this scale. Due to a lack of *in vivo* measurements described in literature it is hard to make a fair with the comparison with the Young's modulus found in our study. Some similar experiments on tongue tissue elasticity were performed by Schiavone et al. 2008 on a tongue at rest. They found a shear modulus of 1.4 kPa, which equals to a Young's modulus of 5.2 kPa[22]. This is in line with the mean value we found, namely 4.83±1.73. Unfortunately, Schiavone et al. 2008 only performed two measurements on one volunteer. The constitutive law used for the FEA was an incompressible two parameter Yeoh strain-energy function, which could also have some influence on the found parameters. To test this, we performed several FEA using the same two parameter Yeoh strain-energy function. These results can be found in Appendix H in Table 7. The constitutive law of the Yeoh model provided similar results as the Gent model, which strengthens the agreement between both their study and our study.

One other study that provided *in vivo* data of the human tongue was performed by Cheng et al. 2011 Using MRE the elastic properties of 7 volunteers were assessed. They found an average Young's modulus of 8 kPa[23]. These results indicate a stiffer tissue than our results. However, in their study, the tongue was placed against the palate. This may have induced extra muscle tone, consequently leading to a higher stiffness. Also, in MRE the whole geometry of the tongue can be included in the measurements, whereas we only measured the apex of the tongue. With simple palpation techniques, it is observed that the apex is indeed softer than the body of the tongue. The latter is strengthened by our additional tests found in Appendix I. One subject was also measured on the body of the tongue and the results show indeed stiffer behavior.

### *6.3. Constitutive law and FEA*

The main aim of this study was not to provide a universal constitutive law of human tongue tissue elasticity. We wanted to show the results of rather difficult experiments on *in vivo* human tongue elasticity, performed for the first time on this scale. To describe the elastic behavior of biological material several constitutive laws were used in the past, like the Neo-Hookean solid or the Mooney-Rivlin solid strain-energy functions. But these do not describe experimental data adequately for non-crystallizing rubber at high values of strain in particular. Non-crystallizing rubber is a material soft tissue is often compared to. Both strain-energy models are not able to describe significant rapid rise in the stress versus strain curve in simple tension experiments[20]. Although we did not perform such measurements and set the maximum total strain at 50% (see section 4.2), severe strain stiffening may occur at even moderate stretches for biological materials[41]. To model strain stiffening several alternative models have been proposed with, for example, limiting chain extension, like the Gent model. Although the Gent model does not include viscoelastic behavior, it gave a good insight in the elastic response of tongue tissue. Updating both mechanical parameters of the Gent model using an optimization scheme provided adequate fits to the experimentally obtained volume versus pressure characteristic curves, as seen in Figure 12 and the low values for the $RSS$. No direct viscoelastic behavior, stress softening, and residual strain was observed in the

preliminary tests and between the measurements of the subjects. Looking at the dimensionless parameter $J_m$ we obtained and an average value 0.32±0.11. For rubber, typical values for the dimensionless parameter $J_m$ for simple extension range from 30 to 100 whereas for biological tissue, much smaller values of $J_m$ are appropriate. For human arterial wall tissue, for example, values between 0.4–2.3 have been suggested[42,43]. Our results are slightly lower as suggested for arterial wall tissue but in the same order of magnitude. Based on all the aforementioned we believe that our results and the Gent model gave a good estimation of the elastic properties of human tongue tissue elasticity.

The 2D FE model with axisymmetric conditions provided a comprehensive method to inversely analyze the performed experiment. Also, the computational power needed was low because of the 2D model and axis symmetric condition. One iteration took about 28 seconds on a workstation (Intel Xeon E3-1240 v3 3.4GHz., 16GB RAM). One could argue that a 3D FE model would provide a more realistic representation of the tongue geometry, but 3D models showed too similar results in the past to be worth the loss in computational time[17]. In the future, it is therefore recommended to use a 2D axisymmetric model for the FEA. However, some parts of the FE model and the inverse analysis could be improved. In future work, the same set of data obtained in the present study could be used to fit a more advanced elastic material model. Steps towards a more realistic representation of the experiments are already made and are described in section 7.3.

### *6.4. The volume-based technique*

As described in section 2.3, the volume based aspiration method has been tested extensively to assess its ability to estimate the aspirated tissue volume. Although the errors are close to zero when compared to a reference volume, the volume estimation is still very sensitive to errors when measuring human tissue. Before each measurement is started, an initial small negative pressure is applied to check the pressure stability and to asses if there is an airtight connection with no leakage. The initial aspirated tissue volume is therefore unknown. Therefore, based on phantom tests, it is advised to start with a really small negative pressure around 1 millibar[44]. This is feasible for the phantom test, where a phantom is a non-moving object. Unfortunately, unwilling movements of the tongue by the subjects were encountered during the experiments. To obtain a steady airtight connection between the tongue and the aspiration chamber each measurement had to start at pressure difference between -6 and -8 millibars. In order to predict the initial aspirated tissue volume, a second-order polynomial fit was used to extrapolate the data. Although this seems to give a good representation, it is yet another assumption that is made and probably affects the identification of the model parameters. Also, at low strain and pressure sometimes rapid stiffening of the material was observed. When looking at the data the average estimation of the initial volume was on average 0.21 of the shape ratio, this is about 42% of the aspiration limit (See Appendix H, Table 4). Meaning that almost half of the data used for the FEA is an estimation based on the acquired measurement points. To overcome this problem in the future it is advised to assess the lowest initial pressure possible to start per subject. Since it is mainly needed due to unwilling tongue movements. Another solution to get a more accurate estimation is to increase the maximum amount of aspirated volume and get more measurement points. We believe that the volume ratio of 0.5 of half a sphere is chosen with too much caution. During the measurements, no subject experienced unpleasant feelings or pain and the tissue recovered very quickly, without leaving any marks.

To have a neater methodology in the future the estimation of the constitutive law could be done with only the raw measurement data and the estimation of the initial tissue volume can be incorporated in the FEA. A first estimation can be done using the second order polynomial, which can then be used as an extra initial input parameter in the FEA. This method was proposed by Elahi et al. 2018[44], and has already been implemented and is discussed in section 7.3.

Besides these improvements, which can all be implemented in the future, the volume-based measurement technique has a lot of strong points as well. One is the continuous recording of the pressure data and the possibility of performing real-time measurement, allowing the rater to observe the aspirated tissue volume during the measurements. Also, our results showed a good reproducibility within the subjects. In addition, the phantoms tests of Elahi et al. 2018 showed good characterization of silicon phantoms using the same methodology[44]. These silicon phantoms are much stiffer than tongue tissue. This highlights LASTIC its ability to provide contrast between mechanical local behavior of different materials. Lastly, the current design of LASTIC overcomes most practical constraints we were facing during our measurements: the aspiration chamber is small and light; it can withstand the severe

sterilization process; measurements can be performed within short intervals; the whole device consists of a small setup with an aspiration pump, manometer, and a laptop. All of this complies with the limited time and space in the OR and the limited amount of space in the oral cavity. Also, the aspiration chamber and tubes to the aspiration pump are disposable and the additional hardware can be placed 1.5 meters from the patient at the OR. Based on the aforementioned we believe LASTIC is a very promising technique to identify the tongue tissue elastic properties and differences in the elastic properties for our purposes. Yet, it remains an estimation.

### *6.5. Other sources of errors*

Too high volume rate applied by the syringe pump can be a source of error due to viscoelastic behavior the system. Low enough volume rate should thus be used. Such a volume rate can be partially estimated during rigid tests performed and by ensuring that the volume rate has no effect on the obtained function $V_{rigid}^{total}$. This was not tested for our system. However, almost all connecting tubes were replaced with rigid tubes to reduce possible bias by viscoelastic behavior of the system itself.

Water vapor was sometimes observed on the surface of the aspiration chamber. A special hydrophilic treatment of the aspiration chamber should solve this issue.

The left and right side from the midline of the tongue were considered equal in healthy tongue tissue, we made no distinction. However, this could be investigated in several subjects. If there is indeed no difference we do not have to measure the same spot on one side each time but could switch from left to right to maintain a short interval and especially be sure that the tissue is recovered in between the measurements.

## 7. FUTURE PERSPECTIVES

### *7.1. Extend current results*

One hypothesis of our research team that is still not confirmed is that there is a difference in tongue elasticity between young and elder people. Aging brings structural and physiological changes to the tongue muscle[45,46], thus it is necessary to investigate if this affects the elasticity. Since the average age of the subjects was 28 years, the cohort with healthy subjects should be extended with more elder subjects (>50 years) to investigate this hypothesis.

The ability to provide contrast between mechanical local behavior of different materials by LASTIC was discussed before, but this feature will enable the creation of contrast maps on the tongue as well. The additional tests in Appendix I indicate that there is a difference in elasticity between the apex and the body of the tongue. Therefore, it would be very interesting to extend the number of measurement locations for several subjects to investigate this phenomenon and create a contrast map of the surface of the tongue. The subjects participating in this study agreed on being contacted again for future research when writing the informed consent. So, the same subject could be asked to participate in these additional experiments.

### *7.2. Additional tests and passive elasticity*

Before the study on the patient cohort starts we believe same additional tests may be wise considering the passive elasticity.

In the preliminary tests, the aspiration rate did not seem to have an effect on the elastic response of the tissue. These tests were performed while the subject was awake. The presence of muscle tonus could provide active resistance to the applied load on the tissue. It is unknown how the tissue will respond when a subject is under general anesthesia and almost no muscle tone is present. It is recommended to perform additional tests with different aspiration rates on the first three subjects as well, i.e. investigate the effect of the aspiration rate on the passive elastic response of the tissue.

Also, due to the lack of muscle tone, it expected that tissue recovery takes longer. Therefore, the interval between the measurements should be reconsidered as well.

### *7.3. FE model and inverse analysis*

In our FEA the pressure was applied on the tissue surface that was initially inside the aperture. The aspirated tissue volume was then calculated based on the displacement of the apex height of the tissue in the y-direction. But, the tissue was allowed to move in the x-direction as well. So, gliding between the aspiration chamber and tissue might have occurred, i.e. other elements possibly intruded in the aspiration chamber from the side. Meaning that only taking the displacement in the y-direction might not properly define the final shape of the tissue inside the aspiration chamber. The effect of this on the eventually calculated tissue volume is unknown. Therefore, it might be wise to also include the

displacement in the x-direction for the calculation of the tissue volume in the future as well. Since the applied pressure remained on only the initial surface in the aperture, the nodes that intrude the aperture should be takin in consideration as well. This way the final surface shape is completely used for calculating the tissue volume instead of only the deformed shape in the y-direction.

We assumed, because of the superficial measurements and small strains, that the bottom layer could be constrained for horizontal and vertical displacements. We assumed that the bottom of the tissue would not be affected by the load applied on the surface. This known as the Saint-Venant principle, which states that the effect of the applied load on a surface will disappear throughout the loaded sample. A rule of thumb, or acceptable approach, is that the distance between the surface on which the load is applied and the bottom of the sample should at least be as large as the largest dimension of the loaded surface. The aperture radius was 5 mm in our model and the distance to the bottom was 15 mm. This is three times the dimension of the loaded surface. However, one could argue that the apex of the tongue *in vivo* is not constrained in any direction and that the bottom layer should be able to move freely. This was tested and unfortunately, the FEA failed because of a wrong constraint model. The stress applied to the sample became too high in several places and also at the bottom. This means that the Saint-Venant principle does not apply for our FE model. This is very unfortunate because it should be. Therefore, we are currently developing a new FE-model in which the tissue can move freely in all dimensions but the Saint-Venant principle still applies, even for the relatively thin apex of the tongue. This model is not yet finished.

The friction between the aspiration chamber and the tongue is unknown and based on an assumption. Because the tongue is wet and a subject can produce saliva between the measurements the friction coefficient is considered low, 0.2 to be exact, in the FEA. In the past, the friction coefficient has proven to have a small impact on the results[44]. Elahi et al. 2018 compared the characterization of two silicon phantoms using a friction coefficient of 0 and 1. For the studied friction coefficients μ=[0, 1]) they showed errors of [8.8, 5.6]% for one phantom and [6.6, 4.1]% for the other. So it expected to have a small impact but yet proper checking of the effect of the friction coefficient could be wise for future work.

In the current biomechanical tongue model of the Virtual Therapy project in ArtiSynth, a five parameter Mooney-Rivlin hyperelastic strain energy function is used to describe the elastic behavior of the tongue. However, the last three mechanical parameters are equal to zero. Meaning that practically we are only using a two-parameter Mooney-Rivlin model. This model is not able to describe the progressive curves as observed in our experiments. Therefore this model should either be adapted with the right material parameters or be extended with more. The latter will definitely increase the computational time since the number of iterations needed to get a good fit between the FEA and the experiment will increase with more parameters. It is advised to perform some FEA on our current data to check if large differences are observed. If not, it is advised to use the robust Gent model. Praised by its simplicity, yet its effectiveness.

The identification of $V_{0,sample}$ with the FEA as mentioned in section 6.4 was tested. The results are shown in Appendix H in Table 5. In Figure 39 the results of the FEA fitting are shown for the same four subjects as in Figure 12, only now the raw measurement data was used and $V_{0,sample}$ as extra input parameter for the FEA. The difference between the estimation of $V_{0,sample}$ with extrapolation versus the identification in the FEA, are shown in Table 6. It can be seen that $V_{0,sample}$ only differs slightly. This indicates that the extrapolation is a good method to estimate $V_{0,sample}$. However, the absolute difference for the Young's modulus was on average 0.79 kPa. This is higher than expected, and it indicates that there is no unique solution for the FEA when incorporating $V_{0,sample}$ as extra parameter. To estimate a range for the solutions provided by the FEA will take a lot of time using a direct inverse FEA procedure for each measurement. To overcome the long computational time one could use a library of prearranged FE simulations results. The $RSS$, or other cost function, could then be used to give a range of satisfactory results for the Young's modulus and the parameter $Jm$.

### *7.4. Measuring fibrotic tissue*

The elastic properties of the tongue are strongly influenced by fibrotic changes after treatment. In order to predict movements and load-bearing tasks of the tongue and to present the individual treatment effects on mastication, swallowing, and speech, fibrosis and other effects on tissue elasticity should be studied

closely. To extend the biomechanical tongue with elastic properties of fibrotic tissue is, therefore, essential in the future for the Virtual Therapy project. The ability to provide contrast between mechanical local behavior of different materials by LASTIC has been proven in previous studies and our study. Assuming that fibrotic tissue is at least some kilopascal stiffer than healthy tissue it should be possible to identify the elastic properties of fibrotic tissue as well.

Since LASTIC is used for superficial measurements, a cohort with patients who underwent a partial glossectomy is most suitable to investigate fibrosis. One of the major constraints that we could be facing is obtaining an airtight connection with the tissue. If fibrotic tissue is too stiff this could give problems. In the past, ultrasonic gel was used on phantoms to improve the airtight connection. Biocompatible gel or even glue could solve this problem in human trials.

### *7.5. User Recommendations*

In order to use the volume-based aspiration method, the user should take several considerations into account. Some of them are already mentioned but here an overview will be given:

1. Special attention should be paid to prevent any leakage in both the rigid and sample test. Before any test, a small initial negative pressure $P_0$ should be applied and its stability over time should be checked. For the rigid test, a fixture apparatus with an undeformable surface should be used. The use of ultrasonic gel contributes to a better airtight connection with a deformable surface as well.
2. The initial pressure $P_0$ should be really small compared to the pressure range of the measurement. In soft material like tongue tissue, this is an arduous task because of unwilling tongue movements and consequently losing the airtight connection. Therefore, it is advised to assess the lowest initial pressure possible per subject
3. To avoid potential effects of the temperature on the error, the main and rigid tests should be performed in the same environment and within a short interval.
4. On the OR sterilized conditions are required during the sample test. To be able to estimate the aspirated tissue volume real-time the rigid test should be performed before the main test. But, to avoid any possible system contamination it advised to use a generic calibration file. i.e. rigid volume curve, for the OR for each measurement. Since the environmental conditions on the OR are kept as constant as possible this should not affect the real-time measurement a lot. Then, after performing all sample measurements, a rigid test can be done for that specific moment and subject. Since the aspiration chamber and the connected tube are disposable, one could perform the rigid test before the sample tests. But this would require two tubes and two aspiration chambers, which is in our opinion a waste of material and sterilization costs.
5. The use of a rigid holder for the aspiration chamber, as seen in Figure 11, would be advisable in order to avoid applying external load on aspiration chamber

## 8. CONCLUSION

In conclusion, we can state that the results presented in this report gave a good initial estimation of the elastic behavior tongue tissue. Although the Gent model does not include viscoelastic behavior, it provided great insight in what the elastic properties might be. Also, we obtained a lot of data which can be evaluated using different material models in the future as well. The design of LASTIC and its ability to provide contrast between the mechanical local behavior of different materials, makes it a very promising and feasible technique to measure the elastic properties of the human tongue. We consider LASTIC to be a suitable technique for our future purposes. Therefore, we believe the first step towards extending the biomechanical tongue model of the Virtual Therapy project was made.

## 9. REFERENCES


1. Dutch Head and Neck Oncology Cooperative Group of the Association of Comprehensive Cancer Centres, Utrecht the N. National guideline, version 1.4, 2004. www.oncoline.nl. Accessed February 20, 2006.

2. IKNL. Nederlandse Kankerregistratie. www.cijfersoverkanker.nl. Published 2018. Accessed December 12, 2016.

3. Rosebush MS, Kishan Rao S, Samant S, et al. Oral cancer: enduring characteristics and emerging trends. *J Tenn Dent Assoc*. 2011;91(2):24.

4. Blot WJ, McLaughlin JK, Winn DM, et al. Smoking and drinking in relation to oral and pharyngeal cancer. *Cancer Res*. 1988;48(11):3282-3287.

5. Neville BWDD, Allen CM, Bouquot JE. *Oral and Maxillofacial Pathology*. St. Louis, MO.; 2009.

6. da Silva SD, Ferlito A, Takes RP, et al. Advances and applications of oral cancer basic research. *Oral Oncol*. 2011;47(9):783-791.

7. Van Alphen MJA. *Towards a Predictive Model for Functional Loss after Oral Cancer Treatment*. University of Twente; 2015. doi:10.3990/1.9789036539173

8. Weber C, Dommerich S, Pau HW, Kramp B. Limited mouth opening after primary therapy of head and neck cancer. *Oral Maxillofac Surg*. 2010;14(3):169-173. doi:10.1007/s10006-010-0220-2

9. Warnakulasuriya S. Global epidemiology of oral and oropharyngeal cancer. *Oral Oncol*. 2009;45(4–5):309-316. doi:http://dx.doi.org/10.1016/j.oraloncology.2008.06.002

10. Funk GF, Karnell LH, Christensen a. J. Long-term Health-Related Quality of Life in Survivors of Head and Neck Cancer. *Arch Otolaryngol - Head Neck Surg*. 2012;138(2):123-133. doi:10.1001/archoto.2011.234

11. Dwivedi RC, Kazi RA, Agrawal N, et al. Evaluation of speech outcomes following treatment of oral and oropharyngeal cancers. *Cancer Treat Rev*. 2009;35(5):417-424. doi:10.1016/j.ctrv.2009.04.013

12. Kreeft AM. *Functional Inoperability of Oral And*. University of Amsterdam; 2013.

13. Kreeft A, Tan IB, Van Den Brekel MWM, Hilgers FJ, Balm AJM. The surgical dilemma of "functional inoperability" in oral and oropharyngeal cancer: Current consensus on operability with regard to functional results. *Clin Otolaryngol*. 2009;34(2):140-146. doi:10.1111/j.1749-4486.2009.01884.x

14. Schiavone P, Promayon E, Payan Y. LASTIC: A light aspiration device for in vivo soft tissue characterization. *Lect Notes Comput Sci (including Subser Lect Notes Artif Intell Lect Notes Bioinformatics)*. 2010;5958 LNCS(January 2010):1-10. doi:10.1007/978-3-642-11615-5_1

15. Lloyd JE, Stavness I, Fels S. ArtiSynth: A Fast Interactive Biomechanical Modeling Toolkit Combining Multibody and Finite Element Simulation. *Soft Tissue Biomech Model Comput Assist Surg*. 2012:355-394. doi:10.1007/8415_2012_126

16. Wells PNT, Liang H-D. Medical ultrasound: imaging of soft tissue strain and elasticity. *J R Soc Interface*. 2011;8(64):1521-1549. doi:10.1098/rsif.2011.0054

17. Deram A, Luboz V, Promayon E, Payan Y. Using a 3D biomechanical model to improve a light aspiration device for in vivo soft tissue characterisation. *Comput Methods Biomech Biomed Engin*. 2012;15(sup1):41-43. doi:10.1080/10255842.2012.713711

18. Hermant N, Perrier P, Payan Y. *Human Tongue Biomechanical Modeling*. Elsevier Inc.; 2017. doi:10.1016/B978-0-12-804009-6.00019-5

19. Puglisi G, Saccomandi G. The Gent model for rubber-like materials: An appraisal for an ingenious and simple idea. *Int J Non Linear Mech*. 2015;68:17-27. doi:10.1016/j.ijnonlinmec.2014.05.007

20. Horgan CO. The remarkable Gent constitutive model for hyperelastic materials. *Int J Non Linear Mech*. 2015;68:9-16. doi:10.1016/j.ijnonlinmec.2014.05.010

21. Gérard J-M, Ohayon J, Luboz V, Perrier P, Payan Y. Non-linear elastic properties of the lingual and facial tissues assessed by indentation technique: application to the biomechanics of speech production. *Med Eng Phys*. 2005;27(10):884-892.

22. Schiavone P, Boudou T, Promayon E, Perrier P, Payan Y. A light sterilizable pipette device for the in vivo estimation of human soft tissues constitutive laws. *Conf Proc Annu Int Conf IEEE Eng Med Biol Soc IEEE Eng Med Biol Soc Conf*. 2008;2008(May 2014):4298-4301. doi:10.1109/IEMBS.2008.4650160

23. Cheng S, Gandevia SC, Green M, Sinkus R, Bilston LE. Viscoelastic properties of the tongue and soft palate using MR elastography. *J Biomech*. 2011;44(3):450-454.

24. Hollenstein M, Jabareen M, Breitenstein S, et al. Intraoperative mechanical characterization of human liver. In: *PAMM: Proceedings in Applied Mathematics and Mechanics*. Vol 9. Wiley Online Library; 2009:83-86.

25. Sigrist RMS, Liau J, Kaffas A El, Chammas MC, Willmann JK. Ultrasound elastography: Review of techniques and clinical applications. *Theranostics*. 2017;7(5):1303-1329. doi:10.7150/thno.18650

26. Carter FJ, Frank TG, Davies PJ, McLean D, Cuschieri A. Measurements and modelling of the compliance of human and porcine organs. *Med Image Anal*. 2001;5(4):231-236.

27. Samur E, Sedef M, Basdogan C, Avtan L, Duzgun O. A robotic indenter for minimally invasive measurement and characterization of soft tissue response. *Med Image Anal*. 2007;11(4):361-373.

28. Yao W, Yoshida K, Fernandez M, et al. Measuring the compressive viscoelastic mechanical properties of human cervical tissue using indentation. *J Mech Behav Biomed Mater*. 2014;34:18-26.

29. Brown JD, Rosen J, Kim YS, Chang L, Sinanan MN, Hannaford B. In-vivo and in-situ compressive properties of porcine abdominal soft tissues. *Stud Health Technol Inform*. 2003:26-32.

30. Agache PG, Monneur C, Leveque JL, De Rigal J. Mechanical properties and Young's modulus of human skin in vivo. *Arch Dermatol Res*. 1980;269(3):221-232.

31. Badir S, Mazza E, Bajka M. Objective assessment of cervical stiffness after administration of misoprostol for intrauterine contraceptive insertion. *Ultrasound Int open*. 2016;2(2):E63.

32. Diridollou S, Patat F, Gens F, et al. In vivo model of the mechanical properties of the human skin under suction. *Ski Res Technol*. 2000;6(4):214-221.

33. Elahi SA, Connesson N, Payan Y. Disposable system for *in-vivo* mechanical characterization of soft tissues based on volume measurement. *j mech med biol*. 2018;18(04):1850037. doi:10.1142/s0219519418500379

34. Khazaka, Courage. Cutometer. https://www.courage-khazaka.de/index.php/en/products/scientific/140-cutometer. Accessed February 1, 2018.

35. Vuskovic V. Device for in-vivo measurement of mechanical properties of internal human soft tissues. 2001.

36. Badir S, Bajka M, Mazza E. A novel procedure for the mechanical characterization of the uterine cervix during pregnancy. *J Mech Behav Biomed Mater*. 2013;27:143-153.

37. Nava A, Mazza E, Furrer M, Villiger P, Reinhart WH. In vivo mechanical characterization of human liver. *Med Image Anal*. 2008;12(2):203-216.

38. Schiavone P, Chassat F, Boudou T, Promayon E, Valdivia F, Payan Y. In vivo measurement of human brain elasticity using a light aspiration device. *Med Image Anal*. 2009;13(4):673-678. doi:10.1016/j.media.2009.04.001

39. Wu Y, Van der Schaft DWJ, Baaijens FP, Oomens CWJ. Cell death induced by mechanical compression on engineered muscle results from a gradual physiological mechanism. *J Biomech*. 2016;49(7):1071-1077.

40. Oomens CWJ, Bader DL, Loerakker S, Baaijens F. Pressure induced deep tissue injury explained. *Ann Biomed Eng*. 2015;43(2):297-305.

41. Holzapfel GA. Similarities between soft biological tissues and rubberlike materials. *Const Rubber IV*. 2005;(March):607-617. http://www.biomech.tugraz.at/images/pdf/Holzapfel-Constitutive_Models_for_Rubber_IV-2005.pdf.

42. Goriely A, Destrade M, Ben Amar M. Instabilities in elastomers and in soft tissues. *Q J Mech Appl Math*. 2006;59(4):615-630. http://dx.doi.org/10.1093/qjmam/hbl017.

43. Horgan CO, Saccomandi G. A description of arterial wall mechanics using limiting chain extensibility constitutive models. *Biomech Model Mechanobiol*. 2003;1(4):251-266. doi:10.1007/s10237-002-0022-z

44. Elahi SA, Connesson N, Chagnon G, Payan Y. In-vivo soft tissues mechanical characterization: volume-based aspiration method validated on silicones. *Exp Mech (under Revis*. 2018;(October).

45. Bennett JW, Van Lieshout PHHM, Steele CM. Tongue control for speech and swallowing in healthy younger and older adults. 2007.

46. Bässler R. Histopathology of different types of atrophy of the human tongue. *Pathol Pract*. 1987;182(1):87-97.

47. Dalley. KLM and AF. *Clinically Oriented Anatomy*. 6th ed. Wolters Kluwer Health/Lippincott Williams & Wilkins; 2009.

48. McGinty B. Continuum Mechanics. www.continuummechanics.org.

49. Sarvazyan AP, Urban MW, Greenleaf JF. Acoustic waves in medical imaging and diagnostics. *Ultrasound Med Biol*. 2013;39(7):1133-1146. doi:10.1016/j.ultrasmedbio.2013.02.006

50. Wells PNT. *Scientific Basis of Medical Imaging*. Churchill Livingstone; 1982.

51. Shiina T, Nightingale KR, Palmeri ML, et al. WFUMB guidelines and recommendations for clinical use of ultrasound elastography: Part 1: Basic principles and terminology. *Ultrasound Med Biol*. 2015;41(5):1126-1147. doi:10.1016/j.ultrasmedbio.2015.03.009

52. Computerized Imaging Reference Systems Inc. - A Castleray Company. CIRS Tissue Simulation & Phantom Technology. 2017.

53. Member NR, Member KN. using a 2D Matrix Ultrasound Array. 2013;32(9):1671-1684. doi:10.1109/TMI.2013.2262948.Imaging

54. Topp KA, Brien WDO, Topp KA, Brien WDO. Anisotropy of ultrasonic propagation and scattering properties in fresh rat skeletal muscle in vitro Anisotropy of ultrasonic propagation and scattering properties in fresh rat skeletal muscle in vitro. 2017;1027(2000). doi:10.1121/1.428282

55. Kreeft AM, Van Der Molen L, Hilgers FJ, Balm AJ. Speech and swallowing after surgical treatment of advanced oral and oropharyngeal carcinoma: A systematic review of the literature. *Eur Arch Oto-Rhino-Laryngology*. 2009;266(11):1687-1698. doi:10.1007/s00405-009-1089-2

56. Virtual Therapy for head & neck cancer - prediction of functional loss.

57. Van Alphen MJA, Kreeft AM, Van Der Heijden F, Smeele LE, Balm AJM. Towards virtual surgery in oral cancer to predict postoperative oral functions preoperatively. *Br J Oral Maxillofac Surg*. 2013;51(8):747-751. doi:10.1016/j.bjoms.2013.06.012

58. Tang A, Cloutier G, Szeverenyi NM, Sirlin CB. Ultrasound elastography and MR elastography for assessing liver fibrosis: Part 2, diagnostic performance, confounders, and future directions. *Am J Roentgenol*. 2015;205(1):33-40. doi:10.2214/AJR.15.14553

59. Nightingale KR, Soo MS, Nightingale RW, Trahey GE. Acoustic radiation force impulse imaging: in vivo demonstration of clinical feasibility. *Ultrasound Med Biol*. 2002;28(2):227–235. doi:10.1016/S0301-5629(01)00499-9

60. Philips Healthcare. Shear Wave elastography. Simplify liver disease assessment. http://www.usa.philips.com/healthcare/resources/feature-detail/shear-wave-elastography.

61. ECHOSENS™. Echosens, the liver company.

62. ECHOSENS™. FibroScan - The reference solution for non-invasive liver diagnosis.

63. Roulot D, Czernichow S, Le Clésiau H, Costes J-L, Vergnaud A-C, Beaugrand M. Liver stiffness values in apparently healthy subjects: influence of gender and metabolic syndrome. *J Hepatol*. 2008;48(4):606-613. doi:10.1016/j.jhep.2007.11.020

64. Castera L, Forns X, Alberti A. Non-invasive evaluation of liver fibrosis using transient elastography. *J Hepatol*. 2008;48(5):835-847. doi:10.1016/j.jhep.2008.02.008

65. Giovanna Ferraioli, Carlo Filice, Laurent Castera et al. WFUMB Guidelines and recommendations for clinical use of ultrasound elastography: Part 3: Liver. 2015:Vol. 41, No. 5, pp. 1161–1179.

66. © AICBT Ltd 2017. Al- Therapy Statistics.

## 10. APPENDICES:

### APPENDIX A: ANATOMY OF THE TONGUE

The tongue is a muscular hydrostat that fills the oral cavity. As a mobile organ, it is mainly responsible for licking, articulation, and squeezing food into the oropharynx as part of swallowing. It is positioned partly in the oral cavity and partly in the oropharynx and can be distinguished into an apex or tip, body, and root. Depending on the sex and size of a subject the tongue volume varies between 60-80 $cm^3$, with a length of around 10 cm and a maximum width of 5 cm. The density of the tongue is close to 1, so its weight varies between 60-80 g[18].

The body of the tongue is the anterior part and roughly two-thirds of the tongue between the root and the apex. The body of the tongue is the most essential part for good swallowing and articulation. The posterior one third is the tongue root and essential for the propulsion of the food bolus into the oropharynx.

The tongue contains four intrinsic and four extrinsic muscles. The intrinsic tongue muscles (superior and inferior longitudinalis, transversalis and verticalis) are entirely attached within the tongue and not to any bone. They are mainly responsible for altering tongue shape. In Figure 18 the main three extrinsic muscles are shown. The four extrinsic muscles of the tongue (genioglossus, hyoglossus, styloglossus, and palatoglossus) are attached to the other intrinsic or extrinsic muscles in the tongue but have their origin outside the tongue. Their main function is moving the tongue, but they can alter its shape as well. The main intrinsic muscles are shown in Figure 19. In Table 2 an overview is shown of all muscles and their origin, insertion, and function.

The cranial nerve XII or hypoglossal nerve is responsible for the innervation of all intrinsic and extrinsic tongue muscles. The palatoglossus is the only exception and is innervated by the pharyngeal nerve. The tongue muscles are vascularized by the lingual artery, which arises from the external carotid artery [47].

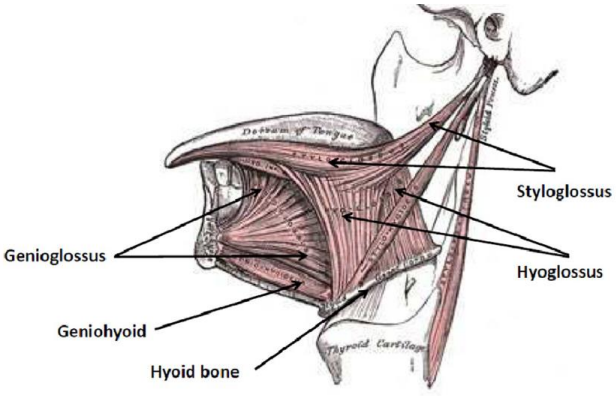


Figure 18: Lateral view of the three main extrinsic muscles of the tongue. The anterior part of the tongue is on the left. The Geniohyoid is shown as well, it connect the mandibula and the hyoid bone as part of the mouth floor. *Image retrieved from Herman et al. 2017.*

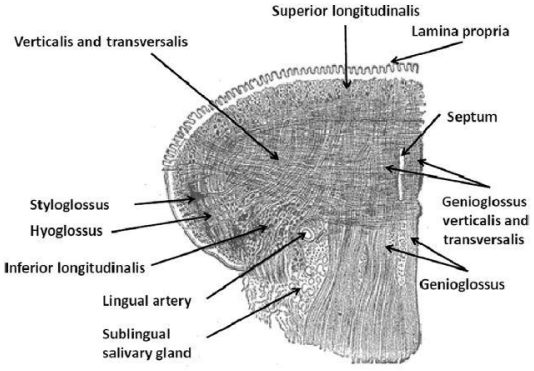


Figure 19: Anterior cut of the tongue showing the main extrinsic and intrinsic muscles. The center of the tongue is on the right, marked by the septum. *Image retrieved from Herman et al. 2017.*

Table 2: Overview of the origin, insertion, and function of the eight tongue muscles.

| Muscle | Origin (proximal attachment) | Insertion (distal attachment) | Function |
|---|---|---|---|
| **Intrinsic muscles** | | | |
| **Superior longitudinalis** | Submucosal fibrous layers and septum | Margins of the tongue and mucous membrane | Shortens tongue; elevating apex and sides of tongue; curls apex upward longitudinally |
| **Inferior longitudinalis** | Hyoid bone and root of the tongue | Apex of the tongue | Shortens tongue; depressing apex; curls apex down longitudinally |
| **Transversalis** | Septum | Fibrous tissue at lateral lingual margins | Elongates and narrows the tongue |
| **Verticalis** | Submucosal fibrous layer of dorsum of the tongue | Inferior surface of borders of the tongue | Broadens and flattens the tongue |
| **Extrinsic muscles** | | | |
| **Genioglossus** | Mental spine of mandible | Lateral and inferior tongue | Depressing and elongating of the tongue |
| **Hyoglossus** | Body and greater horn of hyoid | Inferior aspects of lateral part of the tongue | Depressing and retraction of the tongue |
| **Styloglossus** | Styloid and stylohyoid ligament | Sides of the tongue posteriorly, inter-digitating with the hyoglosses | Retraction of the tongue; curls sides |
| **Palatoglossus** | Palatine aponeurosis of soft palate | Post lateral tongue | Elevating posterior tongue |

The introduction below is mainly derived and summarized from www.continuummechanics.org. Which is written by Bob McGinty[48]. For more information, I would recommend visiting this page.

**Deformation tensors and Invariants**

A tensor is a mathematical object that can be used to describe physical properties. It is a matrix but because it describes a physical property it is called a tensor. In fact, tensors are merely a generalization of scales and vectors. The rank of a tensor is defined by the number of directions, hence the dimensionality of the matrix. A scalar is a zero rank tensor, a vector is a first rank tensor, and a deformation tensor is a second rank tensor.

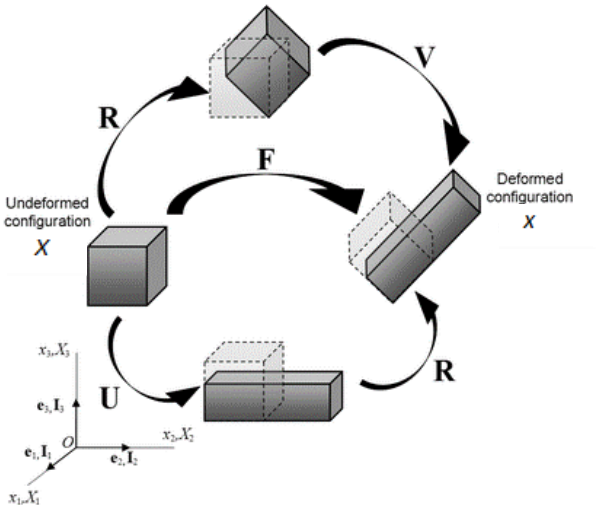


Figure 20: Representation of a deformation of a 3D object. The polar decomposition of the deformation gradient **F** is shown as well. **X** is referred to as the undeformed state and **x** as the deformed state. The symbols $x_1$, $x_2$ , and $x_3$ describe the three direction in which deformation is possible. *Source*: *https://commons.wikimedia.org/wiki/File:Polar_decomposition_of_F.png (adapted version)*

In Figure 20 a representation of a cubic object is shown in a 3D coordinate system on the left. The symbols are now explained step by step. The deformation gradient **F** is the derivative of each component of the deformed vector **x** with respect to each component of the reference vector **X**, i.e. original state. For $\mathbf{x} = \mathbf{x}(\mathbf{X})$, the deformation tensor is as follows:

$$F_{ij} = x_{ij} = \frac{\partial x_i}{\partial dX_j} = \begin{bmatrix} \frac{\partial x_1}{\partial dX_1} & \frac{\partial x_1}{\partial dX_2} & \frac{\partial x_1}{\partial dX_3} \\ \frac{\partial x_2}{\partial dX_1} & \frac{\partial x_2}{\partial dX_2} & \frac{\partial x_2}{\partial dX_3} \\ \frac{\partial x_3}{\partial dX_1} & \frac{\partial x_3}{\partial dX_2} & \frac{\partial x_3}{\partial dX_3} \end{bmatrix} \quad (9)$$

The symbols $x_1$, $x_2$ , and $x_3$ describe the three direction in which deformation is possible. The deformation of an object can be divided in different deformations 1) rigid body translations 2) rigid body rotations 3) combined deformations and rotations. To explain this, simple 2D examples will be used to make it easier to grasp the concepts. Note that $x_{ij}$ represents the new state, i.e. deformed configuration, and $X_{ij}$ the reference state, i.e. undeformed configuration. For 2D deformations the deformation tensor **F** can be rewritten as:

$$F_{ij} = x_{ij} = \frac{\partial x_i}{\partial dX_j} = \begin{bmatrix} \frac{\partial x_1}{\partial dX_1} & \frac{\partial x_1}{\partial dX_2} \\ \frac{\partial x_2}{\partial dX_1} & \frac{\partial x_2}{\partial dX_2} \end{bmatrix} \quad (10)$$

Here $x_1$ represent the transformation in x-direction for a given node in the FE model and $x_2$ in the y-direction. The deformation tensor for the x direction is defined as:

$$x = \frac{\partial x_1}{\partial dX_1} + \frac{\partial x_1}{\partial dX_2} \quad (11)$$

And for the y direction as :

$$y = \frac{\partial x_2}{\partial dX_1} + \frac{\partial x_2}{\partial dX_2} \quad (12)$$

**Rigid body translations**

In Figure 21 an example is shown of rigid body translation.

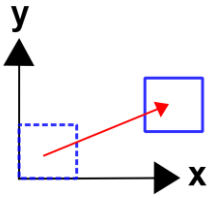


Figure 21: Schematic of rigid body translation

The reference square is translated 5 units in the x-direction and 2 units in the y direction:

$$\begin{aligned} x &= X + 5 \\ y &= Y + 2 \end{aligned} \quad (13)$$

**Rigid body rotations**

In Figure 22 a schematic overview of a rigid body rotation is shown.

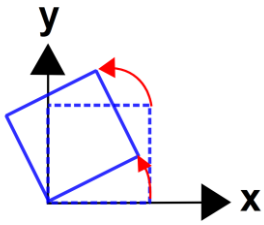


Figure 22: Schematic of rigid body rotation

The rotation is counter-clockwise so the new x and y positions are defined as follows:

$$\begin{aligned} x &= X\cos\theta - Y\sin\theta \\ y &= X\sin\theta + Y\cos\theta \end{aligned} \tag{14}$$

The deformation tensor **F** becomes :

$$\mathbf{F} = \begin{bmatrix} \cos\theta & -\sin\theta \\ \sin\theta & \cos\theta \end{bmatrix} \tag{15}$$

**Simple transformations**

In this section, three simple transformations will be explained: stretching, shearing with rotation and shearing without rotation.

In Figure 23 stretching is shown.

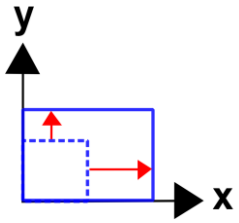


Figure 23 Schematic of stretching

Stretching is observed in both the x and y directions. The following equations describe a 100% elongation in the x-direction and a 50% elongation in the y-direction:

$$\begin{aligned} x &= 2.0X + 0.0Y \\ y &= 0.0X + 1.5Y \end{aligned} \tag{16}$$

The deformation tensor **F** becomes:

$$\mathbf{F} = \begin{bmatrix} 2.0 & 0.0 \\ 0.0 & 1.5 \end{bmatrix} \tag{17}$$

Note that all off-diagonal components are zero. The component $\frac{\partial x_1}{\partial dX_1}$ of the tensor in equation 10 reflects elongation in the x-direction and $\frac{\partial x_2}{\partial dX_2}$ reflects elongation in the y-direction.

In Figure 24 an example of shear with rotation is shown.

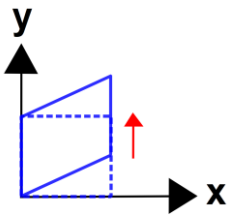


Figure 24: Schematic of shearing with rotation

The elongations in the x and y-direction are 0% but each node for a given location at (x,y), is transformed by increasing each y-value with 50% of the original x-value according to the following equations:

$$\begin{aligned} x &= 1.0X + 0.0Y \\ y &= 0.5X + 1.0Y \end{aligned} \tag{18}$$

The deformation tensor **F** becomes:

$$\mathbf{F} = \begin{bmatrix} 1.0 & 0.0 \\ 0.5 & 1.0 \end{bmatrix} \tag{19}$$

The non-zero off-diagonal value reflects shearing. Figure 24 also shows that the square tends to rotate counter-clockwise. This is reflected in the deformation gradient by the fact that it is not symmetric.

In Figure 25 an example of pure shear is shown.

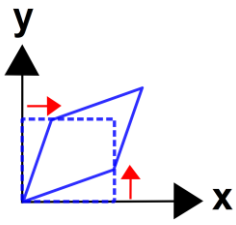


Figure 25: Schematic of shearing without rotation

The elongations in the x and y-direction are 0% but each node for a given location at (x,y), is transformed by increasing each x-value with 50% of the original y-value and each y-value with 50% of the original x-value according to:

$$\begin{aligned} x &= 1.0X + 0.5Y \\ y &= 0.5X + 1.0Y \end{aligned} \tag{20}$$

The deformation tensor **F** becomes:

$$\mathbf{F} = \begin{bmatrix} 1.0 & 0.5 \\ 0.5 & 1.0 \end{bmatrix} \tag{21}$$

The non-zero off-diagonal values mean that shearing is present. The fact that **F** is symmetric reflects that there is no net rotation. The zero net rotation arises from the

fact that while the lower right area of the square tends to rotate counter-clockwise, the upper left area tends to rotate clockwise simultaneously. Therefore, the net rotation for the square as a whole is zero.

**Combined deformations and rotations**

In Figure 26 an object is transformed from a square to the position shown with the arrows.

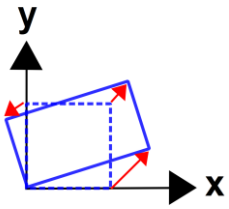


Figure 26: Schematic of a square that is first deformed and then rotated.

The equations to perform this transformation are :

$$\begin{aligned} x &= 1.300X - 0.375Y \\ y &= 0.750X + 0.650Y \end{aligned} \tag{22}$$

And the corresponding deformation tensor **F** is :

$$F = \begin{bmatrix} 1.300 & -0.375 \\ 0.750 & 0.650 \end{bmatrix} \tag{23}$$

Based all the aforementioned transformation and rotations we can say, based on the deformation tensor, that object has been stretched and rotated. However, the rotations do not contribute to stress, but the deformation does. Therefore, it is necessary to extract both mechanisms out of **F** in order to determine the stress and strain state. This can be done by polar decomposition. This will be explained later on, but for now, we just accept that the transformation is done in two steps: first a deformation followed by a rotation. The deformation, in this case, is a 50% stretch in the x-direction and a 25% compression in the y-direction. If **x'** is the intermediate state between both steps we can define the deformations equations as follows :

$$\begin{aligned} x' &= 1.50X + 0.00Y \\ y' &= 0.00X + 0.75Y \end{aligned} \tag{24}$$

The second step to rotate the intermediate **x'** state, in this case with 30° counterclockwise:

$$\begin{aligned} x &= x'\cos(30) - y'\sin(30) = 0.866x' - 0.500y' \\ y &= x'\sin(30) + y'\cos(30) = 0.500x' + 0.866y' \end{aligned} \tag{25}$$

If we write equation 24 and 25 in matrix form, we get a rotation matrix:

$$\begin{Bmatrix} x \\ y \end{Bmatrix} = \begin{bmatrix} 0.855 & -0.500 \\ 0.500 & 0.866 \end{bmatrix} \begin{Bmatrix} x' \\ y' \end{Bmatrix} \tag{26}$$

And a matrix to describe the deformation:

$$\begin{Bmatrix} x' \\ y' \end{Bmatrix} = \begin{bmatrix} 1.50 & 0.00 \\ 0.00 & 0.75 \end{bmatrix} \begin{Bmatrix} X \\ Y \end{Bmatrix} \tag{27}$$

The deformation tensor **F** can be written as the product of the two matrices: a rotation matrix, and a symmetric matrix to describe the deformation :

$$\mathbf{F} = \begin{bmatrix} 0.866 & -0.500 \\ 0.500 & 0.866 \end{bmatrix} \begin{bmatrix} 1.50 & 0.00 \\ 0.00 & 0.75 \end{bmatrix} = \begin{bmatrix} 1.300 & -0.375 \\ 0.750 & 0.650 \end{bmatrix} \tag{28}$$

This product is commonly written as:

$$\mathbf{F} = \mathbf{R} \cdot \mathbf{U} \tag{29}$$

Where **R** is the rotation matrix, and **U** is the right strain tensor. This order of transformations is shown in Figure 20 at the bottom. As one can see at the top the same new configuration can be achieved by rotating first, and then deforming it. In our example of Figure 26 this is shown in Figure 27:

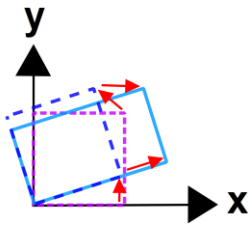


Figure 27: Schematic of a square that is first rotated and then deformed to get the same state as in Figure 26.

In this case, the reference state **X** is first rotated to get the intermediate state **x'** according to:

$$\begin{aligned} x' &= X\cos(30) - Y\sin(30) \\ y' &= X\sin(30) + Y\cos(30) \end{aligned} \tag{30}$$

Then the intermediate state is deformed to get the final state:

$$\begin{aligned} x &= 1.313x' + 0.325y' \\ y &= 0.325x' + 0.938y' \end{aligned} \tag{31}$$

We can see, based on the off-diagonal values, that now the object is being sheared in addition to being stretched and compressed. The deformation tensor **F** is now written as:

$$\mathbf{F} = \begin{bmatrix} 1.313 & 0.325 \\ 0.325 & 0.938 \end{bmatrix} \begin{bmatrix} 0.866 & -0.500 \\ 0.500 & 0.866 \end{bmatrix} = \begin{bmatrix} 1.300 & -0.375 \\ 0.750 & 0.650 \end{bmatrix} \tag{32}$$

This is commonly written as:

$$\mathbf{F} = \mathbf{V} \cdot \mathbf{R} \tag{33}$$

Where $\mathbf{R}$ is the rotation matrix, and $\mathbf{V}$ is the left strain tensor. In each example, the rotation is the same. It's important to understand that the deformations are also the same. They only appear to be different because one is imposed before rotation, the other after.

**Polar decomposition and Invariants**

In these simple examples, the two matrices were known. To subtract them from the deformation tensor $\mathbf{F}$ one can use polar decomposition. Combining this with the product of the matrix $\mathbf{F}$ its transpose gives a surprising result:

$$\mathbf{F} \cdot \mathbf{F}^T = (\mathbf{V} \cdot \mathbf{R}) \cdot (\mathbf{V} \cdot \mathbf{R})^T = \mathbf{V} \cdot \mathbf{R} \cdot \mathbf{R}^T \cdot \mathbf{V}^T \tag{34}$$

And because the transpose of the rotation matrix is equal to the inverse, the product of $\mathbf{R} \cdot \mathbf{R}^T$ becomes $\mathbf{R}^{-1} \cdot \mathbf{R} = \mathbf{I}$, where I is an identity matrix. Therefore, equation 34 becomes:

$$\mathbf{F} \cdot \mathbf{F}^T = \mathbf{V} \cdot \mathbf{R} \cdot \mathbf{R}^T \cdot \mathbf{V}^T = \mathbf{V} \cdot \mathbf{V}^T \tag{35}$$

One can see here that the rotation matrix, $\mathbf{R}$, has been eliminated from the equation. The next step is to find $\mathbf{V}$ from $(\mathbf{V} \cdot \mathbf{V}^T)$, but this is out of the scope of this report. The result $(\mathbf{V} \cdot \mathbf{V}^T)$ is called the left Cauchy Green deformation tensor, i.e. strain tensor. Alternatively, one can perform the operation for equation 35 to obtain the right Cauchy-Green deformation tensor $\mathbf{F}^T \cdot \mathbf{F} = \mathbf{U}^T \cdot \mathbf{U}$.

The Gent model expresses the strain energy in terms of the invariant of the left Gauchy-Green strain tensor, which are expressed in functions of stretch, i.e. strain, ratios.

As stated before the product of the deformation tensor with its transpose, results in a symmetric matrix. This makes it possible to calculate the principal values, i.e. principal stretches/strains. The principal stretches for $\mathbf{V}$ are:

$$\mathbf{V}_{pr} = \begin{bmatrix} \left(\Delta L / L_0\right)_1 & 0 & 0 \\ 0 & \left(\Delta L / L_0\right)_2 & 0 \\ 0 & 0 & \left(\Delta L / L_0\right)_3 \end{bmatrix} \tag{36}$$

If the ratios $\left(\Delta L / L_0\right)_i$ are replaced with the symbol $\lambda_i$, called stretch ratios, the tensor becomes:

$$\mathbf{V}_{pr} = \begin{bmatrix} \lambda_1 & 0 & 0 \\ 0 & \lambda_2 & 0 \\ 0 & 0 & \lambda_3 \end{bmatrix} \tag{37}$$

Therefore, the principal stretches of the left Cauchy-Green strain tensor are:

$$(\mathbf{V} \cdot \mathbf{V}^T)_{Pr} = \begin{bmatrix} \lambda_1^2 & 0 & 0 \\ 0 & \lambda_2^2 & 0 \\ 0 & 0 & \lambda_3^2 \end{bmatrix} \tag{38}$$

Because it is a symmetric tensor it contains three invariants $I_1$ , $I_2$, and $I_3$:

$$\begin{aligned} I_1 &= \mathrm{tr}\left(V \cdot V^T\right) = \lambda_1^2 + \lambda_2^2 + \lambda_3^2 \\ I_2 &= \lambda_1^2\lambda_2^2 + \lambda_2^2\lambda_3^2 + \lambda_1^2\lambda_3^2 \\ I_3 &= \det(V \cdot V^T) = \lambda_1^2\lambda_2^2\lambda_3^2 \end{aligned} \tag{39}$$

The Gent model includes only the first invariant. It is called invariants because no matter what coordinate transformation you apply to the strain tensor, its principal strains do not change.

The invariants are not zero in undeformed state, i.e. when the strain is zero. When no stress is applied $\lambda_i = 1$ . Therefore, the undeformed state gives $I_1 = 3$, $I_2 = 3$, and $I_3 = 1$ For incompressible material $I_3$ will always equal 1. The invariant $I_3$ represents the physical measure for volume change, so it cannot reflect any deformation state since its value never changes. This leaves $I_1$ and $I_2$ to describe the deformation. Even for nearly incompressible materials $I_3$ is often left out of the model. The physical interpretation of the first invariant of a strain tensor it that $I_1$ is directly related to the hydrostatic component of the tensor. The hydrostatic strain is simply the average of all three principal stretches. For this report it is sufficient to know that the hydrostatic strain is closely related to volume changes when the strains are small. The confusing aspect of hydrostatic strain is that it can be nonzero in incompressible materials. This is because the hydrostatic strain is more a mathematical construct than a direct physical measure of volume and its change. After all, the true measure for volume change is the determinant of the deformation gradient, i.e. the invariant $I_3$ . When the strain is small the hydrostatic strain is only a convenient approximation.

## APPENDIX C: EXPLANATION VOLUME BASED MEASUREMENTS

During the *in vivo* and *in situ* test, the system is simply composed of a syringe pump, a manometer and an aspiration chamber (Figure 3). The volume is aspirated by the syringe pump with an adjustable rate in milliliters per minutes, which was kept fixed during both experiments, and the corresponding pressure is measured over time. However, the aspirated volume by the syringe pump is different from the aspirated tissue volume. The difference is mainly caused by volume changes in the system due to the applied pressure and that the system volume is compressible due to air expansion and the elasticity of the components (connections, tubes, syringe, etc).

In order to calculate the aspirated tissue volume, two tests are performed. The first test is to experimentally assess the system volume function using an undeformable material, referred to as the rigid test. The result of this test completely depends on the volume inside the system during aspiration.

The behavior of the pressure and volume inside the system can be described according to the general gas equation of Boyle and Gay-Lussac which is as follows:

$$P \cdot V = nRT \tag{40}$$

With

$P$ = pressure in Pascal

$V$ = volume in $m^3$

$n$ = amount of gas in mole

$R$ = ideal gas constant

$T$ = Temperature in Kelvin

It states that the relationship between pressure $P$ times volume $V$ depends on the amount of gas $n$ in mole, the gas constant $R$ and the temperature $T$. Since the rigid and main/sample test are performed within a short interval we assume that the temperature $T$ is constant. Therefore, equation 40 can be rewritten to the law of Boyle-Mariotte:

$$P \cdot V = c \tag{41}$$

Where $c$ is a constant. Meaning that with a constant amount of gas and a constant temperature the pressure of a gas becomes directly proportional to the volume.

During the *in vivo* tests, the system volume is not constant, but proportionally increasing over time due to a fixed AR. In Figure 28 and Figure 29 a schematic overview of the rigid test is shown. Figure 28 shows the system at the start of the rigid test. Here $P_0$ represents the pressure outside the system, i.e. the atmospheric pressure. At this point, the initial pressure inside the system is equal to the atmospheric pressure $P_0$. The atmospheric pressure is considered constant during the test. The initial volume inside the system, i.e. volume inside the tubes and aspiration chamber, is defined as $V_0$ .

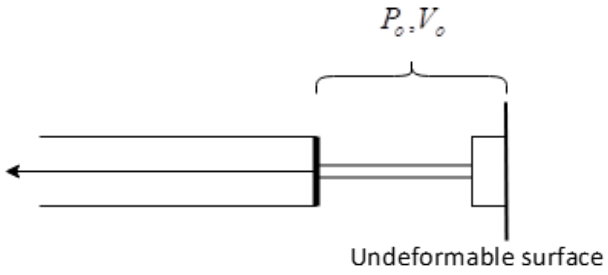


Figure 28: Schematic representation before the rigid test is started. The arrow represents the syringe and the direction it is pulled.

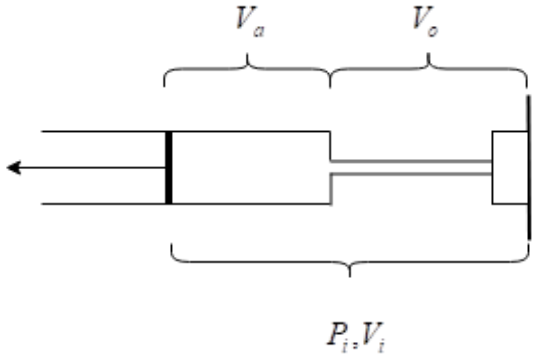


Figure 29: Schematic representation at a given point during the rigid test. The arrow represents the syringe and the direction it is pulled.

Figure 29 shows the system during the rigid test. During the aspiration test, the total volume inside the system, represented by $V_i$, increases over time. The system volume can thus be defined as:

$$V_i = V_0 + V_a \tag{42}$$

Where $V_a$ is the aspirated volume. According to the law of Boyle-Mariotte, the pressure should decrease with an increasing volume. With $P_i$ as the new pressure inside the system, the change in pressure which is given by the manometer is defined as:

$$\Delta P = P_0 - P_i \tag{43}$$

Substituting our model in the law of Boyle-Mariotte gives:

$$P_0 \cdot V_0 = c \tag{44}$$

And:

$$P_i \cdot V_i = c \tag{45}$$

Therefore:

$$P_i \cdot V_i = P_0 \cdot V_0 \tag{46}$$

Substituting equation 42 and 43 in equation 46 gives:

$$(P_0 - \Delta P) \cdot (V_0 + V_a) = P_0 \cdot V_0 \tag{47}$$

Thus, $\Delta P$ can be defined as follows:

$$-\Delta P = \frac{P_0 \cdot V_0}{V_0 + V_a} - P_0 = \frac{P_0 \cdot V_0}{V_0 + V_a} - \frac{P_0 \cdot (V_0 + V_a)}{V_0 + V_a} = \frac{-P_0 \cdot V_a}{V_0 + V_a} \tag{48}$$

This can be rewritten as:

$$\Delta P_{rigid} = \frac{P_0 \cdot V_a}{V_0 + V_a} = \frac{P_0 \cdot V_a}{V_i} \tag{49}$$

Which gives the relationship between the change in pressure and the atmospheric pressure, aspirated volume, and system volume at any given time point during the rigid test.

For the second test, referred to as the main or sample test, a tissue sample is introduced as shown in Figure 30.

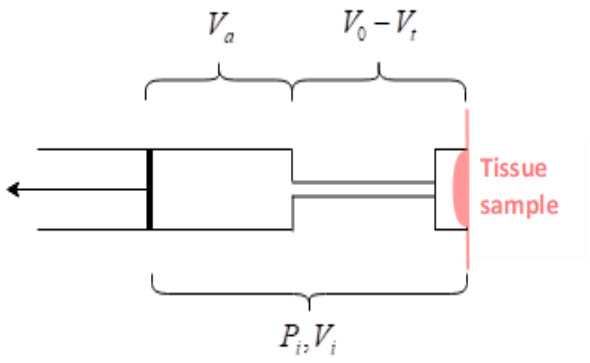


Figure 30: Schematic representation at a given point during the main test. The arrow represents the syringe and the direction it is pulled.

Again the same law is applied as in the rigid test, but the volume $V_i$ is influenced by the aspirated tissue volume $V_t$. Since the latter intrudes the volume of the system during the test $V_i$ is redefined as:

$$V_i = V_0 + V_a - V_t \tag{50}$$

Following the same steps as in (44-49) the change in pressure during the main test is as follows:

$$\Delta P_{main} = \frac{P_0 \cdot V_a - P_0 \cdot V_t}{V_0 + V_a - V_t} = \frac{P_0 \cdot V_a - P_0 \cdot V_t}{V_i} \tag{51}$$

Both (49) and (51) are experimentally assessed by measuring the change in pressure and the corresponding aspirated volume by the syringe. It is assumed that $P_0$ and $V_0$ are constant during both tests since they are performed within a short interval.

According to the ideal gas law $V_i$ should be the same at equal pressures for (49) and (51). So at a given $\Delta P$ for both tests, the volume inside the systems is as follows:

$$\begin{aligned} V_i^{rigid} &= V_i^{main} \\ V_0 + V_a^{rigid} &= V_0 + V_a^{main}{}_a - V_t \\ V_a^{rigid} &= V_a^{main} - V_t \end{aligned} \tag{52}$$

According to equation 52, it is reasoned that $V_a^{main} > V_a^{rigid}$ at equal $\Delta P$ for equation 49 and 51 and that the aspirated tissue volume as a function of the change in pressure can be defined as:

$$V_t(\Delta P) = V_a^{main}(\Delta P) - V_a^{rigid}(\Delta P) \tag{53}$$

In Figure 31 an overview is shown on how $V_t$ is calculated based on the two assessed curves. In section 2.3 a short explanation is given. For clarity reasons here $\Delta P$ is referred to as just $P$, because this is the only pressure measured and is directly provided by the manometer.

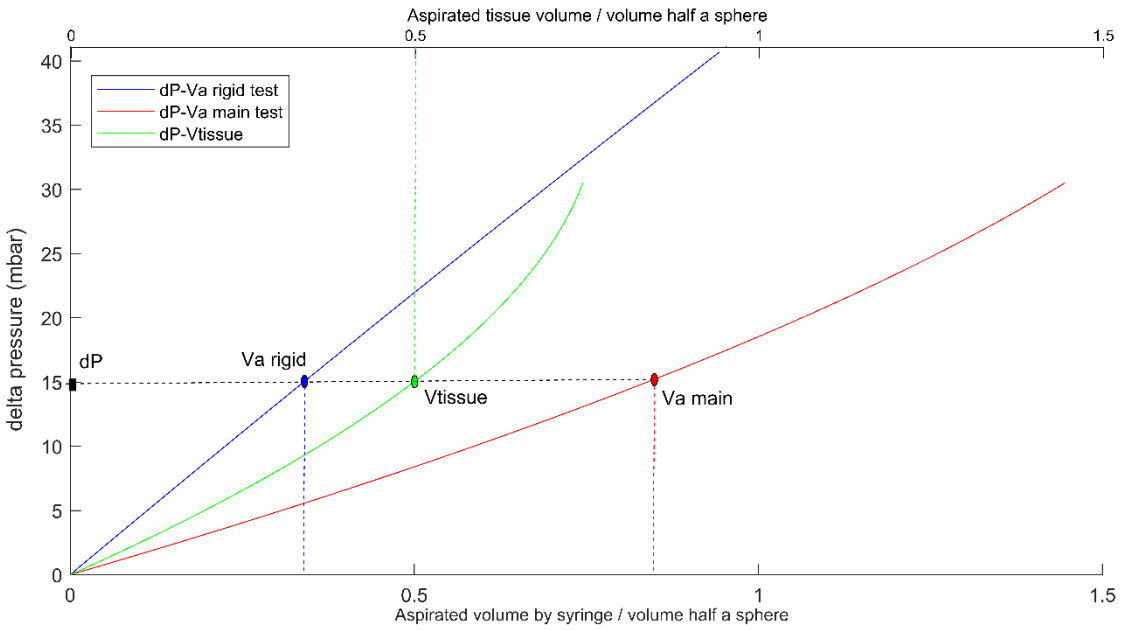


Figure 31: Overview of the experimental assessed rigid test curve (blue) and main test curve (red). The bottom x-axis represents the aspirated volume by the syringe and belongs to the volume versus pressure curve of the rigid test (blue) and the curve of the main test (red). The top x-axis represents the aspirated tissue volume and belongs to the aspirated tissue volume curve depicted in green. The tissue volume curve is calculated according to equation 53.

| # | Risico | Potentiele gevolgen | Potentiele oorzaken | Risico gradering | Vangnet tijdens evaluatie | Rest risico evaluatie | Vangnet uiteindelijk product | Opmerkingen |
|---|---|---|---|---|---|---|---|---|
| 1 | Patiënt ervaart pijn | Negatieve ervaring voor patiënt, weefselschade | Aspiratie vervormd het weefsel teveel,<br>Verschillend pijngrens per patiënt. | 1 | Druk kan volledig en direct verwijderd worden door een klep te openen. Zuignap zal losraken | 0 | Hetzelfde als tijden de evaluatie. Mocht dit teveel gebeuren dan is een ander ontwerp van de zuignap misschien nodig. Denk aan een rubbertje zodat de zuignap zachter is aan de onderkant en minder scherp aanvoelt op het weefsel. | In theorie zal een pijn ervaring alleen voor kunnen komen als de patiënt een lage pijngrens heeft. Door het real-time meetsysteem is het risico van teveel weefsel aspireren gereduceerd tot een uiterst minimum. |
| 2 | Zuignap schiet lost uit de tube | Zuignap valt in mondholte en misschien wel in de trachea of oesophagus | Suboptimale bevestiging | 2 | Tijdens alle experimenten is dit nog nooit gebeurd. De tube zit namelijk erg strak om het verbindstuk van de zuignap heen. | 0 | Extra controle moment voor het plaatsen van de zuignap op het weefsel, zo zijn we er zeker van dat de bevestiging goed is. | Na het controle moment en het starten van de meting zal de kans alleen nog maar kleiner worden door de onderdruk die ontstaat. |
| 3 | Hygiëne | Ontsteking | Niet goed gedesinfecteerd | 1 | Zuignap is disposable, en worden van te voren machinaal gedesinfecteerd. Dit is een gevalideerd proces. | 0 | Idem | De mondholte is van zichzelf al een nest vol bacteriën. Steriel maken van het zuignapje is daardoor niet nodig. Een gedesinfecteerde zuignap zal wat hygiëne betreft geen extra risico's met zich meebrengen. |
| 4 | Trauma tijdens meting | Weefselschade / bloeduitstorting | Teveel weefsel aspireren, hierdoor wordt de druk te hoog en de deformatie te groot | 2 | Real-time metingen en gefixeerd volume of basis van de literatuur. Zie uitleg hierboven | 0 | Idem. | |

## APPENDIX E: REEVALUATION OF ESTIMATING THE INITIAL TISSUE VOLUME

Before a measurement is started an airtight connection between the tissue and aspiration chamber is obtained by creating an initial negative pressure within the aspiration chamber. Consequently, some initial and unknown tissue volume is aspirated. For real-time measurements, a software tool was developed that automatically estimates the initial tissue volume using a linear estimation based on the slope of the first ten measurement points.

The real-time measurement tool provides two outputs. First, the analyzed data where the initial volume is already estimated using the linear estimation. Secondly, the raw measurement data without any estimation yet. Based on the raw data the total volume, i.e. total aspirated volume $V^{total}$ according to equation 4 in section 2.3, can be calculated at the corresponding pressure points. For the silicon phantom, linear estimation works very accurately because of the linear elastic response of the material for small deformations. Human tissue is known to show nonlinear behavior and therefore the initial tissue volume estimation was reevaluated.

In Figure 32 the linear estimation of the initial tissue volume is shown. To smoothen the data a second-degree polynomial fit is calculated through the measurement points.

In Figure 33 the estimation of the initial total volume is done using the raw data output. The raw data is extrapolating to a pressure equal to zero using a second-degree polynomial fit.

Looking at the tissue volume curve in Figure 32, it seems that linear estimation is not necessarily wrong since the curve seems to show a gradual progress. However, when looking more closely at the curve and comparing it with the extrapolated tissue volume curve the flaw becomes very clear. In Figure 34 both tissue volume curves are shown. It can be seen that the blue curve, i.e. the tissue volume with linear estimation, has not a gradual process and the slope of the initial tissue volume at approximately a volume ratio of 0.15 is significantly steeper than the part between 0.15 and 0.3. This means that the linear estimation is highly likely to provide an underestimation of the initial tissue volume. Also, the shape of the curve complicates the fitting of the FEA. The tissue volume curve with after extrapolation of the initial global volume in red shows a gradual process throughout the whole curve. Therefore, the initial volume was estimated by extrapolating the raw total volume first before calculating the tissue volume curve and running the FEA.

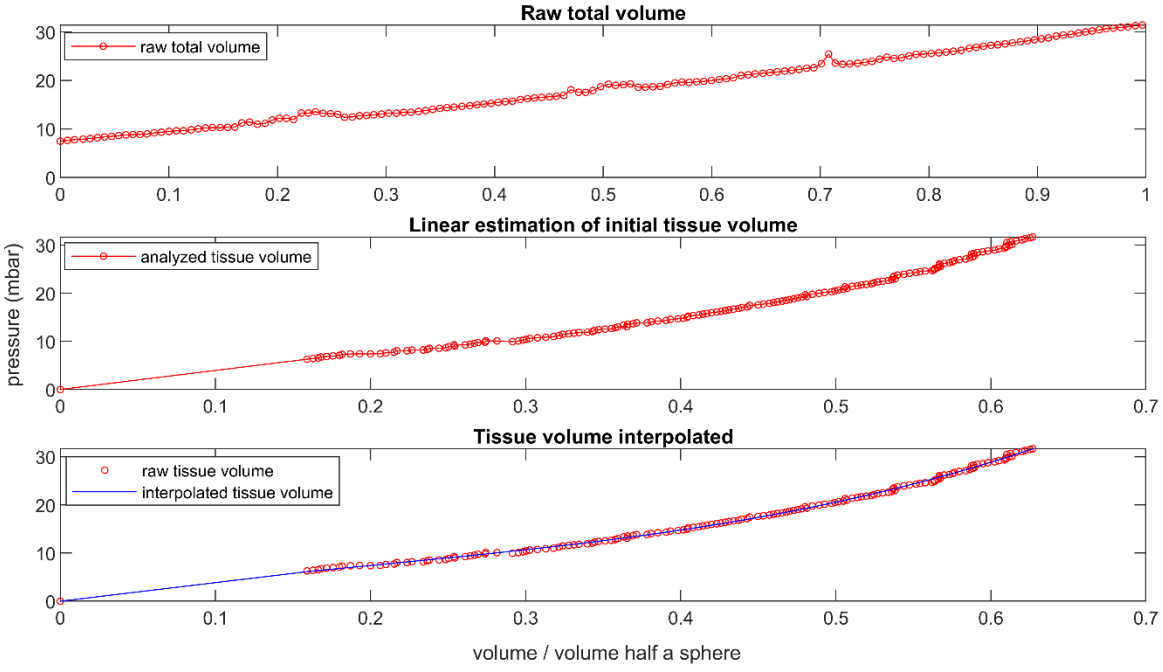


Figure 32: Estimation of the initial volume using linear estimation. **Top:** In red the raw total volume is shown. **Middle:** The analyzed tissue volume is shown, the red dots represent the raw measurement points. **Bottom:** To smoothen the data a second-order polynomial fit is calculated. This is shown in blue. The raw measurements points of the tissue volume are shown in red.

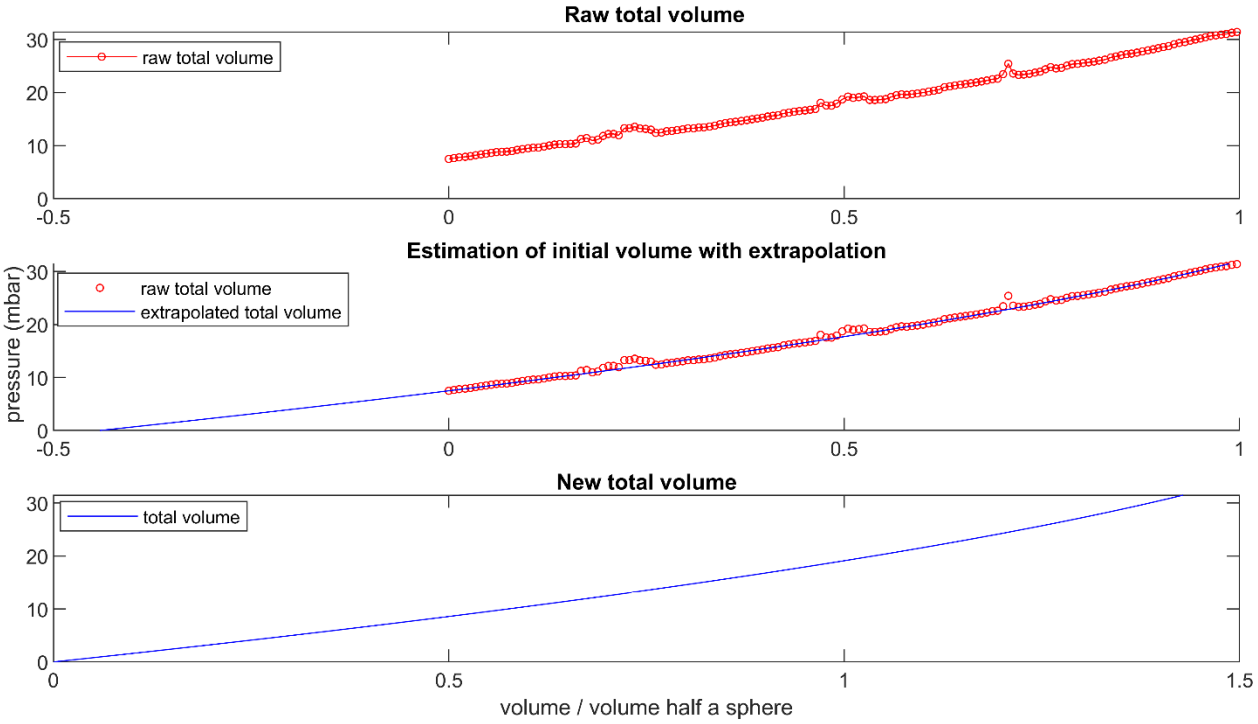


Figure 33: Estimation of the initial volume using extrapolation. **Top:** In red the raw total volume is shown. **Middle:** The extrapolated total volume is shown in blue, the red dots represent the raw measurement points. **Bottom:** The new total volume curve starting from the origin.

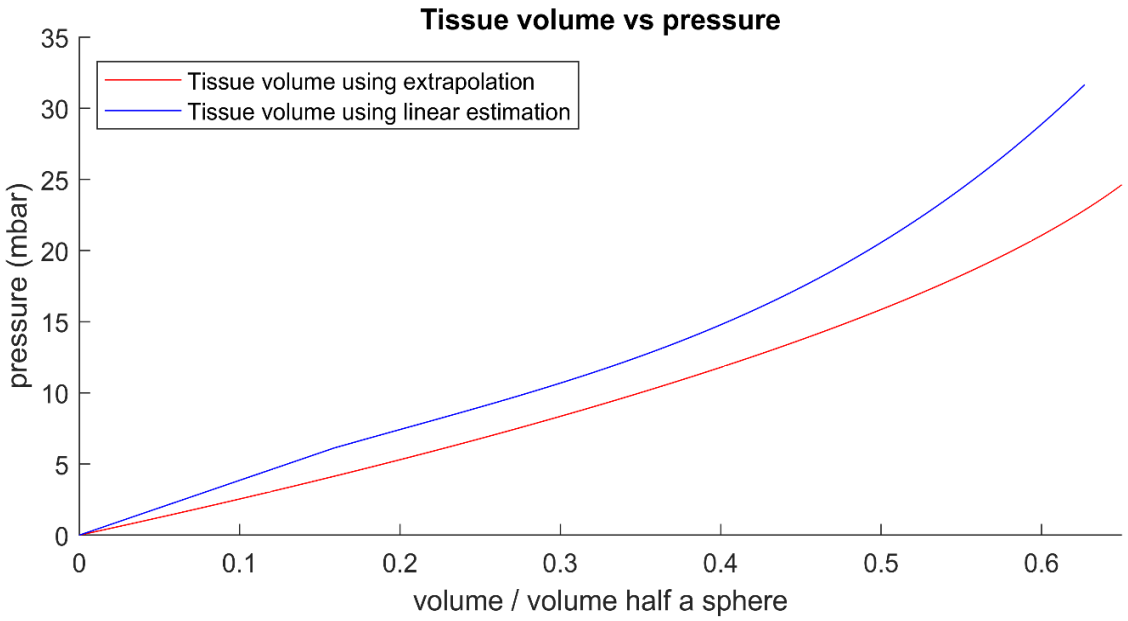


Figure 34: Tissue volume curve using a linear estimation of the initial tissue volume (blue) and extrapolation of the total volume (red).

## APPENDIX F: DATA PRELIMINARY TESTS

**Motivation:**

The human tongue can exhibit nonlinear, time-dependent, inhomogeneous and anisotropic behavior. It is, therefore, considered to be a viscoelastic material showing time-dependent strain. In other words, the rate at which the strain is applied affects the elastic response of the tissue. In order to investigate the effect of the AR on the tissue volume versus pressure curve and to distinguish possible differences in the (visco)elastic response of the tissue, preliminary tests were done on three volunteers. Each subject was measured at an AR of 0.2, 0.4, 0.8 and 1.2 ml/min. For each AR the measurement was repeated three times and the average curve was calculated.

**Results**

In Figure 35 and Figure 37 curves of the preliminary tests of subject H01 and H04 are shown, respectively. Although the three tissue volume vs pressure curves for each subject at a given AR show a wide spread, the calculated Young's modulus for each curve does not differ a lot. The mean Young's modulus is practically the same for each AR. This can be seen in Figure 36 and Figure 38 for H01 and H04, respectively.

For all measurements at every AR, the value of *Jm* was 0.32±0.01 and 0.28 ±0.03 for subject H01 and subject H04, respectively. Since these values are very low with a small standard deviation they are not shown in Figure 35 to 38 for clarity reasons. In Table 3 and 4 all results can be found of subject H01 and H04, respectively.

**Findings summary:**

For each calculated Young's Modulus in Table 3 and 4 the mean is practically the same for each AR. The variation within both subject H01 and H04 is low with a standard deviation of 0.16 and 0.32, respectively.

Although the tissue volume versus pressure curves for each subject at a given AR show a wide spread, they overlap as well (Figure 35 and Figure 37). The calculated Young's modulus for each curve does not differ a lot. In Table 3 and 4 we see that the standard deviation between the three measurements at each AR is the same or even higher compared to the overall results of all ARs together. For subject H03 the same measurements were performed and similar results were observed.

**Conclusion**:

In conclusion, it seemed that the AR does not have a great effect on the tongue muscle (visco)elastic response while the subject is awake. Therefore, one fixed AR is chosen for the remainder of this study. An AR below 0.4 ml/min is not preferable because of the long measurement time. It is very difficult for a subject to relax the tongue for a long period of time. At an AR of 0.8 ml/min, it becomes more difficult to get an accurate measurement since the pressure is decreasing fast which gives the researcher less time to start the measurement at a low negative pressure. Therefore, an AR of 0.6 ml/min was chosen for all the upcoming measurements. At this rate, a single measurement takes 20 to 30 seconds. Although the large spread observed in the pressure versus volume curves did not lead to a large variation in the Young's modulus, each subject will be measured ten times in order to calculate an accurate average curve for the FEA.

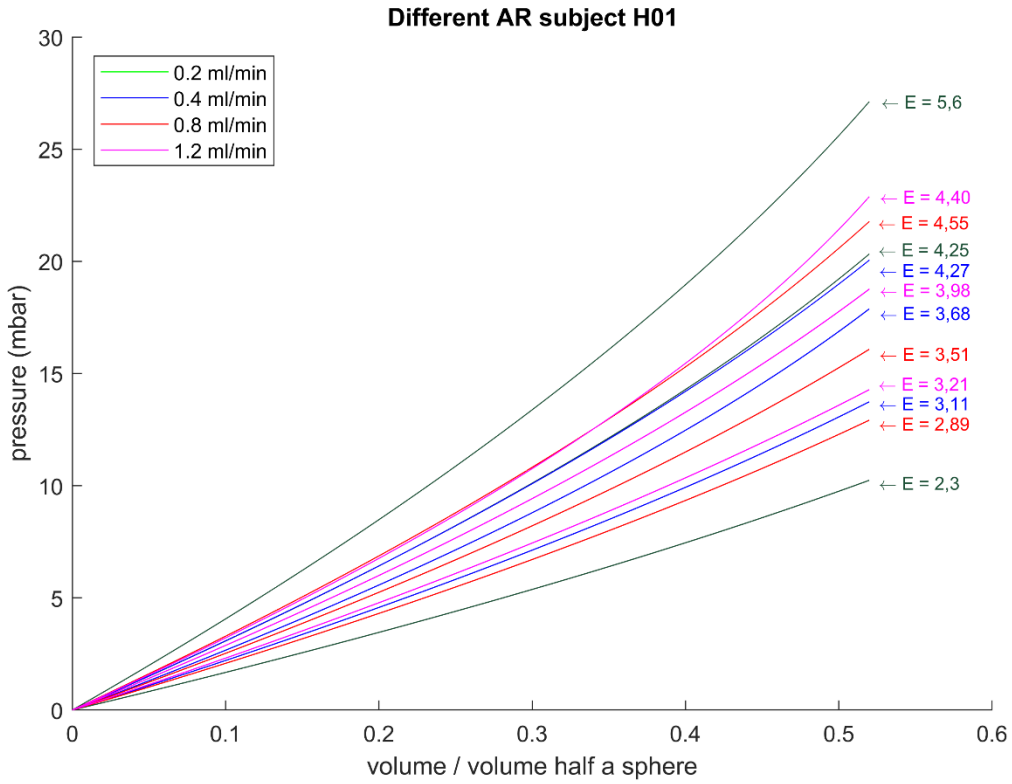


Figure 35: Pressure versus tissue volume curves of subject H01 at four different AR, including the corresponding Young's modulus.

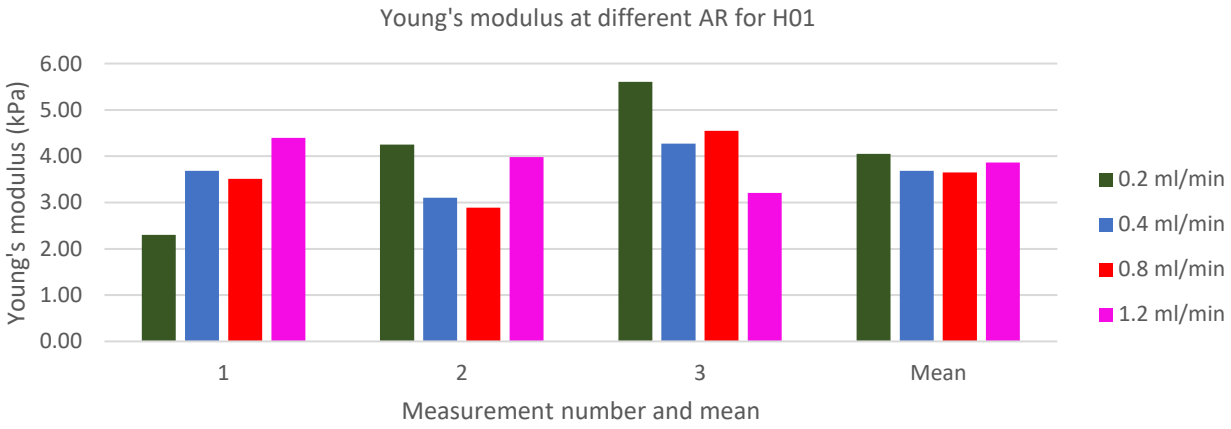


Figure 36: Young's modulus for each AR for three consecutive measurements for H01. On the right the mean is depicted.

Table 3: All results of subject H01.

| Measurement | **1** | | **2** | | **3** | | **Mean** | | | |
|---|---|---|---|---|---|---|---|---|---|---|
| AR(ml/min): | *E(kPa)* | *Jm* | *E(kPa)* | *Jm* | *E(kPa)* | *Jm* | *E(kPa)* | *stdev* | *Jm* | *stdev* |
| 0.2 | 2.30 | 0.41 | 4.25 | 0.28 | 5.60 | 0.27 | 4.05 | 1.35 | 0.32 | 0.06 |
| 0.4 | 3.68 | 0.26 | 3.11 | 0.36 | 4.27 | 0.31 | 3.69 | 0.48 | 0.31 | 0.04 |
| 0.8 | 3.51 | 0.35 | 2.89 | 0.41 | 4.55 | 0.28 | 3.65 | 0.68 | 0.35 | 0.05 |
| 1.2 | 4.40 | 0.20 | 3.98 | 0.30 | 3.21 | 0.42 | 3.86 | 0.49 | 0.31 | 0.09 |
| Overall mean | | | | | | | 3.81 | | 0.32 | |
| Stdev | | | | | | | 0.16 | | 0.01 | |

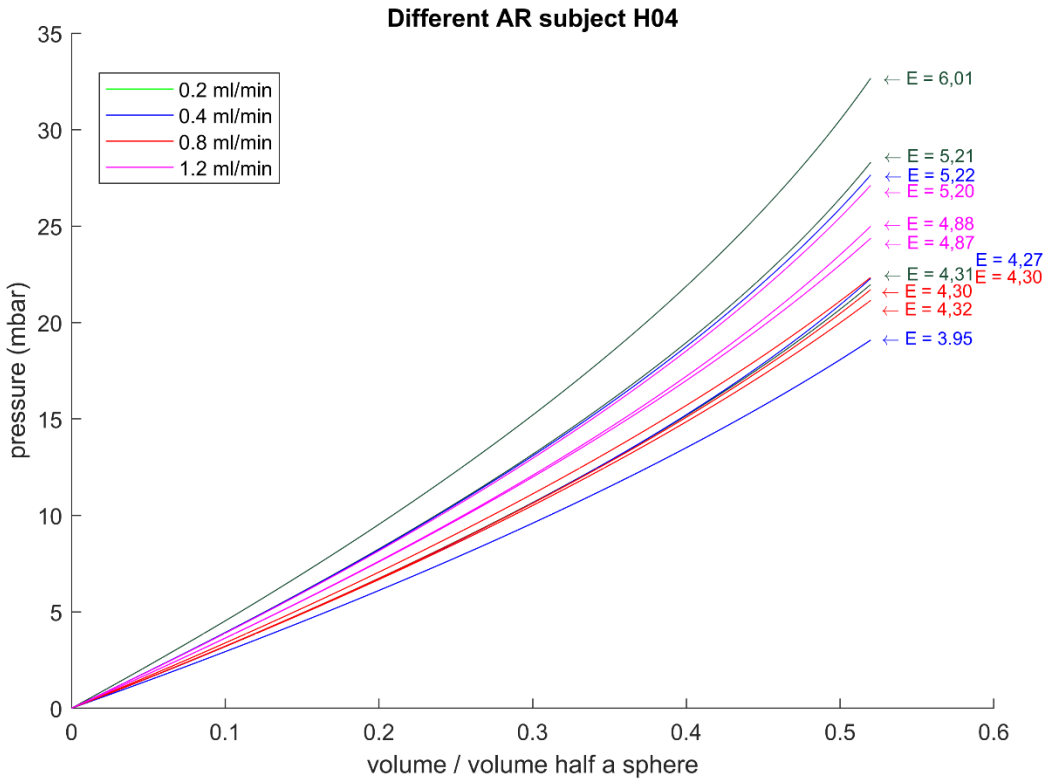


Figure 37: Pressure versus tissue volume curves of subject H04 at four different AR, including the corresponding Young's modulus.

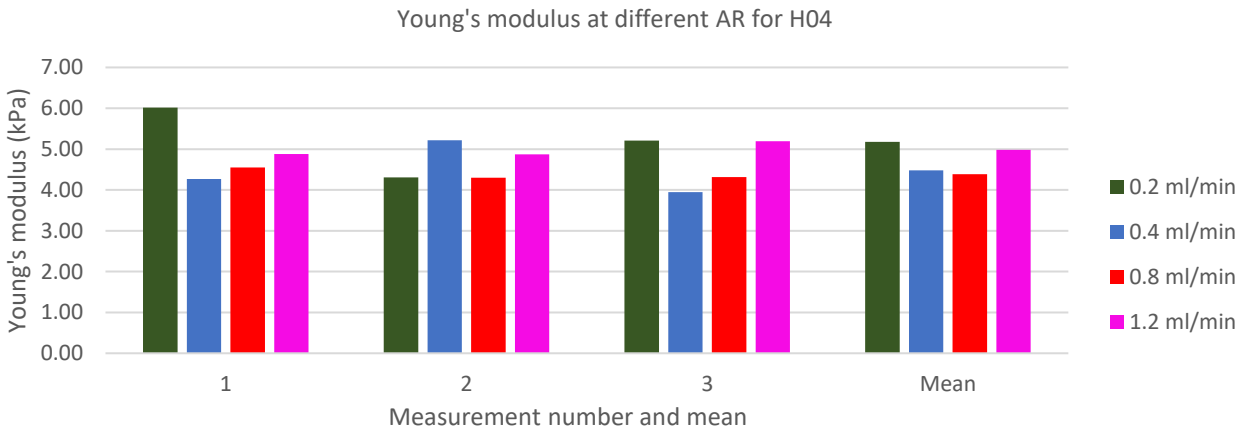


Figure 38 Young's modulus for each AR for three consecutive measurements for H04. On the right the mean is depicted.

Table 4: All results of subject H04.

| Measurement | **1** | | **2** | | **3** | | **Mean** | | | |
|---|---|---|---|---|---|---|---|---|---|---|
| AR(ml/min): | *E(kPa)* | *Jm* | *E(kPa)* | *Jm* | *E(kPa)* | *Jm* | *E(kPa)* | *stdev* | *Jm* | *stdev* |
| 0.2 | 6.01 | 0.22 | 4.31 | 0.28 | 5.21 | 0.22 | 5.18 | 0.70 | 0.24 | 0.03 |
| 0.4 | 4.27 | 0.25 | 5.22 | 0.24 | 3.95 | 0.35 | 4.48 | 0.54 | 0.28 | 0.05 |
| 0.8 | 4.55 | 0.33 | 4.30 | 0.32 | 4.32 | 0.29 | 4.39 | 0.11 | 0.32 | 0.02 |
| 1.2 | 4.88 | 0.30 | 4.87 | 0.27 | 5.20 | 0.25 | 4.98 | 0.15 | 0.28 | 0.02 |
| Overall mean | | | | | | | 4.76 | | 0.28 | |
| Stdev | | | | | | | 0.33 | | 0.03 | |

## APPENDIX G: ALL RESULTS PER SUBJECT

In the tables below the results for each measurements for each subject is shown. Both the Young's modulus and the factor *Jm* are depicted. In the outer right column the *RSS* value of the fitting process is shown, indicating the goodness of fit after 30 iterations.

**H01**

| # | E(kPa) | Jm | RSS |
|---|---|---|---|
| 1 | 3.27 | 0.53 | 0.03 |
| 2 | 3.00 | 0.53 | 0.02 |
| 3 | 3.51 | 0.66 | 0.03 |
| 4 | 3.52 | 0.46 | 0.03 |
| 5 | 3.36 | 0.47 | 0.03 |
| 6 | 4.49 | 0.32 | 0.04 |
| 7 | 4.20 | 0.38 | 0.04 |
| 8 | 3.94 | 0.33 | 0.03 |
| 9 | 3.34 | 0.40 | 0.03 |
| 10 | 3.19 | 0.52 | 0.03 |
| mean | 3.58 | 0.46 | |
| stdev | 0.45 | 0.10 | |
| median | 3.44 | 0.47 | |

**H02**

| # | E(kPa) | Jm | RSS |
|---|---|---|---|
| 1 | 5.88 | 0.20 | 0.97 |
| 2 | 4.23 | 0.30 | 0.04 |
| 3 | 3.47 | 0.37 | 0.03 |
| 4 | 4.03 | 0.23 | 0.17 |
| 5 | 3.80 | 0.32 | 0.03 |
| 6 | 3.73 | 0.29 | 0.04 |
| 7 | 5.27 | 0.21 | 0.50 |
| 8 | 3.97 | 0.29 | 0.05 |
| 9 | 5.01 | 0.27 | 0.09 |
| 10 | 4.42 | 0.27 | 0.07 |
| mean | 4.38 | 0.28 | |
| stdev | 0.73 | 0.05 | |
| median | 4.13 | 0.28 | |

**H03**

| # | E(kPa) | Jm | RSS |
|---|---|---|---|
| 1 | 3.55 | 0.40 | 0.03 |
| 2 | 3.18 | 0.38 | 0.02 |
| 3 | 3.64 | 0.32 | 0.03 |
| 4 | 4.52 | 0.29 | 0.06 |
| 5 | 3.38 | 0.38 | 0.03 |
| 6 | 3.61 | 0.33 | 0.03 |
| 7 | 3.86 | 0.28 | 0.05 |
| 8 | 4.98 | 0.26 | 0.13 |
| 9 | 3.57 | 0.36 | 0.03 |
| mean | 3.81 | 0.33 | |
| stdev | 0.54 | 0.05 | |
| median | 3.61 | 0.33 | |

**H04**

| # | E(kPa) | Jm | RSS |
|---|---|---|---|
| 1 | 4.45 | 0.22 | 0.15 |
| 2 | 4.41 | 0.25 | 0.06 |
| 3 | 4.49 | 0.23 | 0.09 |
| 4 | 4.40 | 0.24 | 0.08 |
| 5 | 4.36 | 0.21 | 0.20 |
| 6 | 4.64 | 0.18 | 0.53 |
| 7 | 4.65 | 0.20 | 0.29 |
| 8 | 4.19 | 0.28 | 0.04 |
| 9 | 4.51 | 0.21 | 0.16 |
| 10 | 4.44 | 0.24 | 0.09 |
| mean | 4.46 | 0.23 | |
| stdev | 0.13 | 0.03 | |
| median | 4.45 | 0.23 | |

**H05**

| # | E(kPa) | Jm | RSS |
|---|---|---|---|
| 1 | 3.33 | 0.46 | 0.03 |
| 2 | 5.72 | 0.76 | 0.07 |
| 3 | 3.88 | 0.66 | 0.04 |
| 4 | 3.67 | 0.49 | 0.03 |
| 5 | 3.76 | 0.45 | 0.04 |
| 6 | 4.28 | 0.45 | 0.05 |
| 7 | 4.03 | 0.46 | 0.04 |
| 8 | 5.06 | 0.38 | 0.06 |
| 9 | 3.63 | 0.40 | 0.03 |
| 10 | 4.13 | 0.46 | 0.04 |
| mean | 4.15 | 0.50 | |
| stdev | 0.69 | 0.11 | |
| median | 3.96 | 0.46 | |

**H06**

| # | E(kPa) | Jm | RSS |
|---|---|---|---|
| 1 | 5.96 | 0.17 | 3.62 |
| 2 | 9.42 | 0.16 | 10.07 |
| 3 | 7.98 | 0.17 | 5.90 |
| 4 | 10.66 | 0.11 | 24.30 |
| 5 | 8.89 | 0.12 | 43.57 |
| 6 | 8.75 | 0.10 | 65.00 |
| 7 | 9.22 | 0.10 | 58.58 |
| 8 | 10.03 | 0.11 | 32.53 |
| 9 | 10.31 | 0.11 | 27.25 |
| 10 | 5.92 | 0.19 | 1.72 |
| mean | 8.71 | 0.13 | |
| stdev | 1.57 | 0.03 | |
| median | 9.05 | 0.12 | |

**H07**

| # | E(kPa) | Jm | RSS |
|---|---|---|---|
| 1 | 3.87 | 0.28 | 0.05 |
| 2 | 4.88 | 0.30 | 0.06 |
| 3 | 3.73 | 0.38 | 0.03 |
| 4 | 3.80 | 0.40 | 0.03 |
| 5 | 3.86 | 0.47 | 0.04 |
| 6 | 4.31 | 0.25 | 0.16 |
| 7 | 4.89 | 0.30 | 0.06 |
| 8 | 4.74 | 0.29 | 0.07 |
| 9 | 4.74 | 0.28 | 0.07 |
| 10 | 4.14 | 0.43 | 0.04 |
| mean | 4.30 | 0.34 | |
| stdev | 0.45 | 0.07 | |
| median | 4.23 | 0.30 | |

**H08**

| # | E(kPa) | Jm | RSS |
|---|---|---|---|
| 1 | 14.36 | 0.10 | 27.79 |
| 2 | 5.95 | 0.22 | 0.49 |
| 3 | 12.14 | 0.11 | 42.49 |
| 4 | 10.51 | 0.13 | 74.26 |
| 5 | 12.22 | 0.10 | 62.12 |
| 6 | 10.48 | 0.17 | 10.04 |
| 7 | 6.74 | 0.20 | 1.46 |
| mean | 10.34 | 0.15 | |
| stdev | 2.81 | 0.05 | |
| median | 10.51 | 0.13 | |

**H09**

| # | E(kPa) | Jm | RSS |
|---|---|---|---|
| 1 | 4.28 | 0.25 | 0.12 |
| 2 | 5.62 | 0.17 | 2.63 |
| 3 | 4.95 | 0.25 | 0.17 |
| 4 | 4.13 | 0.25 | 0.12 |
| 5 | 4.51 | 0.25 | 0.12 |
| 6 | 4.40 | 0.27 | 0.08 |
| 7 | 4.28 | 0.30 | 0.05 |
| 8 | 5.41 | 0.27 | 0.11 |
| 9 | 4.89 | 0.22 | 0.31 |
| 10 | 5.46 | 0.18 | 1.62 |
| mean | 4.79 | 0.24 | |
| stdev | 0.52 | 0.04 | |
| median | 4.70 | 0.25 | |

**H10**

| # | E(kPa) | Jm | RSS |
|---|---|---|---|
| 1 | 3.69 | 0.37 | 0.03 |
| 2 | 4.52 | 0.33 | 0.04 |
| 3 | 4.76 | 0.31 | 0.05 |
| 4 | 4.46 | 0.34 | 0.04 |
| 5 | 3.91 | 0.43 | 0.04 |
| 6 | 4.43 | 0.28 | 0.06 |
| 7 | 4.21 | 0.37 | 0.04 |
| 8 | 4.94 | 0.33 | 0.05 |
| 9 | 4.93 | 0.31 | 0.05 |
| 10 | 4.25 | 0.32 | 0.04 |
| mean | 4.41 | 0.34 | |
| stdev | 0.39 | 0.04 | |
| median | 4.44 | 0.33 | |

**H11**

| E(kPa) | E | Jm | RSS |
|---|---|---|---|
| 1 | 2.97 | 0.46 | 0.78 |
| 2 | 3.15 | 0.53 | 0.03 |
| 3 | 3.50 | 0.54 | 0.03 |
| 4 | 3.14 | 0.74 | 0.02 |
| 5 | 3.15 | 0.49 | 0.02 |
| 6 | 3.17 | 0.45 | 0.02 |
| 7 | 3.23 | 0.43 | 0.03 |
| 8 | 2.56 | 0.56 | 0.02 |
| 9 | 3.07 | 0.47 | 0.02 |
| mean | 3.10 | 0.52 | |
| stdev | 0.23 | 0.09 | |
| median | 3.15 | 0.49 | |

**H12**

| # | E(kPa) | Jm | RSS |
|---|---|---|---|
| 1 | 3.08 | 0.47 | 0.02 |
| 2 | 5.34 | 0.23 | 0.33 |
| 3 | 4.45 | 0.48 | 0.05 |
| 4 | 5.09 | 0.31 | 0.06 |
| 5 | 4.98 | 0.86 | 0.05 |
| 6 | 3.43 | 0.45 | 0.03 |
| 7 | 3.62 | 0.55 | 0.03 |
| 8 | 3.56 | 0.36 | 1.48 |
| mean | 4.19 | 0.46 | |
| stdev | 0.82 | 0.18 | |
| median | 4.04 | 0.46 | |

**H13**

| # | E(kPa) | Jm | RSS |
|---|---|---|---|
| 1 | 5.99 | 0.32 | 0.08 |
| 2 | 6.18 | 0.22 | 0.56 |
| 3 | 5.69 | 0.25 | 0.21 |
| 4 | 4.68 | 0.28 | 0.06 |
| 5 | 8.24 | 0.72 | 0.16 |
| 6 | 8.75 | 0.30 | 0.20 |
| 7 | 5.04 | 0.29 | 0.07 |
| 8 | 6.19 | 0.23 | 0.38 |
| 9 | 8.73 | 0.50 | 0.19 |
| 10 | 6.95 | 0.28 | 0.16 |
| mean | 6.64 | 0.34 | |
| stdev | 1.40 | 0.15 | |
| median | 6.18 | 0.29 | |

**H14**

| # | E(kPa) | Jm | RSS |
|---|---|---|---|
| 1 | 3.71 | 0.26 | 0.06 |
| 2 | 6.19 | 0.14 | 11.18 |
| 3 | 3.11 | 0.43 | 0.02 |
| 4 | 4.04 | 0.26 | 0.07 |
| 5 | 4.00 | 0.28 | 0.05 |
| 6 | 3.66 | 0.29 | 0.04 |
| 7 | 3.81 | 0.39 | 0.03 |
| 8 | 5.33 | 0.22 | 0.36 |
| 9 | 4.85 | 0.24 | 0.21 |
| 10 | 5.74 | 0.23 | 0.36 |
| mean | 4.44 | 0.27 | |
| stdev | 0.97 | 0.08 | |
| median | 4.02 | 0.26 | |

**H15**

| # | E(kPa) | Jm | RSS |
|---|---|---|---|
| 1 | 2.81 | 0.48 | 0.02 |
| 2 | 4.01 | 0.31 | 0.04 |
| 3 | 3.27 | 0.45 | 0.03 |
| 4 | 4.64 | 0.47 | 0.05 |
| 5 | 3.34 | 0.36 | 0.02 |
| 6 | 3.62 | 0.34 | 0.03 |
| 7 | 4.17 | 0.34 | 0.04 |
| 8 | 3.95 | 0.37 | 0.03 |
| 9 | 4.52 | 0.31 | 0.05 |
| 10 | 3.84 | 0.36 | 0.03 |
| mean | 3.82 | 0.38 | |
| stdev | 0.54 | 0.06 | |
| median | 3.90 | 0.36 | |

**H16**

| # | E(kPa) | Jm | RSS |
|---|---|---|---|
| 1 | 4.72 | 0.24 | 0.17 |
| 2 | 4.38 | 0.40 | 0.04 |
| 3 | 4.84 | 0.38 | 0.05 |
| 4 | 5.10 | 0.27 | 0.10 |
| 5 | 3.68 | 0.33 | 0.03 |
| 6 | 3.76 | 0.38 | 0.03 |
| 7 | 4.75 | 0.36 | 0.05 |
| 8 | 5.02 | 0.33 | 0.05 |
| 9 | 4.75 | 0.34 | 0.05 |
| mean | 4.56 | 0.34 | |
| stdev | 0.49 | 0.05 | |
| median | 4.75 | 0.34 | |

Table 4: Average results of all subjects, $V_0$ with extrapolation and depicted as volume ratio.

| *subject #* | *E(kPa)* | *Jm* | *Vo* | *RSS* |
|---|---|---|---|---|
| H01 | 3.53 | 0.45 | 0.27 | 3.08E-02 |
| H02 | 4.27 | 0.27 | 0.25 | 7.25E-02 |
| H03 | 3.74 | 0.33 | 0.26 | 3.01E-02 |
| H04 | 4.34 | 0.26 | 0.21 | 9.08E-02 |
| H05 | 4.05 | 0.46 | 0.25 | 4.08E-02 |
| H06 | 8.52 | 0.13 | 0.12 | 4.59E+00 |
| H07 | 4.25 | 0.33 | 0.25 | 3.89E-02 |
| H08 | 9.52 | 0.13 | 0.12 | 5.95E+00 |
| H09 | 4.74 | 0.24 | 0.20 | 1.98E-01 |
| H10 | 4.37 | 0.34 | 0.20 | 4.08E-02 |
| H11 | 3.09 | 0.53 | 0.26 | 2.44E-02 |
| H12 | 4.06 | 0.43 | 0.19 | 4.01E-02 |
| H13 | 6.36 | 0.27 | 0.13 | 1.69E-01 |
| H14 | 4.26 | 0.26 | 0.18 | 7.95E-02 |
| H15 | 3.74 | 0.37 | 0.17 | 3.03E-02 |
| H16 | 4.50 | 0.33 | 0.23 | 4.35E-02 |
| mean | 4.83 | 0.32 | 0.21 | |
| stdev | 1.73 | 0.11 | 0.05 | |
| median | 4.27 | 0.33 | 0.21 | |

Table 5: Average results of all subjects, $V_0$ identified with FEA and depicted as volume ratio.

| *subject #* | *E(kPa)* | *Jm* | *Vo* | *RSS* |
|---|---|---|---|---|
| H01 | 3.07 | 0.36 | 0.30 | 8.07E-04 |
| H02 | 3.99 | 0.35 | 0.23 | 2.10E-03 |
| H03 | 3.33 | 0.32 | 0.27 | 5.03E-04 |
| H04 | 3.40 | 0.30 | 0.22 | 2.43E-03 |
| H05 | 3.72 | 0.35 | 0.28 | 8.11E-04 |
| H06 | 7.87 | 0.16 | 0.10 | 9.50E-03 |
| H07 | 3.99 | 0.37 | 0.24 | 8.42E-04 |
| H08 | 9.74 | 0.16 | 0.09 | 7.67E-03 |
| H09 | 2.32 | 0.15 | 0.28 | 1.20E-03 |
| H10 | 3.31 | 0.30 | 0.22 | 2.17E-03 |
| H11 | 2.23 | 0.38 | 0.29 | 1.81E-03 |
| H12 | 4.00 | 0.34 | 0.20 | 3.40E-02 |
| H13 | 5.09 | 0.27 | 0.12 | 9.84E-03 |
| H14 | 3.50 | 0.30 | 0.17 | 1.16E-03 |
| H15 | 3.15 | 0.30 | 0.17 | 2.02E-03 |
| H16 | 3.13 | 0.41 | 0.24 | 4.31E-03 |
| mean | 4.11 | 0.30 | 0.21 | |
| stdev | 1.92 | 0.08 | 0.07 | |
| median | 3.45 | 0.31 | 0.22 | |

Table 6: Difference between extrapolation and FEA

| *subject #* | *ΔE(kPa)* | ΔJm | *ΔVo* |
|---|---|---|---|
| H01 | 0.47 | 0.09 | -0.03 |
| H02 | 0.28 | -0.08 | 0.02 |
| H03 | 0.41 | 0.01 | -0.01 |
| H04 | 0.95 | -0.04 | -0.01 |
| H05 | 0.33 | 0.10 | -0.03 |
| H06 | 0.64 | -0.03 | 0.02 |
| H07 | 0.26 | -0.04 | 0.01 |
| H08 | -0.22 | -0.03 | 0.03 |
| H09 | 2.42 | 0.09 | -0.08 |
| H10 | 1.06 | 0.04 | -0.02 |
| H11 | 0.86 | 0.15 | -0.03 |
| H12 | 0.06 | 0.09 | 0.00 |
| H13 | 1.28 | 0.00 | 0.01 |
| H14 | 0.76 | -0.03 | 0.01 |
| H15 | 0.58 | 0.07 | 0.00 |
| H16 | 1.37 | -0.08 | 0.00 |
| abs mean | 0.75 | 0.06 | 0.02 |
| stdev | 0.58 | 0.04 | 0.02 |
| median | 0.61 | 0.01 | 0.00 |

Table 7: Two parameter Yeoh strain energy function

| *subject #* | *E(kPa)* | *c10(kPa)* | *c30(kPa)* | *RSS* | ΔE with Gent |
|---|---|---|---|---|---|
| H01 | 3.62 | 0.60 | 5.33 | 0.30 | 3.62 |
| H02 | 4.43 | 0.74 | 14.61 | 0.38 | 4.43 |
| H03 | 3.86 | 0.64 | 9.25 | 0.34 | 3.86 |
| H04 | 4.50 | 0.75 | 15.59 | 0.38 | 4.50 |
| H05 | 4.16 | 0.69 | 6.05 | 0.39 | 4.16 |
| H07 | 4.39 | 0.73 | 10.33 | 0.44 | 4.39 |
| H09 | 4.92 | 0.82 | 20.11 | 0.44 | 4.92 |
| H10 | 4.51 | 0.75 | 10.34 | 0.47 | 4.51 |
| H11 | 3.16 | 0.53 | 3.72 | 0.21 | 3.16 |
| H12 | 4.17 | 0.69 | 6.56 | 0.40 | 4.17 |
| H13 | 6.60 | 1.10 | 21.96 | 0.84 | 6.60 |
| H14 | 4.41 | 0.74 | 15.00 | 0.37 | 4.41 |
| H15 | 3.89 | 0.65 | 6.76 | 0.51 | 3.89 |
| H16 | 4.64 | 0.77 | 11.10 | 0.49 | 4.64 |
| mean | 4.38 | 0.73 | 11.19 | 0.43 | 4.38 |
| stdev | 0.76 | 0.13 | 5.37 | 0.14 | 0.76 |
| median | 4.40 | 0.73 | 10.34 | 0.40 | 4.40 |

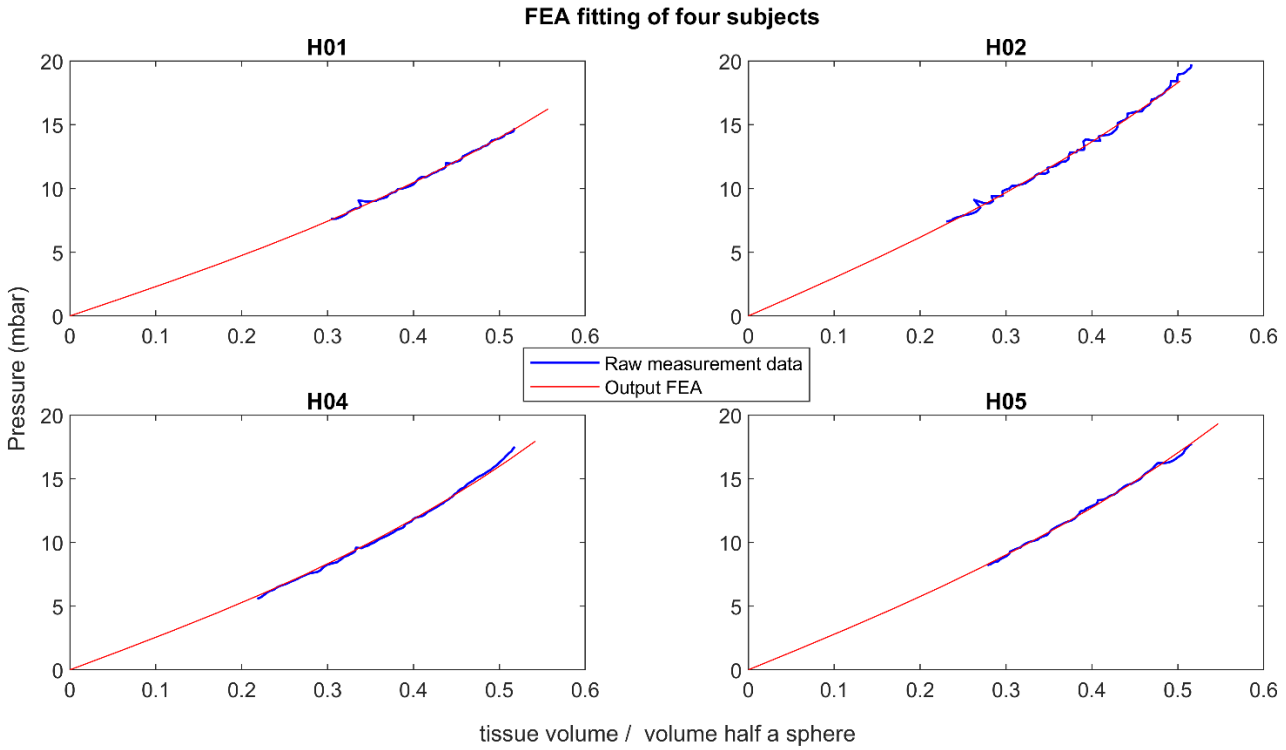


Figure 39: Results of FEA fitting of four subjects using the raw tissue volume data. Note that these are the same subjects as in Figure 12.

## APPENDIX I: ADDITIONAL TESTS

Subject H03 was measured at two locations, the apex and the body of the tongue, with an AD of 10 mm and 15 mm. Each location was measured ten times with each AD. The average curve was calculated and is shown in Figure 40. The results of the simulation are shown in Table 8.

Table 8: Results of additional test subject H03

**Additional tests subject H03**

| | *E(kPa)* | *Jm* | *RSS* |
|---|---|---|---|
| *Apex , AD=10mm* | 3.84 | 0.28 | 0.04 |
| *Body, AD=10mm* | 8.53 | 0.14 | 2.05 |
| *Apex, AD=15mm* | 4.70 | 0.23 | 0.11 |
| *Body, AD=15mm* | 5.35 | 0.13 | 0.77 |

The difference between an AD of 10 mm and 15 mm on the apex is low, 0.86 kPa to be exact. The question remains of this is due to the AD and tissue response itself or just the reproducibility of the experiment, i.e. if the experiment on the apex was redone with both ADs a different Young's modulus might be obtained. The difference between the apex and body measurement with an AD of 15 mm is 0.67 kPa. Here the same question remains. However, the results for an AD of 10 mm are remarkable. The Young's modulus increases from 3.84 kPa for the apex to 8.53 kPa for the body of the tongue. The stiffness is more than doubled. Based on the experience and palpation of surgeons it is known that the anterior part of the tongue is more flexible and less stiff compared to the posterior part of the tongue. So the observed difference could be expected. One could also reason that when the tissue/tongue gets thicker, i.e. more muscle mass underneath the aperture, it will provide more resistance to the aspiration experiment, thus showing a stiffer behavior. When running an FEA with a thicker FE model this is indeed the case. This might also explain the small difference between both ADs on the apex of the tongue. But this does not explain the large difference between both ADs on the body of the tongue. If the exact same tissue is measured one would expect the outcome to be almost the same regardless of the AD, because of the normalized volume (by half a sphere volume). However, increasing the AD to 15 mm does not show a stiffer behavior. This can be explained because of the nature of the measurement. The measurements are performed on the surface of the tongue. Thus, the experiment focuses on the response of the most superficial tissue. If the AD is increased the aspirated volume of the tissue increases to get the same shape ratio and possibly more tissue layers with different elastic behavior are addressed, which will influence the overall response of the tissue.

One hypothetically explanation might be the influence of the mucosal layer of the tongue. Because of the superficial measurements, the thickness of the mucosal layer will influence the measurement. If the mucosal layer of the tongue becomes thicker it will lead to a stiffer response for a fixed AD since the mucosal layer is considered stiffer than the underlying muscle tissue. Measurements on *ex vivo* bovine tongue with and without the mucosal layer have shown the influence of a thick mucosal layer. (*I performed these test during my second visit to Grenoble, see Figure 41).* A fixed AD of 9.9 mm was used. Although the mucosal layer of a bovine tongue is expected to be much ticker compared to a human tongue, these measurements indicate that the mucosal layer is indeed stiffer than the tongue muscle tissue.

Assuming that the mucosal layer is stiffer than the underlying muscle tissue, one could explain the difference in elastic response between the apex and the body of the tongue when using an AD of 10 mm if the thickness of the mucosal layer increases from the apex to the body. To verify this hypothesis a histological study needs to be performed. When the AD is increased and the experiment is performed at the same location a more elastic response is expected because more muscle tissue is addressed. The aspirated volume of the mucosal layer will decrease relatively compared to the total aspirated muscle tissue underneath, so the influence of the mucosal layer on the overall response will decrease. The latter might explain the more elastic response on the body of the tongue when using an AD of 15 mm compared to an AD of 10 mm.

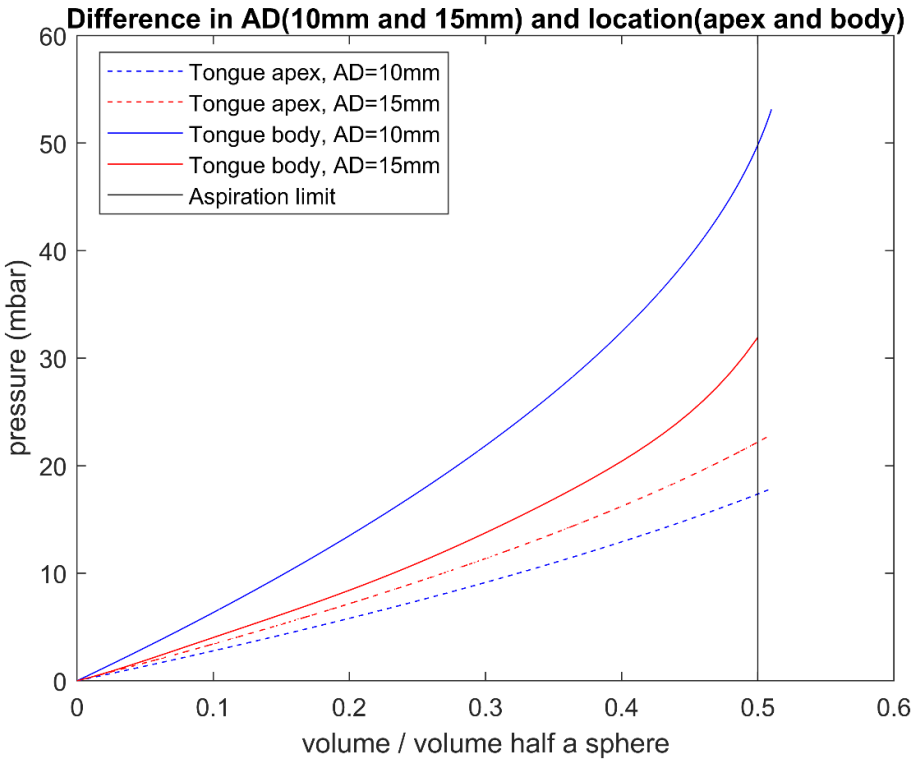


Figure 40: Results of two AD at two locations for subject H03

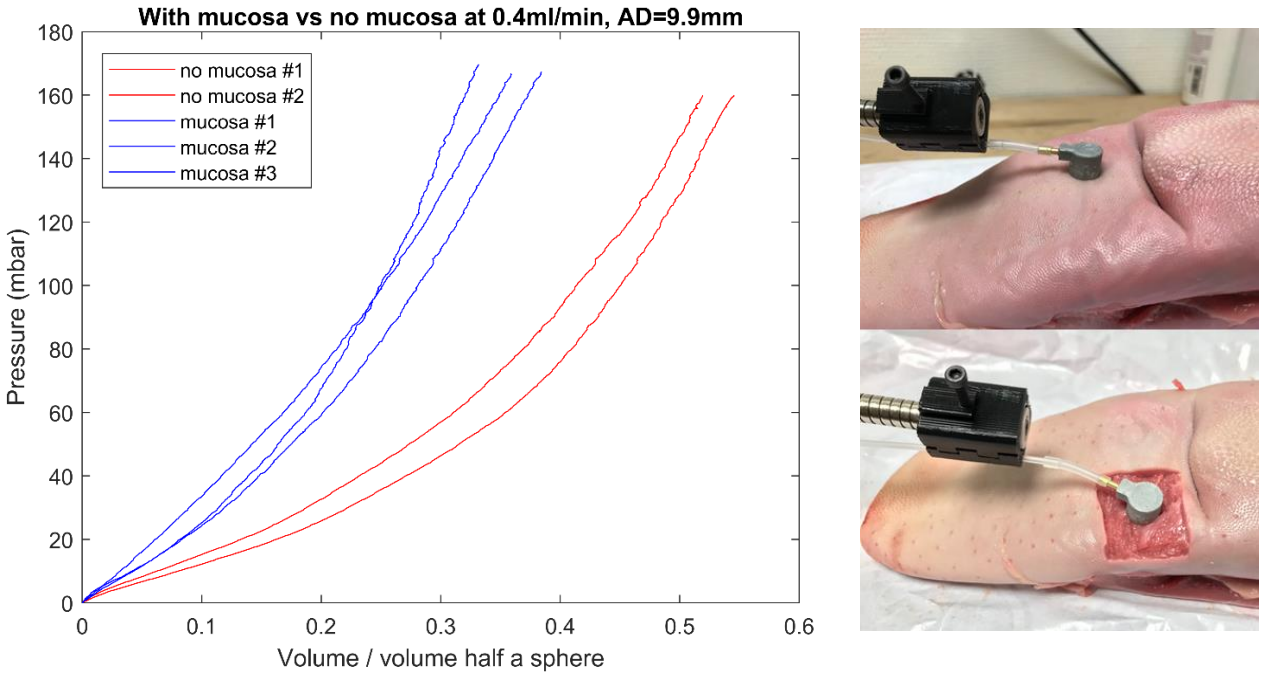


Figure 41: **Left**: Bovine tongue measurements with an AD of 9.9 mm. In blue the results of the measurements including the mucosal layer, in red the results after removing the mucosal layer. **Top right:** The bovine tongue with the mucosal layer. **Bottom right:** The bovine tongue without the mucosal layer.

## APPENDIX J: ACOUSTIC WAVES, ELASTICITY, AND SWE

### Introduction

Over the past decades, ultrasound has become an important diagnostics modality. With continues technological development ultrasound has progressed to a portable, user-friendly and sophisticated instrument. Due to generally real-time imaging, the widespread availability, relatively low cost, and high resolution, ultrasonic imaging is now one of the most common medical imaging technology used in clinical practice.

Although the integration in every day clinical practice nowadays, ultrasonic imaging techniques are subject of intense research[16]. Twenty years ago, the terms 'acoustic imaging' and 'ultrasonic imaging' were synonymous since the only acoustic waves used to image biological structure were longitudinal waves. But from the 1990s a new acoustic imaging technology emerged that was based on transverse waves. The imaging of soft tissue strain and elasticity aims to provide information about the mechanical properties of tissues, e.g. hardness and stiffness[49].

### Elasticity and acoustic waves

Elasticity is a measure of the stiffness of a material. It describes the tendency of the material to return to its original size and shape after experiencing external force or stress. The change in size or shape is known as the strain. The force acting on an unit area is known as the stress and is responsible for the strain. Assuming a material to be completely elastic and its deformation to be time-independent, the elasticity can be described according to Hooke's Law:

$$\Gamma = \frac{\sigma}{\varepsilon} \tag{54}$$

Where stress $\sigma$ is the unit force per area in kilopascals, strain $\varepsilon$ is the deformation per unit length which is dimensionless and the elastic modulus $\Gamma$ is the ratio between stress and strain in kilopascals.

Depending on the kind of material the response to an external force differs. Fluids resist a change in volume, but not in shape: they possess only volume elasticity. Solids resist changes in shape and volume: they possess rigidity or shear elasticity, as well as volume elasticity[16].

The elastic moduli $\Gamma$ also describe the propagation speed of waves in a material according to:

$$c = \sqrt{\frac{\Gamma}{\rho}} \tag{55}$$

Here $\rho$ is the density of the material and $c$ is the wave speed. There are three types of elastic moduli $\Gamma$ defined by the way of deformation. This is shown in Figure 42.

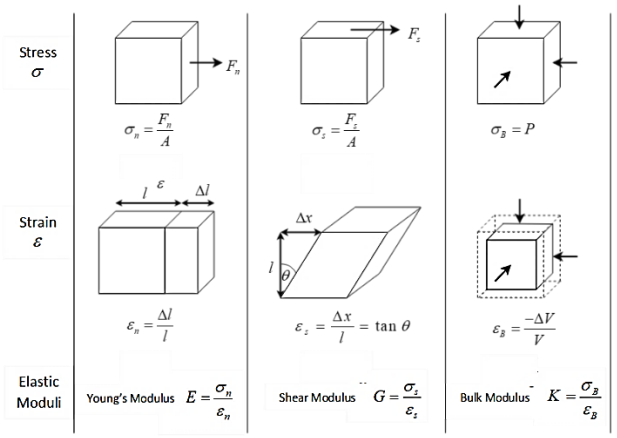


Figure 42: Overview of the three different elastic moduli and their corresponding deformation models. Each is defined by a stress and strain.

The Young's; modulus is defined by uniaxial stress and proportional strain in the same direction, whereas the shear modulus is defined by stress on a surface that is tangential to the strain. The Bulk modulus is defined by a pressure or force inward, causing bulk strain or volume changes.

The two wave types in ultrasound differ in the way the wave propagates through the material. In shear wave imaging the particle motion is perpendicular to the direction of the wave propagation, with shear wave speed $c_s$ related to the shear modulus $G$. The direction of the particle movement can be in any direction, as long as it is perpendicular to the direction of the wave propagation. This makes it a polarized wave and sensitive for anisotropic tissue.

In B-mode ultrasound (with longitudinal waves), particle motion is parallel to the direction of wave propagation, with longitudinal wave speed $c_l$ related to the bulk modulus $K$. Therefore, it is not a polarized wave and not sensitive for anisotropic tissue.

Three elastic moduli are not independent but can be related to each other according to Poisson's ratio $v$. This ratio describes the compressibility of the material, i.e. the ability of a solid to retain its original volume after being subjected to stress. The relationship between the Young's modulus $E$, shear modulus $G$, and bulk modulus $K$ is as follows:

$$E = 2(v+1)G = 3K(1-2v) \tag{56}$$

Since soft tissue has a high-water content the Poisson ratio is nearly 0.5, which represents an incompressible material. Therefore, $E$ is often estimated as follows:

$$E = 3G \tag{57}$$

Based on the relationship of equation 55, 56 and 57, the Young's modulus can be calculated according to:

$$E = 3\rho c_s^2 \tag{58}$$

With $c_s$ as the speed of the shear waves and $\rho$ as the density of the material. In Table 9 and overview is given of the main properties of the two waves types[25,49].

Based on the relationship of wave speed and the elastic modulus, and the relationship between these moduli, one could state that both wave types could be used to measure the elastic properties of tissue. However, longitudinal waves are not used for this purpose simply because their propagation speed too fast to be measured reliably with the available techniques[49]. Also, the variation in speed is low and thus the variation in bulk modulus, so almost no contrast is seen and the ability to reveal the differences in elastic properties is low. The compressional wave is only used to induce a push pulse which creates shear waves inside the tissue. This is called acoustic radiation force impulse (ARFI) and is described shortly in section 2.2 and in Appendix L in the METC protocol. Shear waves are preferred for their low propagation speed and can be easily measured using Doppler processing techniques[25]. But shear waves have more benefits for elasticity imaging, this is explained in the next section

.

Table 9: Overview of the main differences of longitudinal and shear waves

| | **Longitudinal waves** | **Shear waves** |
|---|---|---|
| **Equation for speed** | $c_l = \sqrt{\frac{K}{\rho}} = \sqrt{\frac{E(1-v)}{\rho(1+v)(1-2v)}}$<br><br>Assuming $v$ is near 0.5, $E \approx 3\rho c_l^2$ | $c_s = \sqrt{\frac{G}{\rho}} = \sqrt{\frac{E}{2\rho(1+v)}}$<br><br>Assuming $v$ =0.5, $E = 3\rho c_s^2$ |
| **Speed related to** | Bulk modulus | Shear modulus |
| **Speed in tissue** | 1500-1800 m/s | 0.5-100 m/s |
| **Tissue speed variation** | Low variation in speed. The variation in bulk modulus in soft tissue is significantly less than one order of magnitude. | High variation in speed. The shear modulus in soft tissue varies over several orders of magnitude. |
| **Sensitive for anisotropy** | No polarized waves, not sensitive for anisotropy | Polarized waves, sensitive for anisotropy |

**Why shear waves and elastic imaging?**

The mechanism of providing the contrast in imaging is one of the most important characteristics that distinguishes the practical capabilities and limitations between different imaging techniques[50]. In conventional ultrasound images, i.e. B-mode with longitudinal waves, the anatomy is revealed because of different acoustic properties of soft tissue, mainly by differences in echogenicity and also partly due to attenuation. But in ultrasound based on elasticity images, with shear waves, it is possible to reveal the differences in elastic properties of soft tissue.

The benefit of elasticity imaging lies in the fact that many soft tissues can share similar ultrasonic echogenicity's but may have different mechanical properties that can be used to clearly visualize normal anatomy and delineate pathologic lesions. It is well known that changes in tissue stiffness are involved in various diseases such as cancerous masses, fibrosis associated with liver cirrhosis, and atheroma and calcification associated with arteriosclerosis[51]. Figures 44-46 strengthen the ability of shear waves to provide contrast between healthy and pathologic tissue. In Figures 43 and 44, the wave speed of longitudinal and shear waves are shown for healthy breast tissue and cancerous breast tissue, respectively. In Figure 45 and 46 the same is shown for healthy liver tissue and fibrotic liver. tissue. The numbers to create these graphs were derived from Sarvazyan et al. 2013[49]. It can be seen that the speed of shear waves differs a lot between healthy and pathologic tissue, while the speed of longitudinal waves shows the same speed in both tissue types.

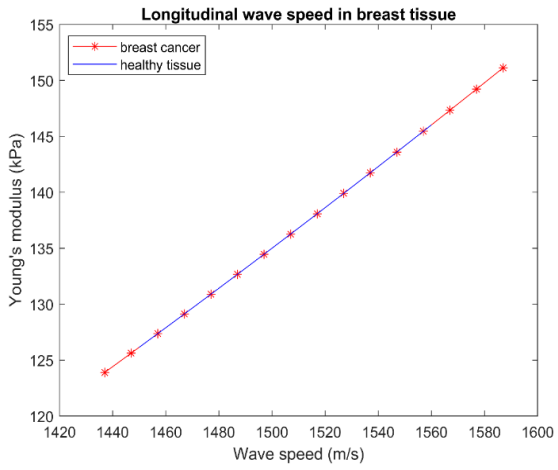


Figure 43: Longitudinal wave speed in breast tissue.

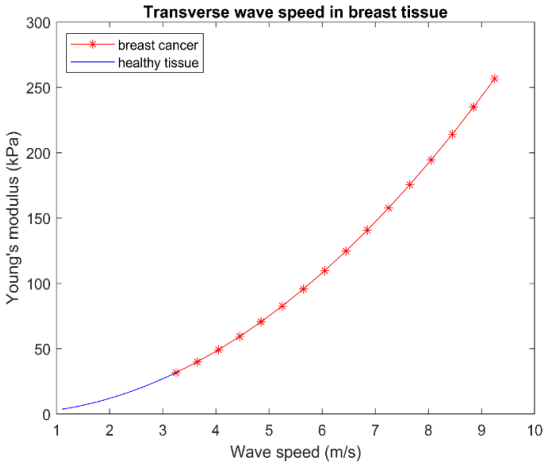


Figure 44: Shear wave speed in breast tissue.

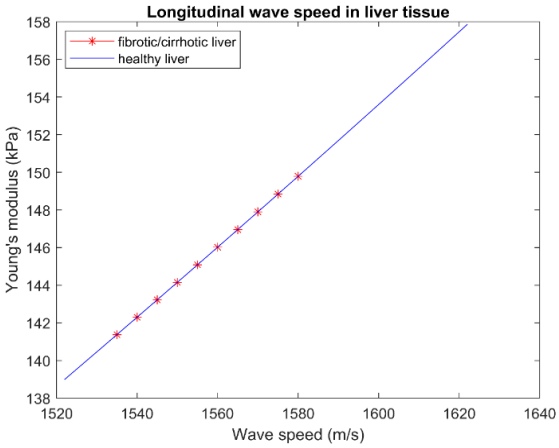


Figure 45: Longitudinal wave speed in liver tissue

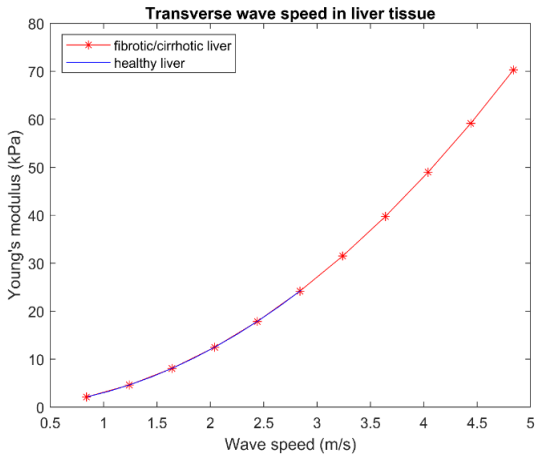


Figure 46: Shear wave speed in liver tissue.

**Our Results & Conclusion**

In our study, a Philips's EPIQ7 Ultrasound system was used in combination with the C5-1 abdominal transducer and ElastQ software. It uses 2D shear wave elastography (SWE) technology to acquire a 2D elastogram. An example of an elastogram is shown in Figure 48.

We performed a phantom study on the tissue mimicking Elasticity QA Phantom (CIRS Model 49)[52]. This phantom box contains four different materials with elastic properties of 8, 14, 45 and 80 kPa and a background of 27 kPa. Each mass was measured 10 times and we calculated the mean and standard deviation. The results can be found in Table 10.

Table 10: Results of the phantom test with SWE. Results are in kilopascals

| ***Reference*** | ***1*** | ***2*** | ***3*** | ***4*** | ***BG*** |
|---|---|---|---|---|---|
| Phantom | 8 | 14 | 50 | 85 | 27 |
| Mean SWE | 9.73 | 13.86 | 40.39 | 65.30 | 22.90 |
| Stdev SWE | 0.18 | 0.36 | 0.83 | 2.14 | 0.36 |

It can be seen that the standard deviations is very low for all the references, indicating high reproducibility. However, the values up to 12 kPa measured with SWE seem to be an overestimation. Higher values seem to be underestimated. This is seen in Figure 47 . A linear fit was calculated on the measurement points, this function could be used to correct the measurements of soft tissue.

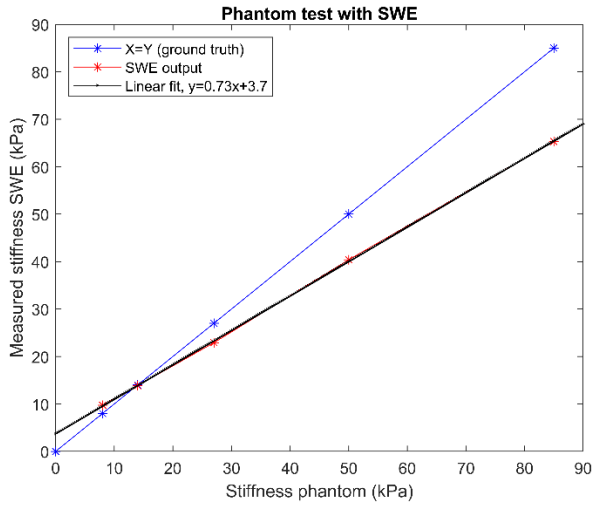


Figure 47: Measured Young's modulus with SWE versus the phantom reference values.

We performed SWE measurements on all 16 healthy subjects on the same spot as we put the aspiration chamber of LASTIC. We took a coronal view as close to the apex as possible, because of the mandibula the outer tip of the tongue was not visible. For each subject, we delineated the same side as we put the aspiration chamber on and calculated the output. In Figure 48 an example is shown. The results for all subjects are shown in Table 11. We obtained an average Young's modulus of 6.93±1.42 kPa for all the subjects. When corrected for the measurement error according to the phantom test we obtained an average Young's modulus of 4.42±1.92 kPa. These results are in the same order of magnitude as LASTIC, the corrected measurements are practically the same. This looks very promising and reliable, however when we look at the difference between LASTIC and SWE we see absolutely no consistency between both measurements techniques. This is seen in the outer right column of Table 11. The difference varies from -4.82-1.69 kPa, whereas the difference for LASTIC varies from 0.13-2.81 kPa. Also, we observed a large variation within each subject. The standard deviation varies from 1.72-4.49 kPa, which we believe is relatively high compared to the obtained mean Young's modulus. For other studies (N17SWE and N17BTM) of our group, we measured three sagittal planes as well. In the sagittal planes, the variation within each subject is even higher compared to taking coronal planes. The obtained Young's modulus and the variation seem to be highly dependent on the angle at which the probe is placed on the submental space of the subject. This is confirmed by literature. In short: the mechanical properties of muscle are different along the fibers than across the fibers. Consequently, leading to anisotropic results, since the shear wave speed dependents on the direction of propagation with respect to the muscle fiber orientation. This confounds SWE measurements in two ways: 1) The fiber orientation is not precisely known usually, also the resolution of the C5 probe is too low to visualize fiber orientation 2) The assumption of isotropy in SWE to calculate the shear or Young's modulus does not apply. The shear modulus is greater along the fibers than across, meaning that if the angle of the push pulse direction varies from parallel to perpendicular to the muscle fiber direction, the shear modulus will increase[53]. Another influence is anisotropic acoustic scattering in muscle tissue, leading to a decrease in signal as the push pulse it tilted from perpendicular towards the muscle fiber direction. It has been shown that the acoustic attenuation is a factor 2 greater at 45° to the fibers than perpendicular[54].Although we knew SWE works more accurate in homogeneous and isotropic matter, we hoped that SWE could be used to measure the elasticity of inhomogeneous and isotropic tissue like tongue muscle. Unfortunately, we have to conclude that the results are not reliable because of the anisotropic nature of the tongue tissue.

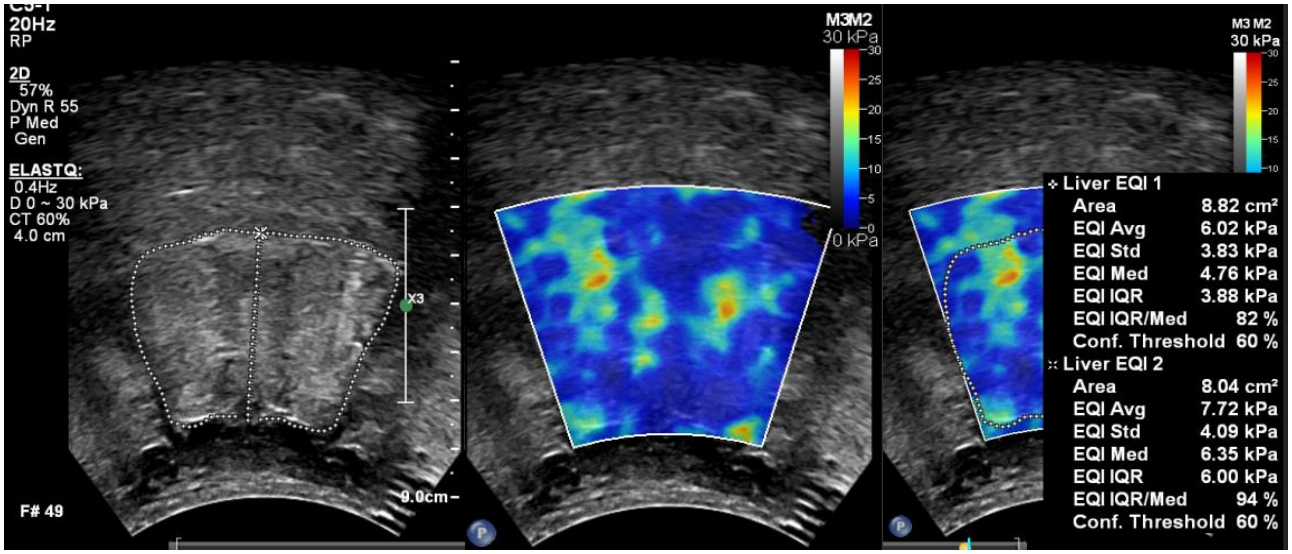


Figure 48: **Left**: Grayscale image of the apex of the tongue (coronal view) with delineations of the left and right side. **Middle:** Elastogram superimposed on grayscale image. **Right:** Results of the delineated parts.

Table 11: Results of the SWE measurement on the healthy subjects

| Results Shear Wave Ultrasound | | | | | | |
|---|---|---|---|---|---|---|
| | **Young's modulus (kPa)** | | | **Corrected Modulus** | | **Difference LASTIC** |
| *Subject* | *Mean* | *Stdev* | *Median* | *Mean* | *Stdev* | *ΔE (kPa)* |
| H01 | 6.72 | 2.47 | 6.18 | 4.14 | | 0.60 |
| H02 | 4.43 | 1.72 | 6.18 | 1.00 | | -3.27 |
| H03 | 7.72 | 4.09 | 6.35 | 5.51 | | 1.76 |
| H04 | 5.30 | 3.03 | 4.41 | 2.19 | | -2.15 |
| H05 | 6.51 | 4.45 | 9.94 | 3.85 | | -0.20 |
| H06 | 10.50 | 4.15 | 10.40 | 9.32 | | 0.80 |
| H07 | 6.88 | 4.99 | 5.12 | 4.36 | | 0.11 |
| H08 | 7.13 | 3.32 | 6.35 | 4.70 | | -4.82 |
| H09 | 6.45 | 3.98 | 4.94 | 3.77 | | -0.97 |
| H10 | 8.13 | 4.84 | 6.53 | 6.07 | | 1.69 |
| H11 | 5.95 | 3.01 | 5.12 | 3.08 | | -0.01 |
| H12 | 8.85 | 3.58 | 7.59 | 7.05 | | 3.00 |
| H13 | 7.44 | 4.39 | 6.35 | 5.12 | | -1.24 |
| H14 | 7.38 | 3.70 | 6.18 | 5.04 | | 0.78 |
| H15 | 5.84 | 2.64 | 5.12 | 2.93 | | -0.81 |
| H16 | 5.65 | 2.78 | 5.12 | 2.67 | | -1.83 |
| All | 6.93 | 1.42 | 6.80 | 4.42 | 1.94 | |

## APPENDIX K: PERSONAL CONTRIBUTIONS TO RESEARCH

The research described in this report was set up from a collaboration between the members of the Virtual Therapy project and researchers from the TIMC-IMAG laboratory in Grenoble. The main motivation to set up this collaboration was the disappointing results of the Shear Wave Ultrasound Elastography and the need for a new measurement technique. In Grenoble, the LASTIC device was designed, which looked very promising for our purposes. Also, in Grenoble they were eager to test LASTIC in a clinical trial. The latter was something we could provide in the NKI. This made it a beneficial collaboration for both sides. In my opinion, we had a good and extensive collaboration, so it is hard to distinguish my personal contribution to this research. I worked together with Nathanael and Ali in many aspects. Most of the aspects were discussed together and choices were made in consultation. In this section, I will try to give an overview of what I think was my personal contribution to this research but also to Virtual Therapy project. I will discuss the main aspects.

**The research protocol**

This is where my first major contribution lies, namely to set up a completely new research line within the Virtual Therapy project. I wrote an application for the medical ethics committee in the NKI and got it approved. This took up a lot of time since we introduced a new measurement technique as well. To get this approved, also for the measurements on the OR, it requires a lot of extra paperwork and convincing of the ethics committee. I performed a risk analysis in order to convince the ethics committee that our proposed measurement technique was safe. During the writing of the application, I often asked Kilian for confirmation. I asked for confirmation mainly because I knew that I could not finish the whole research and Kilian would eventually have to take it over. I wanted to be sure that Kilian stood behind my proposal because he will now be the person responsible for the continuation of the project and be the point of contact. Also, this was the first time I wrote a METC application and I truly believe that reinventing the wheel is a waste of time.

**The measuring device: LASTIC**

Although the device was designed by the researcher in Grenoble, I needed to make some changes for our purposes. I designed a new aspiration chamber during my second week in Grenoble and tested it. Unfortunately, the 3D printing technology in Grenoble was not suitable for creating an airtight chamber. So I had to use chloroform to seal it. The latter was proposed by Nathanael. With a phantom, I tested the new aspiration chamber and investigated if I could achieve the same volume versus pressure curves as with the old aspiration chamber. This was the case. In the NKI the 3D printing technology provided an instant airtight aspiration chamber, this was tested on the same phantom as well. The results of these tests are not shown in this report but were discussed with Kilian and the colleagues in Grenoble.

Another thing we needed was the ability to perform real-time measurements. In the old measurement program, the rigid and sample tests were performed separately as well, but the volume of the tissue sample could only be analyzed retrospectively. As a part of the risk analysis, I concluded that we needed real-time measurements to assure we would not exceed the aspiration limit. We created a tool that automatically saves the data from the rigid test and allows real-time calculation of the tissue sample during a measurement. All the previous measurement programs in Grenoble were written in Python. Because I was not that familiar with Python and due to my limited amount of time in Grenoble, Nathanael wrote the code for the program. This way I was still able to test the new program in my third week in Grenoble with a phantom test. I got similar results as before which I shared with Nathanael and we considered the program to be accurate. The results of these tests are not shown in this report.

**Bovine tongue tests and preliminary tests**

The phantom was known to show linear elastic behavior at an aspiration rate of 0.4 ml/min or lower. At this rate, the elastic response had become rate independent. However, this was not what we did expect for human tongue tissue. In order to investigate the possible viscoelastic response of biological soft tissue, I performed several tests on *ex vivo* bovine tongue tissue with different aspiration rates during my third week in Grenoble. The results are not shown in this report since they do not contribute to the content anymore, but we saw a varying responses. Based on these findings, I decided to perform the preliminary tests on three healthy volunteers as described in this report.

**Measuring the subjects and performing the FEA**

I performed all measurements on the 16 healthy subject myself. Unfortunately, I only had the device for three weeks to perform all the measurements. The application for the ethics committee was approved before the device was at the NKI, but the board of the NKI only gave the approval 1.5 weeks before I had to send the device back to Grenoble. I am very happy with the number of

measurements I could perform and number of subjects I could include in this short period of time. I also performed all Finite Element Analyses to estimate the elastic properties. The results were discussed with Nathanael during a two-hour skype call in October. He was really enthusiastic about the results and agreed on most of my assumptions and conclusions. However, he also had some feedback and thoughts about improvements for the FE model and mainly its boundary conditions. This was discussed in this report in Chapter 7. Changing the boundary conditions did not work out as expected, therefore, a new FE model needs to be developed. Nathanael already worked on this but could not get it working completely. So it is still in development and I recommend Kilian to work with him on the model. I believe we should not try to do this ourselves. The colleagues in Grenoble have more knowledge about creating FE models and performing simulations in Ansys. I noticed that they are eager to work together on this, so I recommend to maintain close contact and use their expertise instead of trying to reinvent the wheel by trying it ourselves from scratch.

In my defense, when I presented my used FE model to Yohan and Ali they believed I could trust my FE model and results. Therefore, I focused on finishing my report rather than changing the FE model.

**The FEA and FE model**

Performing measurements with LASTIC and using an inverse FEA to estimate the elastic properties was already thought of by the researchers in Grenoble in 2008. However, the new volume based version of LASTIC was only tested on phantoms and its corresponding FE model. For this study, I had to learn the coding of the Ansys simulation software in order to understand how the FEA is performed. During my first week in Grenoble, I already shared thoughts with Ali about what the FE model of the apex of the tongue should look like, including the dimensions and boundary conditions. After l performed all the measurements, I adapted Ali his code for the phantoms to make a more realistic representation for the apex of the tongue.

The Gent model was proposed by Ali and his colleagues in Grenoble. It was used for estimating the elastic properties in phantom tests as well and showed almost the same results as the dynamic mechanical analysis (e.g. tensile tests), what is considered to be the ground truth. However, I quickly learned that the Gent model was not the only model suitable for the phantom tests. Because the deformations that were applied were really small, most of the hyperelastic material models will give almost the same results. But, the elastic response of human tongue tissue is nonlinear and strain stiffening was observed for even small deformations. So I did some research in literature and came to the conclusion that the Gent model was suitable for simulating strain stiffening. Other, but more complex, models could also be used but I chose for the Gent model because of its simplicity. The colleagues in Grenoble agreed with this consideration.

**Assisting and contributing to the N17SWU and N17BTM study**

When I started my graduation internship in January, Kilian just started with two new studies. From that moment on I assisted him in (almost) all of the measurements during the past year. We even finished the inclusion for the N17SWU study. For this study I performed measurements on 10 healthy subjects to serve as a second observer to test the reproducibility of the SWE.

**APPENDIX L: RESEARCH PROTOCOL METC**

**Active and passive elasticity measurements of the tongue using in vivo measurement techniques**

**ACTIVE AND PASSIVE ELASTICITY MEASUREMENTS OF THE TONGUE USING IN VIVO MEASUREMENT TECHNIQUES**

| | |
|---|---|
| **Protocol ID** | NL64588.031.18 |
| **Short title** | Active and passive elasticity measurements of the tongue using *in vivo* measurement techniques |
| **Simplified title in Dutch, for PIF** | *Het meten van de stijfheid van de tong met behulp van nieuwe meettechnieken* |
| **EudraCT number** | *Not applicable* |
| **Version** | 4.0 |
| **Date** | 19-11-2018 |
| **Principal investigator(s)** | *Prof. dr. L.E. Smeele (l.smeele@nki.nl)* |
| **Research team** | *S. Boonstra BSc. (sa.boonstra@nki.nl)*<br>*K.D.R. Kappert MSc. (k.kappert@nki.nl)* |
| **Sponsor** | *Netherlands Cancer Institute* |
| **Independent expert (s)** | *Drs. P.F.E. Schutte (p.schutte@nki.nl)* |

**PROTOCOL SIGNATURE SHEET**

| **Name** | **Signature** | **Date** |
|---|---|---|
| **Head of Department:**<br>Prof. Dr. M.W.M. van den Brekel, MD PhD | | |
| **Principal Investigator:**<br>Prof. dr. L.E. Smeele (l.smeele@nki.nl) | | |

**TABLE OF CONTENTS**

**LIST OF ABBREVIATIONS AND RELEVANT DEFINITIONS**

| | |
|---|---|
| ABR | ABR form, General Assessment and Registration form, is the application form that is required for submission to the accredited Ethics Committee (In Dutch, ABR = Algemene Beoordeling en Registratie) |
| AE | Adverse Event |
| AR | Adverse Reaction |
| CA | Competent Authority |
| CCMO | Central Committee on Research Involving Human Subjects; in Dutch: Centrale Commissie Mensgebonden Onderzoek |
| CV | Curriculum Vitae |
| DSMB | Data Safety Monitoring Board |
| EU | European Union |
| EudraCT | European drug regulatory affairs Clinical Trials |
| GA | General Anaesthesia |
| GCP | Good Clinical Practice |
| IB | Investigator's Brochure |
| IC | Informed Consent |
| LASTIC | Light Aspiration device for *in vivo* Soft TIssue Characterization |
| METC | Medical research ethics committee (MREC); in Dutch: medisch ethische toetsing commissie (METC) |
| (S)AE | (Serious) Adverse Event |
| SPC | Summary of Product Characteristics (in Dutch: officiële productinfomatie IB1-tekst) |
| Sponsor | The sponsor is the party that commissions the organisation or performance of the research, for example a pharmaceutical company, academic hospital, scientific organisation or investigator. A party that provides funding for a study but does not commission it is not regarded as the sponsor, but referred to as a subsidising party. |
| US | Ultrasound |
| Wbp | Personal Data Protection Act (in Dutch: Wet Bescherming Persoonsgevens) |
| WMO | Medical Research Involving Human Subjects Act (in Dutch: Wet Medisch-wetenschappelijk Onderzoek met Mensen |

**SUMMARY**

**Rationale:** Among all treatments of cancer, surgery of locally advanced head and neck cancer has one of the highest risks of loss of vital functions. Speech, mastication and swallowing are complex functions that are easily affected. The term "functional inoperability" is used when unacceptable function loss after surgery is to be expected. It is hard to reach a consensus for the majority of surgical interventions regarding functional inoperability. Making effective patient counselling on the expected outcome impossible. To make a better prediction of functional loss after treatment a project was launched called Virtual Therapy. This project aims to develop a biomechanical model to simulate different treatment options and predict functional outcome on founded expectation. To make this model as accurate patient specific as possible, it is important to have knowledge of elastic properties of tissues in the oral region, e.g. the tongue. Elastic properties of the tongue are strongly influenced by postoperative fibrotic changes. But before we can say anything about the effects of fibrosis in patients we need to measure the passive and active stiffness of healthy tongue tissue. Shear wave ultrasound elastography and LASTIC are promising techniques to measure *in vivo* tissue elasticity.

**Objective**: The primary objectives of this study are:
-Analyse if shear wave ultrasound elastography with ElastQ and LASTIC are both feasible techniques to identify differences in tongue tissue elasticity and analyse if there is a correlation between both techniques.
-Investigate if shear wave ultrasound elastography and/or LASTIC can be used to distinguish the 'active' and ' passive' component of the tongue muscle elastic properties.

**Study design:** Prospective feasibility study

**Study population:** We aim to include 19 healthy volunteers (group 1). In addition we aim to include 19 patients (group 2) who are scheduled for OR and will receive general anaesthesia. These patients should not have any pathologies or impaired functionality in the oral cavity and oropharynx region or larynx.

**Intervention (if applicable)**: Shear wave ultrasound elastography is performed and an light aspiration device will be placed on the tongue surface.

**Main study parameters/endpoints:**
Group 1 (healthy volunteers):
- (Active) Elasticity of the tongue.

Group 2 (patients) before GA:
- Active component of tongue muscle elasticity

Group 2 (patients) during GA:
- Passive component of tongue muscle elasticity

**Nature and extent of the burden and risks associated with participation, benefit and group relatedness:** The measurement for the active component of tongue stiffness takes up to twenty minutes and will be scheduled on a moment that is most suitable for the patient and healthy volunteer. The passive component measurement will be performed under general anaesthesia. No extra OR/anesthesia time is requested. No risks are expected with the SWE. There is a possible risk of tissue damage using LASTIC.

The risk of possible tissue damage with LASTIC has been reduced to a very minimum. Several articles describe that human cells and tissue will be damaged after applying 50% or more strain to the tissue for 5-10 minutes. To set the strain limit on 50% and only applying it for a few seconds we assure no damage to the tissue will be done. If the volunteer experiences pain and wants to terminate to measurement all pressure can be released with the turn of one valve to assure direct and safe removal of the suction cup.

## 1. INTRODUCTION AND RATIONALE

Among all treatments of cancer, surgery of locally advanced head and neck cancer has one of the highest risks on loss of vital functions. Speech, mastication and swallowing are complex functions that are easily affected. A systematic review on swallowing dysfunction and speech intelligibility after oral cancer surgery demonstrated that serious swallowing deficiencies were experienced by over 80% of patients and severe impairment of speech intelligibility was observed in 20% of patients [55]. The term “functional inoperability” is used when unacceptable function loss after surgery is to be expected [1312]. In an international survey among surgeons and radiotherapists no consensus was reached for the majority of surgical interventions regarding functional inoperability [12]. Effective counselling of patients on the expected functional outcome is therefore currently impossible. Although severely needed, no standardized evaluation tool exists to help predict a personalized functional outcome of oral cancer therapies. To make a better prediction of functional loss after treatment a project was launched called Virtual Therapy [56]. This project aims to develop a model to simulate different treatment options and predict functional outcome on founded expectation [57].

At the moment ArtiSynth, a platform to simulate biomechanical models, is used to create a model for simulation of different treatments. To make this model as accurate patient specific as possible, it is important to have knowledge of elastic properties of tissues in the oral region. Elastic properties of the tongue in the biomechanical model are now based on assumptions and probabilities, while changing the elastic properties of the model results in a different mobility. Elastic properties of the tongue are strongly influenced by fibrotic changes due to treatment. Therefore fibrosis and other effects on tissue elasticity should be studied closely. Since the (*in vivo*) elastic properties of the tongue are unknown, a study cohort with volunteers should be studied to determine a realistic range and variation for the elastic properties of the human tongue. The elastic properties of the human tongue are expected to be influenced by muscle activation of the tongue muscles. A study cohort of patients, with no pathologies or impaired functionality in the oral cavity and oropharynx region., measured before (active stiffness) and during (passive stiffness) general anesthesia are expected to show the difference between the active and passive tongue muscle elastic properties.

The elasticity of a material, known as the Young's modulus (E), describes the tendency of the material to return to its original size and shape after experiencing stress and determined by stress (the force on the material) and strain (deformation of the material) [16]. Elastography is the technology used to noninvasively assess mechanical tissue properties and is nowadays implemented in clinical ultrasound and MR systems [58]. The most practical method to determine the elasticity of the tongue is shear wave ultrasound elastography. Shear waves used in ultrasound are transiently generated by applying external mechanical vibration to the body or by focusing acoustic radiation force impulses, or push pulses, inside the region of interest. This push pulse in the region of interest results in absorption or reflection of the wave and causes a body force in the direction of wave propagation. Some of the absorbed energy is released as shear waves. [5859] This principle is shown in figure 1.

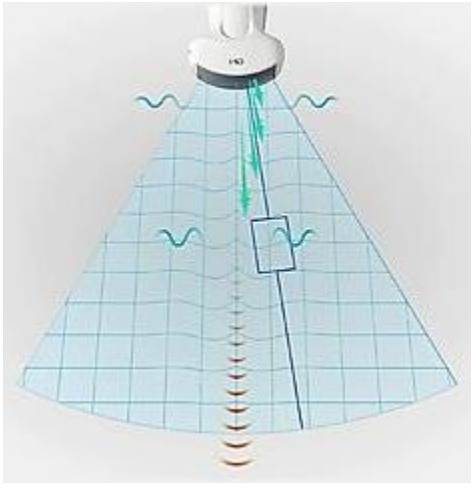

*Figure 1. Shear wave ultrasound. Shear waves oscillate perpendicular to the direction of wave propagation* [60]

Shear wave ultrasound elastography is a technique which is nowadays clinically used for liver stiffness measurement to diagnose liver diseases as fibrosis and neoplastic lesions. Manufacturers as Philips, Siemens, Toshiba and GE have included shear wave elastography in some of their ultrasound devices. The French high-technology company Echosens is specialized in non-invasive diagnostic products and services for hepatology. This company developed Fibroscan, a device using shear waves for the detection of liver fibrosis which is used worldwide. [6162]

Figure 2 shows an example of tongue elasticity measurement. Philips's EPIQ7 Ultrasound system was used in combination with the C5-1 abdominal transducer and ElastQ software. Shear wave ultrasound elastography is easy to perform and a promising technique for determining tongue elasticity. This technique results in a quantitative elasticity measurement which could be included directly into the biomechanical Artisynth model and therefore it is an added value for the virtual therapy project.

ElastQ is a new software program designed by Philips which allows the user to measure the stiffness of the tissue on a larger surface. It provides a 2D elastogram as shown in Figure 2 on the right. Philips has more elastography software, the older version ElastPQ uses a different technique and can only measure the elasticity at one focal point. ElastPQ was used in the N17SWE study at the beginning but gave unsatisfying results. Therefore, we want to use ElastQ to see whether this new software performs better. For this reason we explicitly mention ElastQ in the goal of our study.


*Figure 2. An example of ultrasound tongue elasticity measurement using the ElastQ software. On the right the colored box represents the elastogram.*

Elastography is not yet validated for tongue measurements, and that's why, in addition, we want to introduce a second measurement.The second technique we want use is a Light Aspiration device for *in vivo* Soft TIssue Characterization (LASTIC). LASTIC is developed in Grenoble by Schiavone et al. and uses a negative pressure to deform soft tissue within a small suction cup. [22] Each experiment consist of several negative pressures with corresponding tissue deformation measurements. Based on the amount soft tissue deformation, measured in height in millimetres, the elastic parameters of the soft tissue are estimated by inverting a Finite Element Model of the suction experiment. The parameters are the coefficients of the mechanical constitutive law of soft tissue according to the Mooney-Rivlin strain-energy function, *W* [38]:

$$W = a_{10}(I_1 - 3) + a_{30}(I_1 - 3)^3$$

Using an optimisation scheme a best fit, shown in Figure 3, between experimental data and the calculations of deformation vs. negative pressure is computed, providing the coefficient $a_{10}$ and $a_{30}$. These are two material constants with a unit of stress, while $I_1$ is the first invariant of the right Cauchy-Green strain tensor. Using *W* it is possible to compute the stress/strain relationship, and eventually estimate the Young's Modulus.

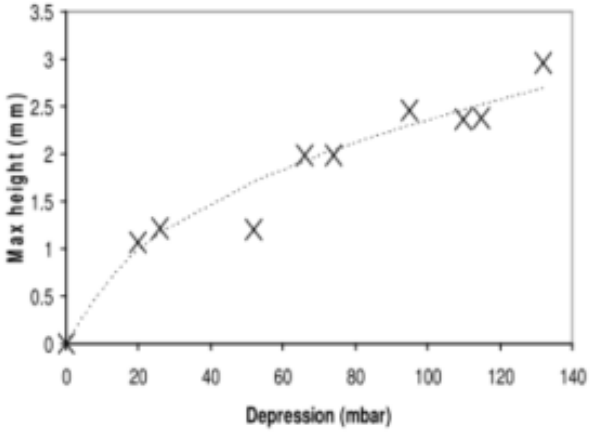


*Figure 3: Tissue bump height as function of the depression in the suction cup, each cross is one measurement. The dotted line plots the simulated results with the estimated constitutive law*.

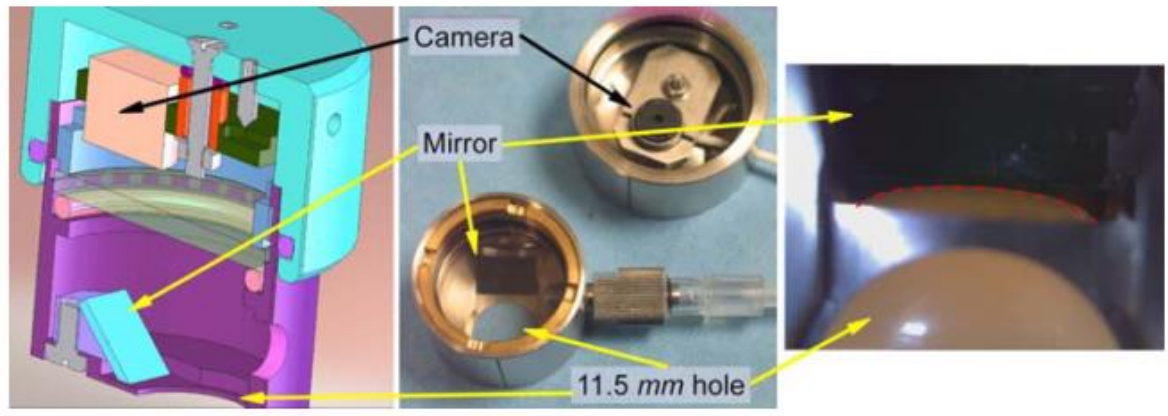


*Figure 4 shows an example of the setup. The camera and mirror are used to measure the deformation of the tissue*

The LASTIC model shown in Figure 4 is an older model. The new version has not yet been published but allows *in vivo* measurement without the use of a mirror and camera and therefore is even smaller, which is more ideal for intra-oral measurements. LASTIC is developed in such a way it is compatible with the sterilization process required by intra operative use. [14] An even older model is already used for *in vivo* brain elasticity measurements. [38]

The risk of possible tissue damage with LASTIC has been reduced to a very minimum. Several articles describe that human cells and tissue will be damaged after applying 50% or more strain to the tissue for 5-10 minutes.[39,40] To set the strain limit on 50% and only applying it for a few seconds we assure no damage to the tissue will be done. If the volunteer experiences pain and wants to terminate to measurement all pressure can be released with the turn of one valve to assure direct and safe removal of the suction cup. Based on experiments with phantom 50% of strain is know to be sufficient to determine the Young's modulus. We know that 50% of strain is around 25% of sphere volume. Based on the radius of the hole we can calculate this volume and use it as maximum volume that can aspirate. For a complete elaboration on risk management see attachment VI in the 'Investigational Medical Device Dossier'.

**Rationale**
Investigate if we can distinguish the active and passive component of the tongue muscle elastic properties.

## 2. OBJECTIVES

**Primary objective:** The primary objectives of this study are:

- Analyse if shear wave ultrasound elastography with ElastQ and LASTIC are both feasible techniques to identify differences in tongue tissue elasticity and analyse if there is a correlation between both techniques.
- Investigate if shear wave ultrasound elastography and/or LASTIC can be used to distinguish the 'active' and ' passive' component of the tongue muscle elastic properties.

**Secondary objective:** The secondary objective is to adapt the biomechanical tongue model with patient specific elastic properties.

## 3. STUDY DESIGN

Study design

This study is a prospective **feasibility** study among patients who are scheduled for surgery with general anesthesia with no pathologies or impaired functionality in the oral cavity and oropharynx region. In addition healthy volunteers will be included to test the repeatability and inter and intra observer variability. A written and signed informed consent will be obtained from each subject prior to inclusion.

The subjects and also colleagues are approached by us and with interest in participation the PIF is send to them. The PIF explicitly states that participation is completely voluntary. We ask the subjects to read them carefully and we give them at least two days to make a choice. Because we can imagine that colleagues might experience extra pressure to participate in the research of their colleagues, we will ask once more before the measurements if they are absolutely sure and mention that they are not obliged to participate.

Study setting

This study will be performed at the Department of Head and Neck Cancer Oncology & Surgery, at the Netherlands Cancer Institute – Antoni van Leeuwenhoek in Amsterdam, the Netherlands.

Study duration

Based on the large population and broad inclusion criterion we expect the measurements to take four weeks within the year 2018.

## 4. STUDY POPULATION

One of our hypothesis is that the elasticity of (tong) tissue is decreasing when people get older. For this reason we want to divide each group into two age categories. The first half should be younger than 50 years old and the other half should be 50 years or older. In this way want to make sure that the age of the volunteers will not be a possible bias for the eventual results, and are able to compare possible differences due to age.

### 4.1 Population (base)

Group 1:

19 Healthy volunteers. Those volunteers will be used for the repeatability and intra observer reliability for the LASTIC device. Approximately 50% of the subjects should be younger than 50 years. Approximately 50% of the subjects should be 50 or older than 50.

Group 2:

19 Patients who are scheduled for surgery with general anesthesia without Laryngeal mask airway and no pathologies or impaired functionality in the oral cavity and oropharynx region. Approximately 50% of the subjects should be younger than 50 years. Approximately 50% of the subjects should be 50 or older than 50.

### 4.2 Inclusion criteria

In order to be eligible to participate in this study, a subject must meet all of the following criteria:

- Older than 18 years
- Informed consent
- For group 2: Patients need to have an ASA score of at least I or II.

### 4.3 Exclusion criteria

A potential subject who meets any of the following criteria will be excluded from participation in this study:

- Pathologies or impaired functionality in the oral cavity and oropharynx region.
- Use of Laryngeal mask airway
- Unforeseen practical problems that make it impossible to carry out the measurements before the start of surgery.

### 4.4 Sample size calculation

The elastic properties of tongue muscle tissue measured by shear wave ultrasound are unknown. Other quantifications methods used in previous studies found a tongue elasticity
in the range of 1-8 kPa [21,23]. To stay in line with another study of our department (AVL N17SWU , NL60754.031.17), in which we want to investigate changes in tongue elasticity due to fibrosis caused by different therapies, we again assume that relative changes in elastic properties of the tongue are in the same region as the liver.

More research has been performed on ultrasound elasticity measurements of the liver. A study with 429 healthy volunteers showed that the mean liver stiffness value in these patients was 5.5 ± 1.6 kPa [63].

Figure 5 shows the clinical significance of liver stiffness cut-offs in chronic liver diseases. Significant fibrosis was found from a value of 7 kPa.

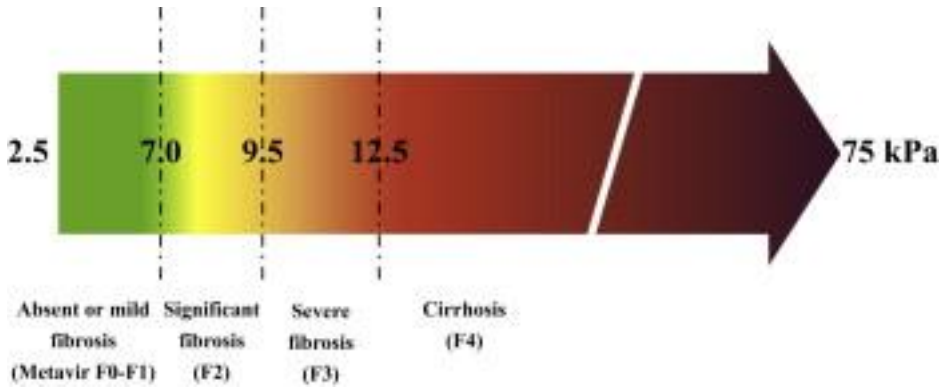


*Figure 5. clinical significance of liver stiffness cut-offs in chronic liver diseases* [6465].

Therefore information from those studies is used to calculate Cohen's d:

$$d = \frac{M_1 - M_2}{\sigma} = \frac{7 - 5.5}{1.6} = 0.94$$

Using a paired t-test, a sample size of 11 participants is needed to have 80% power to detect an effect size of 0.94 with a significance level of 0.05. [66]

In our active study (AVL N17SWU , NL60754.031.17) we included 19 subjects in each group to compare the means of each group with a power of 80% power to detect an effect size of 0.94 with a significance level of 0.05. [66]

To stay in line with this number and possible comparison with the healthy volunteers between both studies we aim to include 19 volunteers for this study for both groups and increase the power to detect an effect size of 0.94 with a significance level of 0.05 to 97%. We expect to be able to include more patients due to the broad inclusion criteria and large patient population in the NKI-AvL.

## 5. METHODS

### 5.1 Study parameters/endpoints

#### 5.1.1 Main study parameter/endpoint

Group 1:

- (Active) Elasticity the tongue

Group 2 before GA:

- Active component of tongue muscle elasticity

Group 2 during GA:

- Passive component of tongue muscle elasticity

#### 5.1.2 Secondary study parameters/endpoints (if applicable)

<not applicable>

#### 5.1.3 Other study parameters (if applicable)

Age; gender; BMI; amount of muscle relaxants during GA; tobacco consumption

### 5.2 Study procedures

The included volunteers from group 1 will be asked to participate in a repeatability study for the LASTIC device. The repeatability of shear wave ultrasound will be tested in the active study( AVL N17SWU , NL60754.031.17) of our department. The fully conscious is asked to position the tongue in a relax position at the floor of the mouth. The LASTIC is positioned left or right from the midline of the tongue. An ultrasound probe placed on the chin is used to ensure that the location of the LASTIC is also visible with ultrasound. Then using the probe, the elasticity of the tissue underneath the LASTIC device is determined using ultrasound elastography. After this the LASTIC device will be used to measure the elasticity on the same spot. Based on the first results the procedure will be repeated up to ten times by one observer to get an accurate average result. The inter observer reliability will be done using a phantom test, in order to reduce the measurement time. The intra observer repeatability will only be performed for active measurements on healthy volunteers using the ten measurements. We will not put healthy volunteers under GA. It can be reasoned that because of the lack of muscle tone, the repeatability can only be better in comparison to the active measurement.

Included volunteers from group 2 will be asked to participate in only the LASTIC measurements. Based on the first result of group 1 and previous studies we see that that the SWE results are unreliable and show high standard deviations for anisotropic tissue (like tongue muscle). Also, there is no correlation between both techniques. The subjects will participate in two measurements: The active measurement and the passive measurement. The active measurement will be performed just before or after a regular appointment at the Netherlands Cancer Institute. The fully conscious is asked to position the tongue in a relax position at the floor of the mouth. The LASTIC is positioned left or right from the midline of the tongue. The measurement is repeated 10 times in order to calculate an accurate average result. The measurements on the OR can be done simultaneously with the surgical procedure, so no addition OR/anaesthesia time is needed.

### 5.3 Withdrawal of individual subjects

Subjects can leave the study at any time for any reason if they wish to do so without any consequences. The investigator can decide to withdraw a subject from the study for urgent medical reasons.

#### 5.3.1 Specific criteria for withdrawal (if applicable)

If one of the two measurements moments (passive of active stiffness measurement) cannot be performed

### 5.4 Replacement of individual subjects after withdrawal

If one of the two measurements moments (passive of active stiffness measurement) cannot be performed a new subject will be included.

### 5.5 Follow-up of subjects withdrawn from treatment

There is no follow-up

### 5.6 Premature termination of the study

No premature termination of any kind is expected.

## 6. SAFETY REPORTING

### 6.1 Temporary halt for reasons of subject safety

In accordance to section 10, subsection 4, of the WMO, the sponsor will suspend the study if there is sufficient ground that continuation of the study will jeopardise subject health or safety. The sponsor will notify the accredited METC without undue delay of a temporary halt including the reason for such an action. The study will be suspended pending a further positive decision by the accredited METC. The investigator will take care that all subjects are kept informed.

### 6.2 AEs, SAEs and SUSARs

#### 6.2.1 Adverse events (AEs)

Adverse events are defined as any undesirable experience occurring to a subject during the study, whether or not considered related to [the investigational product / trial procedure/ the experimental intervention]. All adverse events reported spontaneously by the subject or observed by the investigator or his staff will be recorded.

#### 6.2.2 Serious adverse events (SAEs)

A serious adverse event is any untoward medical occurrence or effect that

- results in death;
- is life threatening (at the time of the event);
- requires hospitalisation or prolongation of existing inpatients' hospitalisation;
- results in persistent or significant disability or incapacity;
- is a congenital anomaly or birth defect; or
- any other important medical event that did not result in any of the outcomes listed above due to medical or surgical intervention but could have been based upon appropriate judgement by the investigator.

An elective hospital admission will not be considered as a serious adverse event.

The procedure is not considered to be of any physical harm to the patient. The investigator will report all SAEs to the sponsor without undue delay after obtaining knowledge of the events.

The sponsor will report the SAEs through the web portal *ToetsingOnline* to the accredited METC that approved the protocol, within 7 days of first knowledge for SAEs that result in death or are life threatening followed by a

period of maximum of 8 days to complete the initial preliminary report. All other SAEs will be reported within a period of maximum 15 days after the sponsor has first knowledge of the serious adverse events.

### 6.3 Follow-up of adverse events

All AEs will be followed until they have abated, or until a stable situation has been reached. Depending on the event, follow up may require additional tests or medical procedures as indicated, and/or referral to the general physician or a medical specialist.
SAEs need to be reported till end of study within the Netherlands, as defined in the protocol

## 7. STATISTICAL ANALYSIS

### 7.1 Primary study parameter(s)

Group1:
19 Healthy volunteers. These volunteers will be used for the intra observer reliability for the LASTIC device. This will be tested using the interclass correlation coefficient (ICC).

Group2:
In total 19 volunteers will be included and undergo two measurement moments:

Before or after GA:

- active component of tongue muscle elasticity

During GA:

- passive component of tongue muscle elasticity

Both measurements will be compared using a paired t-test to investigate if a difference between passive and active tongue muscle elasticity can be distinguished. This will provide insight on the dependency of muscle activations when investigating elastic properties of the tongue.

Compare ultrasound elastography with LASTIC
To asses if there is a correlation between both techniques data of both groups can be used. Using the ICC the agreement between both measurement methods can be evaluated.

## 8. ETHICAL CONSIDERATIONS

### 8.1 Regulation statement

The principal investigator will ensure that this study is conducted in accordance with the principles of the current version of the Declaration of Helsinki or with the laws and regulations of the Netherlands, whichever affords greater protection to the individual. The current version of the Declaration of Helsinki is available in C2.A.

### 8.2 Recruitment and consent

It is the responsibility of the principal investigator to obtain written informed consent from each patient (or the patients' legally acceptable representative - where this is applicable) prior to participation in this study.

The Patient Information Sheet approved by the appropriate independent ethics committee/institutional review board (IEC/IRB) will be used. A copy will be given to the patient (or the patient's legally acceptable representative - where this applicable) and they will be allowed adequate time to make a decision about their participation in the study before giving written informed consent.

All patients will be informed of the aims of the study, the possible adverse events, the procedures and possible hazards to which he/she will be exposed. They will be informed as to the strict confidentiality of their patient data, but that their medical records may be reviewed for trial purposes by authorized individuals other than their treating physician. Information will be given both spoken and written as in the Patient Information text.
It will be emphasized that the participation is voluntary and that the patient is allowed to refuse further participation in the protocol whenever he/she wants. This will not prejudice the patient's subsequent care. Documented informed consent must be obtained for all patients included in the study before they are registered in the study.
Written informed consent form should be signed and personally dated by the patient or by the patient's legally acceptable representative as well as the local investigator.

### 8.3 Objection by minors or incapacitated subjects (if applicable)

The NKI has a liability insurance which is in accordance with article 7 of the WMO.

The NKI (also) has an insurance which is in accordance with the legal requirements in the Netherlands (Article 7 WMO). This insurance provides cover for damage to research subjects through injury or death caused by the study. The insurance applies to the damage that becomes apparent during the study or within 4 years after the end of the study.
Information about the insurance can be found in the patient information letter.

## 9. ADMINISTRATIVE ASPECTS, MONITORING AND PUBLICATION

### 9.1 Handling and storage of data and documents

Every subject is linked to a subject number. Without full access to the key-files, it is not possible to link this number to the subject. This subject number is used to identify data that belongs to one subject. Only the principal investigator and his authorized representative (K.Kappert) have access to these files. This key stays in the Antoni van Leeuwenhoek.

The data of the echo of the subject will be transferred and saved on a secured (research)network directory for researcher in the Antoni van Leeuwenhoek (researchers with access are saved in the delegation log). The network directory is called \\clin-storage\3DMeting\.This disk is managed by the Antoni van Leeuwenhoek. The echo images will be saved with the study number and code which is assigned to the subject. Only the research team has access to this drive.

The measurements with LASTIC will be performed on a coded laptop of the Antoni van Leeuwenhoek, this laptop will never leave the hospital. The results of the measurement will immediately be transferred to the same network directory as described above and won't stay on the laptop. Only the authorized representative (K.Kappert) can access this laptop.

### 9.2 Amendments

Amendments are changes made to the research after a favourable opinion by the accredited METC has been given. All amendments will be notified to the METC that gave a favourable opinion.

### 9.3 Annual progress report

The investigator will submit a summary of the progress of the trial to the accredited METC once a year. Information will be provided on the date of inclusion of the first subject, numbers of subjects included and numbers of subjects that have completed the trial, serious adverse events/ serious adverse reactions, other problems, and amendments.

### 9.4 Temporary halt and (prematurely) end of study report

The investigator/sponsor will notify the accredited METC of the end of the study within a period of 8 weeks. The end of the study is defined as the last patient's last visit.

The sponsor will notify the METC immediately of a temporary halt of the study, including the reason of such an action.

In case the study is ended prematurely, the sponsor will notify the accredited METC within 15 days, including the reasons for the premature termination.

Within one year after the end of the study, the investigator/sponsor will submit a final study report with the results of the study, including any publications/abstracts of the study, to the accredited METC.

## 10. REFERENCES

See section 9 on page 21